AD-A090 127 GENERAL DYNAMICS SAN DIEGO CA CONVAIR DIV F/G 11/4
DEVELOPMENT OF ADVANCED INTERCEPTOR SUBSTRUCTURAL MATERIAL:(U)
AUG 80 J HERTZ, N R ADSIT DAAG46-78-C-0056
UNCLASSIFIED AMMRC-TR-80-44 NL

1 OF 2
AD A 090127

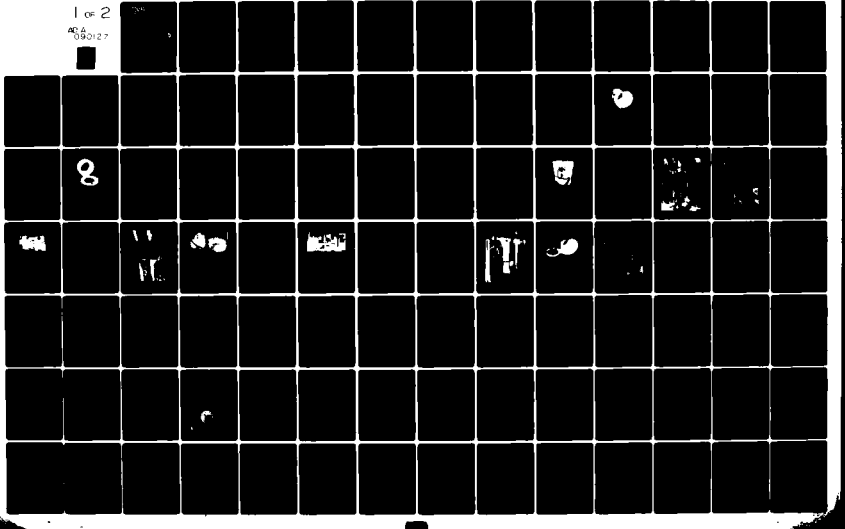

LEVEL II

AD

2

AMMRC TR 80-44

DEVELOPMENT OF ADVANCED INTERCEPTOR SUBSTRUCTURAL MATERIAL

August 1980

J. Hertz And N. R. Adsit
GENERAL DYNAMICS CONVAIR DIVISION
P.O. BOX 80847
SAN DIEGO, CALIFORNIA 92138

FINAL REPORT

CONTRACT DAAG46-78-C-0056

Approved for public release; distribution unlimited

Prepared for
ARMY MATERIALS AND MECHANICS RESEARCH CENTER
Watertown, Massachusetts 02172

The findings in this report are not to be construed as an official Department of the Army position, unless so designated by other authorized documents.

Mention of any trade names or manufacturers in this report shall not be construed as advertising nor as an official indorsement or approval of such products or companies by the United States Government.

DISPOSITION INSTRUCTIONS

Destroy this report when it is no longer needed.
Do not return it to the originator.

UNCLASSIFIED

SECURITY CLASSIFICATION OF THIS PAGE (When Data Entered)

REPORT DOCUMENTATION PAGE	READ INSTRUCTIONS BEFORE COMPLETING FORM
1. REPORT NUMBER: AMMRC TR-80-44	2. GOVT ACCESSION NO.: AD-A090127
	3. RECIPIENT'S CATALOG NUMBER:
4. TITLE (and Subtitle): Development of Advanced Interceptor Substructural Material,	5. TYPE OF REPORT & PERIOD COVERED: Final Report, 2 Sept 1978 - 15 Nov 1979
	6. PERFORMING ORG. REPORT NUMBER:
7. AUTHOR(s): J. Hertz, N.R. Adsit	8. CONTRACT OR GRANT NUMBER(s): DAAG46-78-C-0056
9. PERFORMING ORGANIZATION NAME AND ADDRESS: General Dynamics, Convair Division, P.O. Box 80847, San Diego, CA 92138	10. PROGRAM ELEMENT, PROJECT, TASK AREA & WORK UNIT NUMBERS: D/A Project 1W16211A661, AMCMS Code 62113.11.07000
11. CONTROLLING OFFICE NAME AND ADDRESS: Army Materials and Mechanics Research Center, Watertown, Massachusetts 02172	12. REPORT DATE: August 1980
	13. NUMBER OF PAGES:
14. MONITORING AGENCY NAME & ADDRESS (if different from Controlling Office)	15. SECURITY CLASS. (of this report): Unclassified
	15a. DECLASSIFICATION DOWNGRADING SCHEDULE: N/A

16. DISTRIBUTION STATEMENT (of this Report)

Approved for public release, distribution unlimited.

17. DISTRIBUTION STATEMENT (of the abstract entered in Block 20, if different from Report)

18. SUPPLEMENTARY NOTES

19. KEY WORDS (Continue on reverse side if necessary and identify by block number)

Composite materials
Composite structures
Graphite
Missile airframes
Interceptors
Epoxy resins
Fibers

20. ABSTRACT (Continue on reverse side if necessary and identify by block number)

The work reported herein represents a continuation of previous work reported in AMMRC-TR-78-4 and TR-78-38 and is aimed at the development of ultra-high-modulus graphite/epoxy structures for use in future advanced terminal interceptors. The work has produced a preliminary full-scale design and demonstrated, experimentally and analytically, that the design will carry the loads. More study needs to be conducted and

DD FORM 1 JAN 73 1473 EDITION OF 1 NOV 65 IS OBSOLETE

UNCLASSIFIED

SECURITY CLASSIFICATION OF THIS PAGE (When Data Entered)

some further experimental work is recommended before a full-scale article is tested. Work reported here has concentrated on testing the aft joint and an intermediate ring for holding an equiment package in the frusta.

TABLE OF CONTENTS

TABLE OF CONTENTS, Contd

TABLE OF CONTENTS, Contd

LIST OF FIGURES

LIST OF FIGURES — *Continued*

LIST OF TABLES

PREFACE

This final report was prepared by the General Dynamics Corporation Convair Division for the Army Materials and Mechanics Research Center (AMMRC), Watertown, Massachusetts under contract DAAG46-78-C-0056. This work is part of the program on Development of Hardened ABM Materials, Mr. John F. Dignam, Program Manager. The AMMRC technical supervisor is Mr. Lewis R. Aronin.

This report covers work performed during the period 2 September 1978 to November 1979 by personnel from the General Dynamics Convair Division and Prototype Development Associates (PDA). Convair personnel included Mr. Julius Hertz, the program manager; Dr. N.R. Adsit, principle investigator; Mr. Edward E. Spier, Analysis; Mr. Jack Prunty, Design; Mr. Larry Belfer, Structural Testing; and Mr. J.R. Howard, Shock Testing. The frusta test specimens were fabricated by Mr. Charles M. Ogle. PDA personnel included: Mr. Niel Harrington, Structural Analysis and Mr. E.T. Miyazawa, Thermal Analysis.

SECTION 1

SUMMARY

Advanced terminal interceptor (ATI) studies over the last five years have identified the need for lightweight, stiff materials for the missile structure. Previous programs performed for AMMRC by the General Dynamics Convair Division and Martin-Marietta have successfully fabricated and tested half-scale frusta. During these previous studies, three concepts of end joints were fabricated and the first one successfully tested. In addition, one concept of an equipment ring was also fabricated and tested.

The objectives of this study were to continue the effort to develop ultra-high-stiffness graphite/epoxy for use in an ATI structure. Tasks included:

a. Testing the second and third end joint concepts.

b. Designing, fabricating and testing other equipment ring concepts.

c. A preliminary design of the full-scale frusta.

d. Analyzing the test results and an analysis of a full-scale frusta preliminary design.

e. Thermal analysis of the full-scale frusta.

f. A manufacturing study to determine producibility.

Results of this program show that all three end-joint concepts met and exceeded the design requirements. Two of the joint designs were significantly better than the third. All failures were in the basic shell rather than in the joint.

Two equipment-ring concepts have been shown to be adequate for the design. A metal ring (Ti) will perform adequately, but the graphite/epoxy wedge design was chosen since it meets performance requirements and more closely matches the thermal expansion coefficient of the frusta.

The preliminary design and analysis shows that adequate margins of safety exist for all suspected failure modes. The thermal analysis shows that the interior of the basic frusta is not heated during flight.

Finally, the manufacturing studies show that it is possible to produce sections of the ATI guidance and control sections at the rate of 1000 articles per year.

SECTION 2

INTRODUCTION

2.1 BACKGROUND

Advanced terminal interceptor (ATI) configuration studies over the last five years have identified the need for lightweight, stiff missile structures, especially for interceptors designed to engage maneuvering threats. To meet this challenge, the Army Materials and Mechanics Research Center (AMMRC) has conducted research and development on advanced materials including beryllium, metal-matrix composites, and resin-matrix composites. In the last category, ultra-high-modulus (UHM) graphite/epoxy composite structures have been under evaluation and subscale development since 1973 (Reference 1). The results of previous work on UHM materials show significant reductions in launch weight over more conventional materials.

Complementing programs have been performed for AMMRC by General Dynamics Convair Division (References 2 and 3) and Martin Marietta Orlando Division (Reference 1) to pursue the UHM graphite/epoxy conical shell development. Under these programs, ten graphite/epoxy conical frusta were fabricated representing a half-scale version of the aft portion of the guidance and control section of an early ATI configuration. The size of these frusta are shown in Table 2-1. These were successfully tested, and the results closely verified analytical predictions. An intermediate load introduction ring was designed and analyzed. This resulted in a unique wedge shape ring design of high-strength graphite/epoxy composite. The fabrication, assembly, and test of such a ring in a subscale larger frustum was accomplished, and the bonded ring joint resisted ultimate design loading at both room temperature (RT) and 325F without failure. After several tests, the ring was tested to failure at RT. This occurred at 260 percent of the predicted design ultimate load.

Table 2-1. Summary of Frusta Size[1]

	Half Size	Larger Size	Full Size
Length, Inches	9.30	13.4	33.7
OD Forward, Inches	5.78	8.54	8.01
OD Aft, Inches	7.81	10.73	15.41
Thickness, Inches	0.179	0.179 to 0.210	0.380
Cone Angle, Degrees	6.27	4.67	6.27

[1]Half-size frusta represent stations 44.6 to 61.2 of the full guidance and control section as shown in Figure D-1 of Appendix D. This size has been used in developing the layup for the basic shell, in aft joint reinforcement design, and in a portion of the development effort on the equipment ring. Frusta designated as 'larger size' were used for developing the equipment ring. They are half thickness but, to minimize scaling effects, represent a diameter intermediate between half and full scale in the region of station 44.6. The full size dimensions shown above are for a complete guidance and control section.

2.2 PROGRAM OBJECTIVE

The primary objective of the present program and those studies preceding it was to demonstrate the feasibility of using ultra-high-modulus graphite/epoxy as a structural material on future high-performance interceptors. This objective was to be demonstrated by analysis, fabrication, and testing of conical frusta representative of a guidance and controls section of an advanced terminal interceptor (ATI). An early study (Reference 1) showed that approximately two-thirds of the launch weight could be saved by going from an aluminum ATI to one built from ultra-high-modulus graphite/epoxy. This relationship was developed on the basis that all structural frequencies should be proportionally above the control system bandwidth. This criterion establishes that a first structural bending mode frequency above 70 Hz is required at second stage ignition.

Under an earlier program (Reference 2), General Dynamics qualified an ultra-high-modulus graphite/epoxy (GY-70/934) to Material Specification ANA74700314-001, developed a manufacturing process for fabrication of conical frusta using prepreg gore sections laid into and cured in a bulk graphite tool, and developed a manufacturing process for making high-strength joints by interleaving titanium foil between the graphite/epoxy layers in a closed conical shape. Thirteen subscale frusta were successfully built and subsequently tested. The results demonstrated the feasibility of meeting the primary objective.

Once feasibility of shell fabrication was established, it was necessary to demonstrate the ability to fabricate and assemble a simulated equipment mounting ring for a typical ATI guidance and control section. Preliminary analysis, fabrication, and testing were conducted as part of contract DAAG46-76-C-0008 (Reference 3). An experimental high-strength (T-300/934) graphite/epoxy wedge ring concept secondary bonded to the inside of the frusta was successfully demonstrated. Helicoils were used for attaching a simulated equipment mounting plate to the ring.

The primary objective of the present program was to continue the early efforts initiated under contract DAAG46-76-C-0008 in the areas of design, analysis, manufacturing development, and testing while maintaining the end objective, i.e., the use of a graphite/epoxy substructure for an ATI.

Detailed tasks of this program were as follows:

a. Review of government-furnished configuration studies and definition of a baseline ATI forebody configuration.

b. Establishment of static and shock loads for a defined full-scale section.

c. Thermal-structural analysis of the full-scale guidance and control section of the ATI including strength and stiffness continuity at the forward and aft splice rings, structural integrity of the equipment ring and shell attachment, shell strength and stiffness in the location of the antenna cutouts, and shell thermal-structure integrity under heating and loading environments.

d. Testing of four half-scale frusta having interleaved titanium joint reinforcements.

e. Testing of four additional half-scale frusta fitted with two different equipment ring designs.

f. Testing of two additional larger frusta to further evaluate the most promising equipment ring attachment concept.

g. Preparation of three-view detail and assembly drawings of the full scale section.

h. Comparison of the mass properties of the composite design to its aluminum alloy counterpart.

i. A manufacturing analysis to identify methods of manufacturing and assembly, tooling requirements, facility requirements, a preliminary tooling design, and cost projections for an operational configuration.

j. A test plan that defines requirements for full-scale demonstration tests as well as additional subscale hardware tests.

SECTION 3

MATERIALS AND FABRICATION

3.1 RAW MATERIALS

3.1.1 GRAPHITE/EPOXY. At the outset of this program, 20 pounds of an ultra-high modulus (UHM) graphite/epoxy GY70/934 (Fiberite hy-E-1534) prepreg was ordered from Fiberite Corporation of Winona, Minnesota. The prepreg was ordered per material specification ANA74700314-001B developed by Martin Marietta for AMMRC (Reference 1). As noted in Section 2.2, this material is used in fabricating the basic shell.

The Fiberite certification test data on prepreg Lot C9-086 for 20.8 pounds is given in Table 3-1. A summary of prepreg properties obtained at General Dynamics on Roll 2 are given in Table 3-2. A unidirectional panel was made from the prepreg using the cure cycle previously reported (Reference 2). Flexure and short beam shear specimens were machined from each panel so that the length of the specimens were in the 0° direction. The specimens were tested at ambient temperature and that data, as well as cured panel resin content, fiber volume, and specific gravity are reported in Table 3-3. All data meet the requirements of ANA74700314-001B.

Table 3-1. Fiberite hy-E 1534 Certified Data

Quantity Shipped On 11/1/78	20.8 lbs				
Lot No.	C9-086				
Roll No.		1	2	3	4
Tape Size, Inches		3.0	3.0	3.0	3.0
Resin Solids, %		42.9	42.4	41.2	42.1
Volatile Content, %		0.5	0.5	0.5	0.5
Laminate Flow, % @ 50 p.s.i.		21.0	21.3	22.0	22.7
Gel Time, Minutes @ 377°C		6.3	6.5	6.8	6.0
Tack		Pass	Pass	Pass	Pass
Specific Gravity —					
Tensile Strength (p.s.i.) —			**Fiber Data**		
Tensile Modulus (10^6 p.s.i.) —			**Strength**	**Modulus**	**Density**
Flexural Strength (p.s.i.) R.T.	115,893*	**Lot**	**(ksi)**	**(msi)**	**g/cc**
350°F	118,987*	227(05)	284.9	74.7	1.973
Flexural Modulus (10^6 p.s.i.) —		227(06)	284.9	74.7	1.975
		227(07)	284.9	74.7	1.983
Compression Strength (p.s.i.) —		224(01)	263.6	78.9	2.000
Horizontal Beam Shear (p.s.i.) —					
Cured Ply Thickness, Inches	.0044	*Normalized to 63% fiber volume			
Date of Manufacture	10/19/78				
Shelf Life	6 months @ 0°F Max.	I.R. scan attached			
Ref: Packing List No.	011237				

Table 3-2. Prepreg Properties Obtained at General Dynamics

Material	% Volatiles		% Resin Solids		% Resin Flow		Process Gel*	Infrared Curve
	Spec. Req.	GD Average	Spec. Req.	GD Average	Spec. Req.	GD Average	No Spec. Requirement	
hy-E-1534 (GY-70/934) Batch C9-086, Roll 2	2.0 max	0.5	40 ± 3	41.4	20 ±3	21.4	290F	Meets Standard
hy-E-1034C (T-300/934) Batch C9-101, Roll 1	2.0 max	0.3	40 ± 3	36.8**	20 ± 5	19.4	290F	Meets Standard

*Process gel is temperature at which resin gels when prepreg is processed through normal cure cycle.

**Meets specification when rounded off to nearest percent. Panel made with this prepreg met specification requirements.

Table 3-3. Cured Laminate Properties of Unidirectional Laminates

Material Identification	Longitudinal Flexure Strength, ksi	Longitudinal Short Beam Shear Strength, ksi	Resin Content Wt. %	Fiber Vol. %	Specific Gravity
hy-E-1534 (GY-70/934)	110	7.81	29.78	61.48	1.71
Batch C9-086, Roll 2	122	7.15	30.77	59.88	1.70
	104	7.15	28.43	62.54	1.72
	Avg. 112	7.37	29.66	61.30	1.71
Normalized to 63% F.V.	115				
ANA74700314-001B requirement	95* min.	6.0 min.			
hy-E-1034C (T-300/934)	283	14.8	24.20	70.06	1.60
Batch C9-101, Roll 1	290	15.0	24.09	70.19	1.62
	291	13.9	23.71	70.63	1.61
	Avg. 288	14.5	24.00	70.30	1.61
Normalized to 63% F.V.	258				
ANA74700314-001B requirement	220* min.	14.0 min.			

*Normalized to 63 percent fiber volume

High strength graphite/epoxy prepreg, T300/934, was purchased for use in fabricating equipment rings. It was obtained from Fiberite Corporation as hy-E-1034E, batch C9-101. The certification test data is summarized in Table 3-4. A summary of the prepreg property test results obtained by General Dynamics is given in Table 3-2. This shows that the material met specification requirements except that it was slightly low on resin content.

A unidirectional panel was made from the T300/934 prepreg using the cure cycle previously reported in AMMRC TR78-38. Flexure and short-beam shear specimens were machined from the panel so that the length of the specimens were in the 0° direction. The specimens were tested at ambient temperature and that data, as well as cured panel resin content, fiber volume, and specific gravity are reported in Table 3-3. All data meet the requirements of ANA74700314-001B.

Table 3-4. Fiberite hy-E 1034C Certified Data

Quantity Shipped On 11/1/78	19.8 lbs
Lot No.	C9-101
Roll No.	1
Tape Size, Inches	12.0
Resin Solids, %	37.0
Volatile Content, %	0.3
Laminate Flow, % @ 50 p.s.i.	15.0
Gel Time, Minutes @ 377°C	8.4
Tack	Pass
Fiber Areal Wt. (g/m^2)	152.3
Specific Gravity —	
Tensile Strength (p.s.i.) —	
Tensile Modulus (10^6 p.s.i.) —	
Flexural Strength (p.s.i.) R.T.	274,173*
350°F	172,595*
Flexural Modulus (10^6 p.s.i.) —	
Compression Strength (p.s.i.) —	
Horizontal Beam Shear (p.s.i.) —	
Cured Ply Thickness, Inches	.005
Date of Manufacture	10/25/78
Shelf Life	6 months @ 0°F Max.
Ref: Packing List No.	011238

Fiber Data

Lot	Strength (ksi)	Modulus (msi)	Density g/cc
515-2	470	34.2	1.77
516-2	455	33.9	1.75
567-27	457.9	34.4	1.75
570-2	465	33.9	1.75

*Normalized to 63% fiber volume

I.R. scan attached

3.1.2 TITANIUM. The material used for equipment rings was Ti-6Al-4V obtained as an 8-inch billet from Timet. The properties of the billet are shown in Figure 3-1. This alloy was chosen because of its high strength and on experience obtained in using it for reinforcing the joint specimens.

3.1.3 GRAPHITE. The material used for equipment rings was a fine-grain isotropic graphite from Electro-Nite (E-216). The material properties are shown in Figure 3-2. Because the material is low cost and machines easily, it was an attractive candidate.

3.2 FURNISHED MATERIALS (FRUSTA)

Eight half-scale reinforced joint specimens per Drawing 48126 (Figure 3-3) were furnished by AMMRC. These specimens had been fabricated by General Dynamics under Contract DAAG46-76-C-0008. There were two specimens of Design 1, three of Design 2, and three of Design 3. The remaining four specimens of Design 1 had been previously tested by Martin-Marietta under Contract DAAG46-75-C-0097. The test results are given in Report AMMRC TR 78-4 (Reference 1).

3.3 FRUSTA AND EQUIPMENT RING FABRICATION PROCEDURES

3.3.1 LARGE-SCALE FRUSTA. Two additional large-scale frusta containing wedge-type equipment rings, similar to the one fabricated as part of the supplemental effort on Contract DAAG46-76-C-0008, were fabricated as part of this program. The materials for these frusta and the fabrication and installation of the equipment rings are discussed in the following paragraphs.

Two 13.4-inch-long conical frusta were prepared from hy-E-1534 (GY-70/934) prepreg using batch C9-086 material. The cone size selected was influenced by the availability of an existing bulk-graphite female tool used previously (Reference 3).

The frusta layup was the same as that used in the earlier cones, i.e., $[0_2/45/90/-45/90/45/0_3/-45/0_3/45/0_2/-45/0]_s$. Figure 3-4 shows the bulk-graphite tool used for the fabrication of the 13.4-inch-long frusta. Only the conical section of the tool was used when laying up the prepreg. The cone angle for the bulk graphite tool is 4.67 degrees, whereas the cone angle for the ATI guidance and control section is 6.27 degrees. This difference in cone angles was not considered significant in evaluating the bulkhead ring and the resulting cone-ring joint.

The layup technique, ply orientations, segment wrap angle, and ply starting point were all identical to those used on the earlier cones (Reference 3). The theoretical segment dimensions were calculated, and gore dimensions are given in Figure 3-5. Plastic templates were prepared for use in cutting prepreg gores, and these were then trimmed, as required, for subsequent plies. Layup procedure, debulking, and curing of these 13.4-inch-long frusta was identical to that used in the preparation of the first large-scale frustum.

Thickness measurements were made of the completed frusta. The value ranged from 0.170 to 0.187 inch with an average of 0.180 inch. This means that the cured ply thickness is approximately 0.0047 inch. The previous large-scale frustum (Reference 3) had a ply thickness of 0.0055 inch and the earlier half size frusta had a ply thickness of 0.0052 inch. The anticipated thickness of the large-scale frusta according to the specification was 0.171 to 0.190 inches. The previous thicker frusta and resulting thicker ply dimensions may be attributed to the use of aged material.

Titanium Metals Corporation of America

CERTIFICATE OF TEST

CHEMICAL ANALYSIS

HEAT NO.	C	Fe	N	Al	Va	Cr	Mo	H	Zr	Sn	Mn	O_2
P4757	.011	.17	.007	6.4	4.2			.006				.17

YTTRIUM LESS THAN 50 PPM

MECHANICAL PROPERTIES

HEAT NO.	TEST NO.	SIZE OR GAUGE	YIELD STRENGTH	TENSILE STRENGTH	ELONG	R A %	HARDNESS	BEND TEST
			KSI	KSI	%			BETA TRANSUS
P4757			138	152	19	47		1825°F.
			139	152	18	45		1830°F.

MACRO & MICROSTRUCTURE EXAMINED AND ACCEPTABLE

AIR COOL ANNEALED FROM FINAL FORGING TEMPERATURE

SUBSCRIBED AND SWORN TO BEFORE ME

THIS DATE 1/3/79

RESULTS AS ABOVE CERTIFIED
TITANIUM METALS CORPORATION OF AMERICA

P. Connell

653219-1

Figure 3-1. Ti-6Al-4V Certificate of Test

Electro-Nite Co.
West Coast Division: P.O. Box 1208, Long Beach, Calif. 90801
2000 Gaylord Street, Long Beach, Calif. 90813 213—436-9281

Summary of Typical Properties of Gr. E216 Graphite

Chemical Composition - 99.85% Carbon		0.15% Ash	
Physical Properties			
	Apparent Density	1.77 gm/cc	
	Real Density	2.14 gm/cc	
	Porosity	17.0%	
	Average Pore Size	1.5 microns	
	N_2 Permeability	2.9 millidarcys	
	H_2O Permeability	0.04 millidarcys	
	Maximum Grain Size	.0017 inches	
Mechanicals Properties		With Grain	Against Grain
	Hardness	50	50
	Flexural Strength (PSI)	5500	4800
	Compressive Strength (PSI)	13,000	9500
	Tensile Strength (PSI)	4000	3900
	Modulus of Elasticity (in tension)	1.34	1.31
	x 10^6 PSI (in compression)	1.16	1.10
Thermal Properties			
	CTE (Room Temp. to 600°C;/°C x 10^{-6})	3.2	3.8
	Thermal Conductivity at 200°F (cal/cm. sec. °C)	0.15	0.15
Electrical Properties			
	Specific Resistance (ohm/in.)	.0007	.0007
Maximum Sizes Available		Approximate Weight (Pounds)	
	10" Dia. x 72"	357	
	13" Dia. x 72"	690	
	15" Dia. x 72"	1024	
	19" Dia. x 72"	1377	
	13" x 13" x 72"	844	
	6" x 18" x 72"	690	
	9" x 16" x 72"	885	
	11" x 26" x 65"	1188	

653219-2

Figure 3-2. Summary of Typical Properties of E-216 Graphite

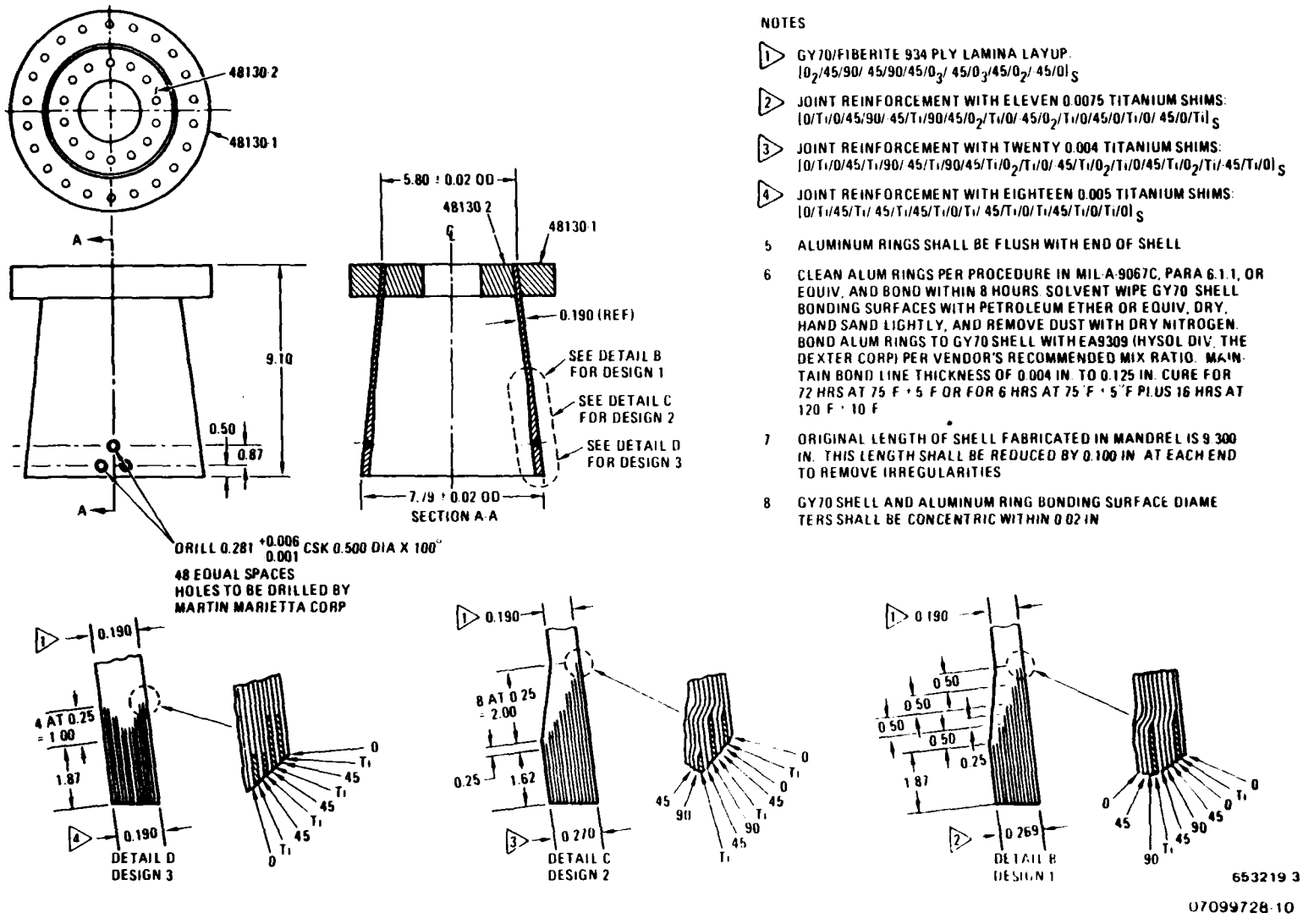

NOTES

1. GY70/FIBERITE 934 PLY LAMINA LAYUP: $[0_2/45/90/\ 45/90/45/0_3/\ 45/0_3/45/0_2/\ 45/0]_S$
2. JOINT REINFORCEMENT WITH ELEVEN 0.0075 TITANIUM SHIMS: $[0/T_i/0/45/90/\ 45/T_i/90/45/0_2/T_i/0/\ 45/0_2/T_i/0/45/0/T_i/0/\ 45/0/T_i]_S$
3. JOINT REINFORCEMENT WITH TWENTY 0.004 TITANIUM SHIMS: $[0/T_i/0/45/T_i/90/\ 45/T_i/90/45/T_i/0_2/T_i/0/\ 45/T_i/0_2/T_i/0/45/T_i/0_2/T_i/-45/T_i/0]_S$
4. JOINT REINFORCEMENT WITH EIGHTEEN 0.005 TITANIUM SHIMS: $[0/T_i/45/T_i/\ 45/T_i/45/T_i/0/T_i/\ 45/T_i/0/T_i/45/T_i/0/T_i/0]_S$
5. ALUMINUM RINGS SHALL BE FLUSH WITH END OF SHELL
6. CLEAN ALUM RINGS PER PROCEDURE IN MIL-A-9067C, PARA 6.1.1, OR EQUIV, AND BOND WITHIN 8 HOURS. SOLVENT WIPE GY70 SHELL BONDING SURFACES WITH PETROLEUM ETHER OR EQUIV, DRY, HAND SAND LIGHTLY, AND REMOVE DUST WITH DRY NITROGEN. BOND ALUM RINGS TO GY70 SHELL WITH EA9309 (HYSOL DIV, THE DEXTER CORP) PER VENDOR'S RECOMMENDED MIX RATIO. MAINTAIN BOND LINE THICKNESS OF 0.004 IN. TO 0.125 IN. CURE FOR 72 HRS AT 75 F ± 5 F OR FOR 6 HRS AT 75 F ± 5 F PLUS 16 HRS AT 120 F ± 10 F
7. ORIGINAL LENGTH OF SHELL FABRICATED IN MANDREL IS 9.300 IN. THIS LENGTH SHALL BE REDUCED BY 0.100 IN. AT EACH END TO REMOVE IRREGULARITIES
8. GY70 SHELL AND ALUMINUM RING BONDING SURFACE DIAMETERS SHALL BE CONCENTRIC WITHIN 0.02 IN

Figure 3-3. Joint Design Specimens (Reference 1)

653219.4
CV098379

Figure 3-4. Graphite Mold

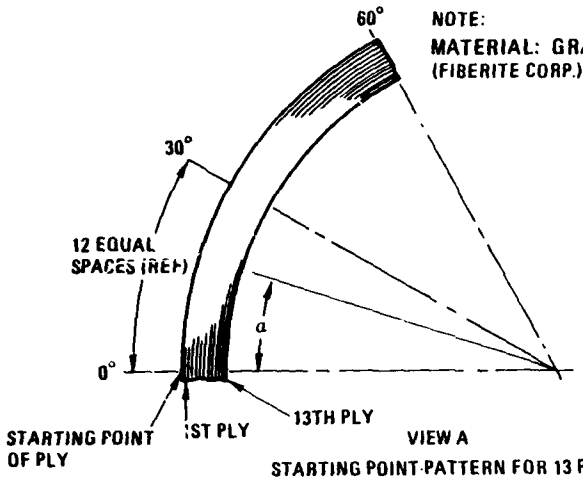

NOTE:
MATERIAL: GRAPHITE/EPOXY, GY 70/934
(FIBERITE CORP.)

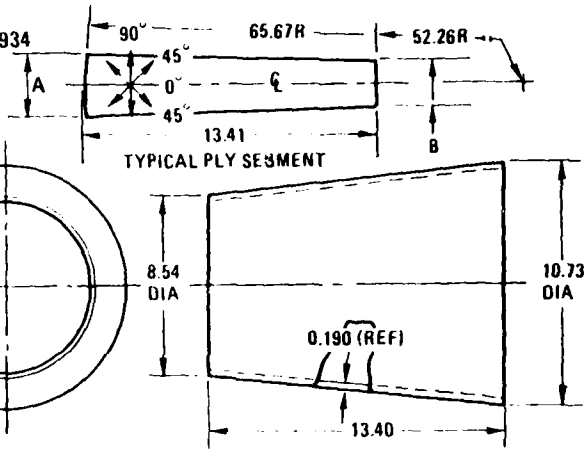

STARTING POINT PATTERN FOR 13 PLIES
PATTERN REPEATS AT 14TH & 27TH PLIES

	PLY NO.	THEORETICAL SEGMENT DIM. A	B	ORIENTATION OF PLY	a	SEGMT WRAP ANGLE	PLY NO.	THEORETICAL SEGMENT DIM. A	B	ORIENTATION OF PLY	a	SEGMT WRAP ANGLE	
	1	2.777	2.210	0"	0° 0'	30"	20	2.682	2.115	0"	20"45'	30"	
	2	2.772	2.205	0"	18"30'	30"	Δ 21	8.031	6.330	-45"	9"15'	90"	
	3	8.301	6.600	+45"	7"0'	90"	22	2.572	2.105	0"	27"45'	30"	
	4	8.286	6.585	90"	25"30'	90"	23	2.567	2.100	0"	16"15'	30"	
	5	8.271	6.570	-45"	13"45'	90"	Δ 24	7.686	6.285	+45"	4"30'	90"	
	6	8.256	6.555	90"	2"15'	90"	25	2.557	2.090	0"	23"0'	30	
	7	8.241	6.540	+45"	20"45'	90"	26	2.552	2.085	0"	11"30'	30"	
	8	2.742	2.175	0"	9"15'	30"	27	2.547	2.085	0"	0"0'	30"	
	9	2.737	2.170	0"	27"45'	30"	Δ 28	7.626	6.240	-45"	18"30'	90"	
PRE-PLY	10	2.732	2.165	0"	16"15'	30"	29	2.537	2.075	0"	7"0'	30"	PRE-PLY
	Δ11	8.181	6.480	-45"	4"30'	90"	30	2.532	2.070	0"	25"30'	30"	
	12	2.722	2.155	0"	23"0'	30"	31	2.527	2.065	0"	13"45'	30"	
	13	2.717	2.150	0"	11"30'	30"	32	7.566	6.180	+45"	2"15'	90"	
	14	2.712	2.145	0"	0"0'	30"	33	7.551	6.165	90"	20"45'	90"	
	Δ15	8.115	6.420	+45"	18"30'	90"	34	7.536	6.150	-45"	9"15'	90"	
	16	2.702	2.135	0"	7"0'	30"	35	7.521	6.135	90"	27"45'	90"	
	17	2.697	2.130	0"	25"30'	30"	36	7.506	6.120	+45"	16"15'	90"	
PRE-BLEED TO 0.103 THICKNESS	Δ18	8.076	6.375	-45"	13"45'	90"	37	2.497	2.035	0"	4"30'	30"	
	19	2.687	2.120	0"	2"15'	30"	38	2.492	2.030	0"	23"0'	30"	FINAL CURE

Δ ADD 0.25 TO A & B DIMS TO PROVIDE 0.25 OVERLAP OF SEGMENTS

653219 5

Figure 3-5. Large Scale Frustum

3.3.2 EQUIPMENT RINGS. Three types of equipment rings from three different materials were tested as part of this study. These included a titanium ring, a bulk-graphite ring, and a graphite/epoxy composite ring. A metal ring has the advantage of being strong, being machinable, and being able to provide a base for attachments. Titanium was chosen because its coefficient of thermal expansion (CTE) is a good match to that of the graphite/epoxy frusta. If there were no change in temperature during manufacture or flight, an aluminum ring (with a CTE twice of that of Ti) might well be chosen since thermal stresses would not be a consideration.

Bulk graphite was picked as a candidate ring since it has a low CTE and is inexpensive. Bulk-graphite parts can be easily fabricated. However, the material itself is somewhat brittle.

3.3.2.1 Graphite/Epoxy Equipment Rings. The design of these rings was basically the same as the previous ring (Reference 2). The concept was to make a ring that has a near zero coefficient of thermal expansion to minimize thermal stresses. The design of the rings is shown in Figure 3-6. The material used was a high strength graphite/epoxy — T300/934. This was chosen because the fiber has high-strength and the resin is the same as that used in the frusta. The ring is designed by strength and thermal characteristics rather than stiffness. A pseudoisotropic layup was used to reduce the CTE to approximately zero.

The layup of the rings was made using the female graphite tool shown in Figure 3-7. Modules of $(0/45/-45/90)_s$ material were placed into the tool in a stepwise fashion, using 0.25-inch steps to give a total of $[0/45/-45/90)_s]_{18}$. An additional overlay resulted in a total of 152 plies. Each ply consisted of six gore sections. The longitudinal butt joints were offset approximately 1.0 inch for each succeeding module. Five precompactions were conducted during the processing. These consisted of vacuum bagging, heating to 150F, applying 50 psig autoclave pressure, and holding 15 minutes at temperature. The bleeder used for each precompaction cycle was one ply of Style 181 fabric and two plies of Style 1534 glass fabric.

The bleeder for the final cure was three plies of Style 7781 glass fabric. The part was vacuum bagged and held in an autoclave under full vacuum at room temperature for a minimum of 30 minutes. The part temperature was raised to 250 $\pm$10F at 2 to 4F/minute and held at temperature for 45 $\pm$5 minutes. Autoclave pressure of 100 $\pm$5 psig was applied and the part was maintained at 250 $\pm$10F for an additional 45 $\pm$5 minutes. The part temperature was raised at 2 to 4F/minute to 350 $\pm$10F and held for a minimum of two hours at temperature. The part was cooled under vacuum and pressure to below 175F and then debagged.

The ring was trimmed to a 3.0-inch length so that the top face was approximately 0.2-inch wide. The facings of the ring and cone were flat and parallel to 0.002-inch TIR (total indicated reading). Thirty-two MS124816 (0.25 inch — 28 thread) helicoils were installed around the bottom face of the ring.

3.3.2.2 Titanium Equipment Ring. The titanium ring was designed to make a shelf for attachment of equipment. A drawing of the cross section is shown in Figure 3-8. The upstanding legs (the bonded surface) were tapered to reduce the stress concentration at the end of the bonded surface. The parts were machined on a lathe using standard machine shop practices. This included use of high-speed steel tools and coolant to ensure proper cutting action.

3.3.2.3 Graphite Equipment Ring. Because graphite is a rather weak material, the concept for this ring was different from that of the metal ring. The design selected is shown in Figure 3-8. This uses a large cross section that could cause a stress concentration in the frusta wall. The ring was simply machined on a lathe with standard tools. It was machined dry (i.e., no coolant) and a vacuum cleaner was used at the tool post to collect the dust.

3.4 ASSEMBLY

3.4.1 BONDING EQUIPMENT RINGS. A total of six equipment rings were bonded into frusta during this program. The procedure was always the same. The rings were bonded into each frusta using Hysol EA934 modified epoxy adhesive with a ambient temperature cure. Each ring was held at the correct position by blocks on a surface table. The frusta were inverted and placed over their respective rings during bonding. To further control the bond-line thickness to 0.005 inch, wire shims were inserted into the space. Bondlines were allowed to cure for 72 hours prior to frusta testing.

3.4.2 FINAL FABRICATION. The joint-test specimen had two sets of holes in the specimen. The attachment at the small end was by bolts through the aluminum rings. These holes were drilled by conventional techniques. The tool used for locating the holes was made for a prior program by Martin-Marietta (Reference 1).

The holes at the base joint were drilled according to Drawing 48126 (Figure 3-1). This involved drilling through graphite/epoxy composite interleaved with titanium foils. To do this, an aluminum plug was first machined that just fit into the joint area. This was shimmed with tooling compound that provided the support necessary to do the actual drilling and prevented breakout at the backface. The drilling was done on a milling machine using a rotary indexing fixture. Conventional high-speed steel drills and countersink tools were used.

The frusta with equipment rings were fitted with end plates to prevent brooming of the graphite/epoxy during test. Aluminum plates with slots were used for this support. The frusta were potted into place with EA934 and cured at ambient temperature.

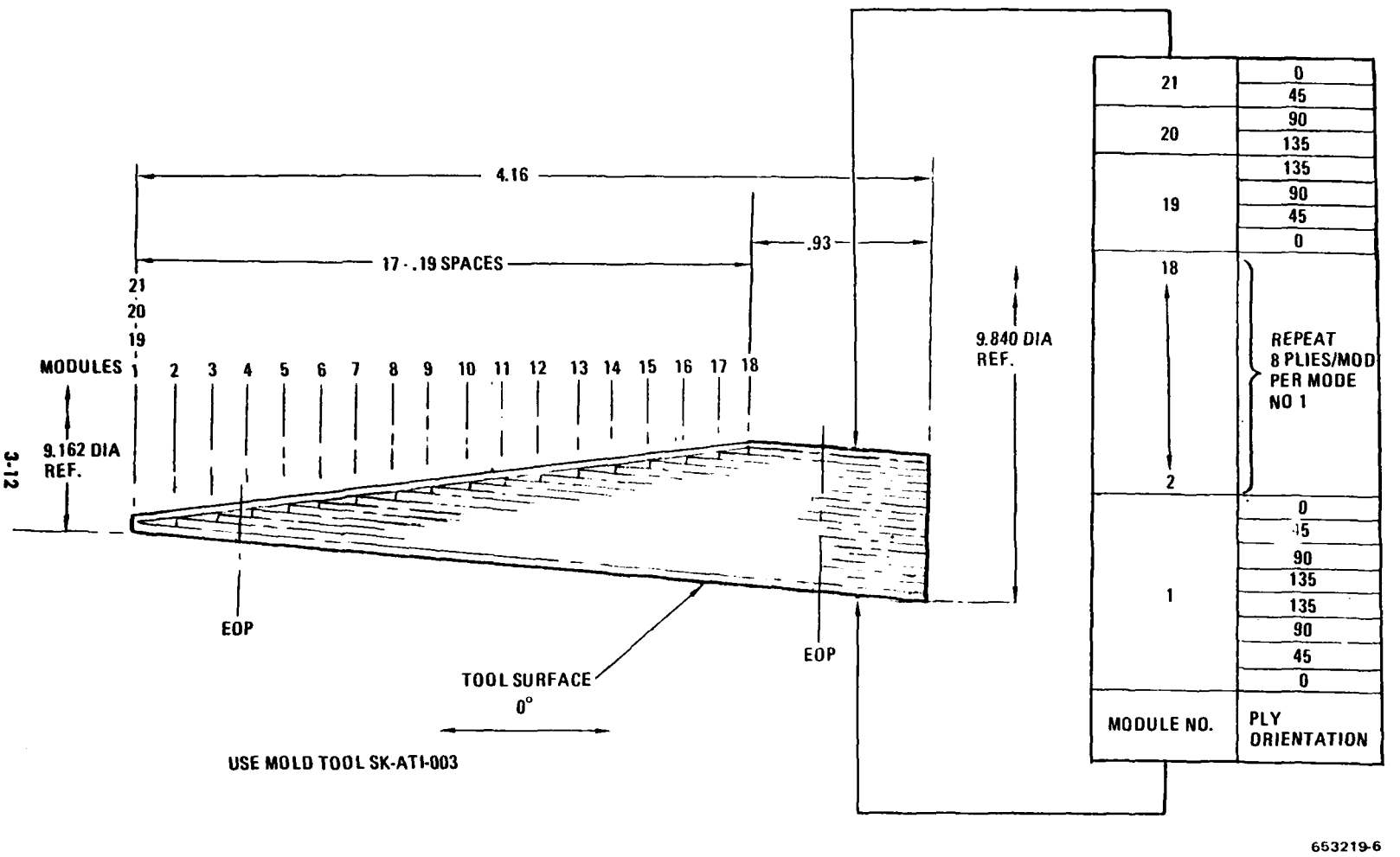

Figure 3-6. Graphite/Epoxy Equipment Ring Design

653219-7
CV119533

Figure 3-7. Female Graphite Tool for Equipment Ring

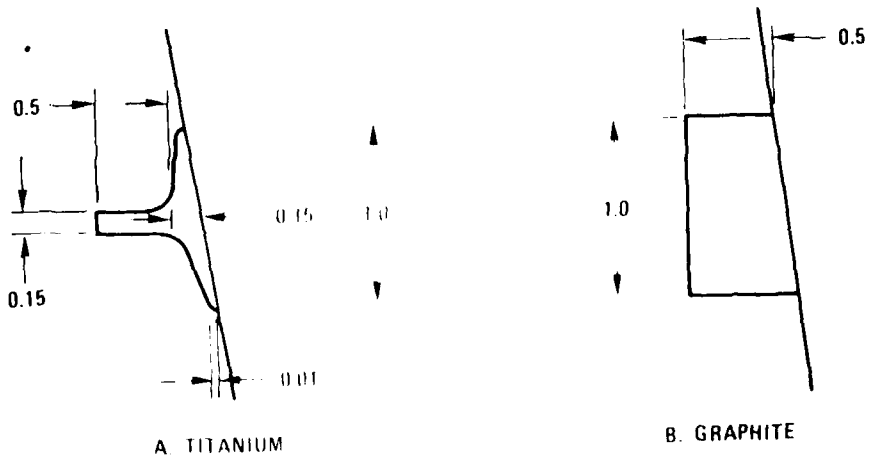

A. TITANIUM

B. GRAPHITE

653219-8

Figure 3-8. Cross Section of Equipment Rings

SECTION 4

TESTING

4.1 STATIC JOINT SPECIMENS

Under DAAG46-76-C-0008, four half-scale joint reinforcement specimens (Figure 3-1) were fabricated (Reference 2) and then tested (Reference 1). These tests were all of joint design 1. In this program, the other two joint concepts were evaluated so that a comparison could be made. The tests were run according to the test plan given in Appendix A.

Each of the four half-scale frusta to be tested were instrumented with 16 single-element strain gages as shown in Figure 4-1. These were BLH gages designated FAE-25-12-SO. The gages were bonded to the frusta with Eastman 910 cyanoacrylate adhesive. A three-wire system was used to connect the gages to the strain readout system. Figure 4-2 shows one frustum ready for installation in the test fixture. Each joint specimen was attached to the end fixture with 48 NAS1154-25 bolts.

4.1.1 COMBINED LOAD TESTS. One frustum each of joint designs 2 and 3 were tested with a combination of loads. As in the previous tests (Reference 1), the design limit loads are defined as:

P (axial compression) = 19,000 lb

V (shear at joint end) = 12,000 lb

M (moment at the joint end) = 158,000 in-lb

A schematic of the test setup is shown as Figure 4-3. Figure 4-4 shows a closeup of the test fixture, while Figure 4-5 shows the overall test setup. After the fixtures were attached, the instrumentation was calibrated and set to zero.

The load on each of the five actuators was increased simultaneously. This is accomplished by using a pressure valving system. The hydraulic pressure creating the loading is stopped at increments while all the loads, strains, and deflections are read and recorded. Increments of 20 percent of the design limit loads (DLL) were used until 100 percent DLL was reached, and then further loading at 10 percent increments were used until failure occurred. A typical printout of this is shown as Figure 4-6. A summary of the test results is given as Table 4-1.

Test C1 was a joint specimen of design 3. There is some evidence that the specimen failed by buckling of the shell at 150 percent of DLL. This can be seen by examining the behavior of gage No. 12 in Figure 4-7. (All of the load-strain and load-deflection curves are included in Appendix B.) This gage shows reversal while gage No. 11, which was on the opposite side of the wall, increased rapidly. Note that failure occurred at a maximum strain of approximately 2000$\mu\epsilon$. This will be noted in other tests. While it was not possible to identify the origin of the failure, we note that the joint did not fail. The failure occurred at the end of the titanium reinforcement. It almost appeared that the frustum was sheared off at that point. Test C3 of joint

Table 4-1. Summary of Base Joint Tests on Half-Scale Frusta**

Cone No.	Joint* Design	Test No.	Type of Test	Results	Failure Mode
7	3	I	Shock	33,000g at 7 kHz	No failure
8	3	C1	Static Combined	150% DLL	Shear at end of Ti foils
9	3	C2	Static Shear/Bending	22,000 lb (133% of Moment)	Shear at end of Ti foils
10	2	II	Shock	40,000g at 7 kHz	No failure
11R	2	C4	Static Shear/Bending	35,000 lb (212% of Moment)	Tensile at forward ring
12	2	C3	Static Combined	189% DLL	45° shear failure

*Per drawing 48126 (Figure 3-1)

**Shock spectra for Cones 7 and 10 are given in Appendix C. Stress-strain curves for Cones 8, 9, 11R and 12 are given in Appendix B.

design 2 showed that failure again occurred when the maximum strain reached approximately 2000$\mu\epsilon$. The failure of this specimen (Figure 4-8) did not appear to be associated with either end. The failure appears to be a 45° shear.

4.1.2 SHEAR/BENDING TESTS. One frustum each of joint designs 2 and 3 were tested with a load applied at the end of the frusta — this produces shear and bending. A schematic of the test setup is shown as Figure 4-9 and the set up is shown in Figure 4-10. The hydraulic actuator used for this test was loaded incrementally. Load, strain, and deflections were read at each increment. Increments of 2000 lb were used to 20,000 lb, and then 1000-lb increments were used until failure occurred. The test results are included in Table 1.

Test C2 was a specimen of joint design 3. This specimen failed the shell exactly at the end of the titanium foils (Figure 4-11). The joint did not appear to be the primary position of failure. This failure is strong evidence of a stress concentration at the end of the titanium foils.

Test C4 of a specimen containing joint design 2 appeared to fail at the forward ring. The failure may have been caused by the load ring.

4.1.3 RESULTS. The loads from these four joint specimens is summarized in Table 4-1. These data were then plotted (Figure 4-12) on the same axial load-moment interaction curve used by Martin-Marietta (Reference 1) to describe the results of their basic frusta and joint specimen tests. Figure 4-12 simply measures the axial behavior of the frusta. One very important feature noted from this curve is that the reinforced joint specimens fit the same data population as the simple frusta specimens. This simply means that the failures of the frusta were all associated with the shell and not the joint. Put another way, the joint is stronger than the shell. It is important to use this fact in our later design of the full scale frusta.

A more meaningful data plot is the axial stress versus shear stress plot shown in Figure 4-13. This curve clearly shows that specimens No. 2 and C2 do not fit with the remaining data. It also shows that these failures are not shear-type failures. Data from tests C4 and 4A are 60 percent higher than the data from tests No. 2 and C2. Also, three other tests reached slightly higher shear stresses. The failure of specimen C2 strongly suggests that a stress concentration exists at the abrupt ending of the titanium foil. While the design limit load was exceeded, the stress concentration did not allow the frustum to reach its full potential.

The data in Figure 4-13 suggest that all the failures are dominated by the axial stress (i.e., the axial line load). The average axial stress is 42 ksi with a standard deviation of 5.7 and a coefficient of variation of 13.4 percent. This coefficient of variation is in line with General Dynamics previous experience with GY-70 systems.

Data obtained at General Dynamics Convair Division under Contract AF 33615-77C-5679 (Reference 4) showed that the shear strength of a (0/45/90/135) layup of GY70/X30 was 14 ksi. This means that we should have expected a shear strength of the ATI material of approximately 10-11 ksi. We exceeded that for tests 4A and C4. Examination of the failed C4 specimen indicates that a possible failure mode was shear, followed by redistribution of stress and then a secondary tensile failure.

No discontinuities are apparent in the deflection readings. This indicates that the bolts held the frusta secure with no slop at the joints. This is important to the vehicle because it will not segment or move as a series of rigid bodies.

4.2 SHOCK TESTS

Two reinforced joint specimens (one each of design 2 and 3, Figure 3-1) were loaded in conditions simulating the second stage ignition shock. Each test specimen was bolted to the test fixture through the 48 countersunk holes that make the base joint. An equipment ring had been installed in each frusta to test that joint as well as the base joint.

The PYRO technic shock machine generates a high-intensity shock spectra. The shock spectra are generated by a steel plate when excited by impact with a fixed mass and velocity. By varying the terminal velocity of the fixed mass, the intensity of the shock spectrum can be varied with a high degree of accuracy and repeatability. The impact energy is induced by using the HYGE shock machine Pneumatic RAM System.

A schematic of the shock machine and the recording system is shown by Figure 4-14 and a photograph of the setup is shown by Figure 4-15.

The test results were included in Table 4-1. A typical shock spectrum is shown as Figure 4-16. This closely simulates the spectrum used previously (Reference 1). The remaining spectrum are given in Appendix C.

Twelve axial strain gages were installed on each frustum before the start of testing. The strain data from the tests on Frustum No. 7 are given in Table 4-2. These are very low and do not approach the limiting strain of 2000$\mu\epsilon$. It is obvious, then, that we should not expect any damage to the frusta, and even at the maximum shock levels no damage was observed.

Table 4-2. Maximum Peak Strains ($\mu\epsilon$) During Shock Testing of Half-Scale Frusta

No. Gage	Run 1	Run 2	Run 3	Run 4	Run 5	Run 6	Run 7	Run 8
1	—	—	—	—	—	—	—	—
2	+50	+50	+75	+90	+150	+180	+240	+200
	−60	−90	−70	−100	−350	−360	−300	−100
3	+80	+100	+120	+150	+350	+320	+250	
	−90	−120	−150	−120	−190	−250	−300	−250
4	+50	+50	+60	+70	+90	+160	+140	+180
	−60	−65	−90	−80	−120	−180	−170	−180
5	+50	+80	+90	+100	+130	+200	+180	+160
	−90	−120	−85	−40	−80	−100	−200	−180
6	+60	+30	+90	+125	+210	+140	+200	+180
	−40	−60	−90	−110	−150	−180	−250	−110
7	—	+60	+90	+50	+120	+160	+100	+200
		−80	−60	−65	−100	−100	−200	−100
8	—	—	—	—	—	—	—	—
9	—	—	—	—	—	—	—	—
10	—	+60	+100	+160	+210	+270	+400	+350
		−50	−60	−100	−120	−160	−150	−160
11	+100	+50	+80	+200	+300	+310	+300	+280
	−50	−90	−100	−180	−210	−320	−320	−200
12	+30	+35	+35	+90	+110	+120	+60	+90
	−30	−30	−40	−45	−80	−60	−40	−50

4.3 EQUIPMENT RING TESTS

4.3.1 STATIC TESTS OF HALF-SCALE FRUSTA. The two remaining joint specimens were fitted with equipment rings, one with a titanium and one with a bulk-graphite ring. These tests were designed to determine what ring concepts would meet the design load conditions. Each frustum had ten strain gages bonded to it in the positions shown in Figure 4-17. BLH FAE-06-12S0 gages were used for this application. An elevated-temperature adhesive (Micromeasurements M Bond 600) was used. The test setup is shown schematically in Figure 4-18. One actual setup is shown in Figure 4-19. Each frustum and ring were tested to the loads given in Table 4-3. The elevated temperature tests were conducted in a universal test machine fitted with a Missimer's environmental chamber.

All of the data for the equipment-ring tests are given in Table 4-4. The titanium equipment ring met all of the loading conditions. Failure occurred in the innermost ply of the graphite/epoxy frustum (See figure 4-20). This could have been a shear failure in the graphite/epoxy or a normal stress failure in the through-the-thickness direction of the graphite/epoxy. It is significant

Table 4-3. Static Test Sequence for Cones with Equipment Rings (Half Scale)

Test Number	Temperature	Loading	Design Limit Load (DLL) (lb)
1	Ambient	Cone and Equipment Ring	P_F = 72,200 P_R = 7,010
2	Ambient	Equipment Ring	P_R = 7,010
3	Elevated	Equipment Ring	P_e = 5,668
4	Ambient	Equipment Ring	To Failure

Table 4-4. Summary of Equipment Ring Tests

Cone	Size of Frustum	Equipment Ring Material	Results	Failure
5	Half Scale	Titanium	Met all conditions — broke at 27,000 lbs	Pulled first layer of graphite/epoxy from frustum wall
6	Half Scale	Graphite	Met ambient loads — failed at 325F	Failure of the graphite at 78% of DLL
LS-3	Larger Size	Graphite/Epoxy	Failed frustum at 98% of requirements	Crippling failure of frustum
LS-2	Larger Size	Graphite/Epoxy	Met all conditions* — broke at 69,700 lbs	Pulled out helicoils

*The loads for test 1 (Table 4-5) were reduced by 50% to prevent crippling.

that the DLL were exceeded by a factor of four. The drawback to the titanium ring design is that a thermal stress is generated as the temperature of the frustum is changed.

The bulk-graphite equipment ring met the ambient-load conditions but the graphite failed at 78% of DLL during the elevated-temperature test. It was initially chosen as a candidate to minimize thermal stress caused by exit heating. Because it failed at the elevated-temperature, the bulk-graphite ring was eliminated from consideration for the final design.

4.3.2 STATIC TEST OF LARGE SCALE FRUSTA. Two large frusta (13.4 in. high) were fabricated and fitted with wedge-shaped graphite/epoxy equipment rings as discussed in Section 3.3.3. These equipment rings were very close to full size, but the frusta were only 0.19-inch thick rather than the 0.38-inch thick for the full-scale frusta. A frustum with a graphite/epoxy ring, tested previously under DAAG46-76-C-0008, was 10 inches high.

The schematic of the test setup is the same as in Figure 4-18. The loads were the same as for the previous large size frustum (Reference 3) and are given in Table 4-5. Reanalysis (see Section 5) suggests that these test loads were too low. However, the failure load obtained in Test No. 4 shows that the frusta can adequately meet the reanalyzed design requirements.

Table 4-5. Static Test Sequence for Large-Scale Frusta with Equipment Rings (Large Size)

Test Number	Temperature	Loading	Design Limit Loads (DLL) (lb)
1	Ambient	Cone and Equipment Ring	P_F = 129,500 P_R = 12,600
2	Ambient	Equipment Ring	P_R = 12,600
3	Elevated	Equipment Ring	P_e = 10,080
4	Ambient	Equipment Ring	To Failure

Specimen LS-2 was tested to the first set of loads, test No. 1 in Table 4-5, when the ring-to-shell bond failed at a very low load. Examination of the failure showed that the adhesive had not adhered to the ring surface. It was found that this ring was the first part from a new tool and had picked up release agent. The surface of the ring was ground to clean off the contamination and rebonded into the frustum. In this series of tests, the frustum and ring were first loaded to 64,750 lb shell load and 6,300 lb on the equipment ring. The ring was then loaded to 12,600 lb at ambient temperature and then 10,080 lb at 325F. This latter test was conducted with the frustum in a Missimer's test chamber. The ring was then tested to failure at ambient temperature. Failure occurred at 69,700 lb when the helicoils pulled out.

Specimen LS-3 was tested at ambient temperature. This frustum reached 98 percent of the DLL when failure occurred. The failure mode was crippling of the shell wall (Figure 4-21). The readings of the strain gages near the ring indicated high reversal loads (Figure 4-22).

There is no previous data available on the crippling of these materials. The only method of obtaining this data is by experiment. It was not possible to predict crippling, but it is possible to predict buckling. From these recent tests, we now have the outline of the crippling curve (see Figure 4-23).

Work reported on a similar material (GY70/HM-S/X904 [Reference 5]) has a crippling curve that is very similar to that plotted in Figure 4-23. This lends credibility to the frusta test results obtained in this program.

It is important to note that the r/t ratio of the full-scale vehicle at its design limit loads is well away from the crippling limit as well as considerably below the strength limit.

4.4 STIFFNESS DATA

The critical design parameter for the ATI frusta is their required natural frequency. This is controlled by the modulus of elasticity (E) of the material and the section modulus (I). In an

attempt to measure this, the modulus of elasticity of the frusta were obtained by analysis of the preceding test data. These values are shown in Table 4-6. The values for the large frusta are very close to that expected. The two small frusta gave high values and the values were checked by rerunning the tests when only load was applied to the frusta and not to the equipment rings. These values are in line with the expected value of 26.5×10^6 psi. Examination of the test data from Tests 1 and 6 from Reference 1 show that the initial modulus (up to DLL) was in the 25 to 26×10^6 psi range. All of these data show good correlation between predicted and measured values.

Table 4-6. Modulus of Elasticity for G/E Frusta

Frustum Identification	Size	Load (lbs)	Strain ($\mu\epsilon$)	Area (in^2)	Modulus of Elasticity (msi)
LS-1	Larger	129,500	925	6.060	23.1
LS-3	Larger	64,750	500	5.004	25.9
Joint No. 6	Half Size	72,200	637	3.920	28.9
Joint No. 5	Half Size	72,200	657	3.920	28.0
Retest Joint No. 6	Half Size	25,000	236	3.920	27.0
Retest Joint No. 5	Half Size	25,000	239	3.920	26.6

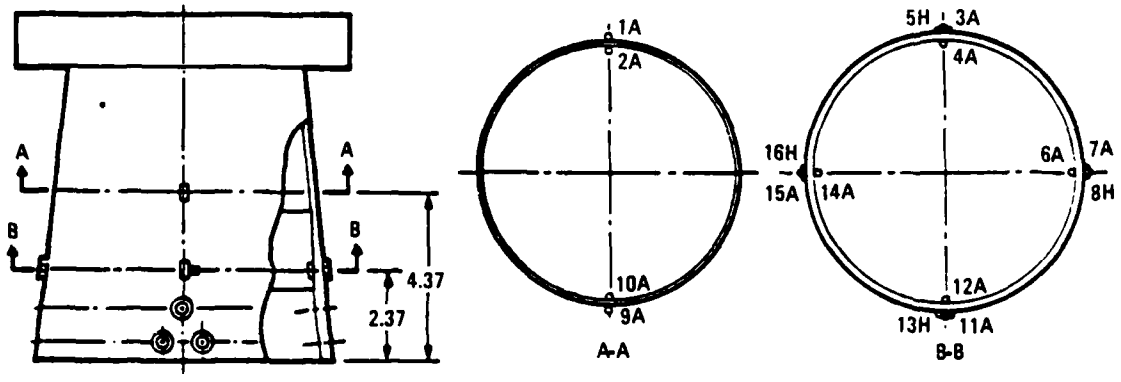

Figure 4-1. Strain Gage Location — Static Tests

653219-10
CV019732

Figure 4-2. Joint Test Specimen Ready for Test

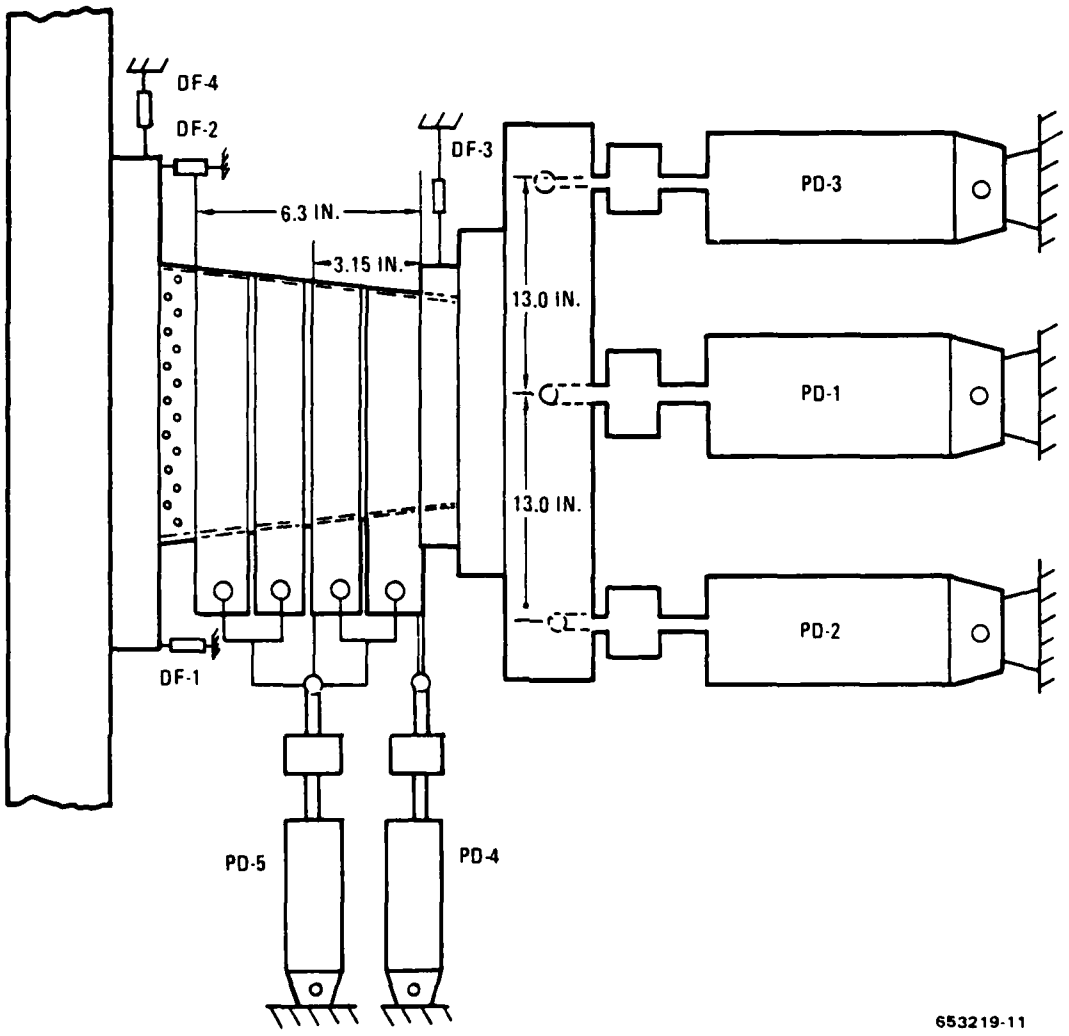

Figure 4-3. Combined Axial, Compression, and Shear Bending Test Configuration

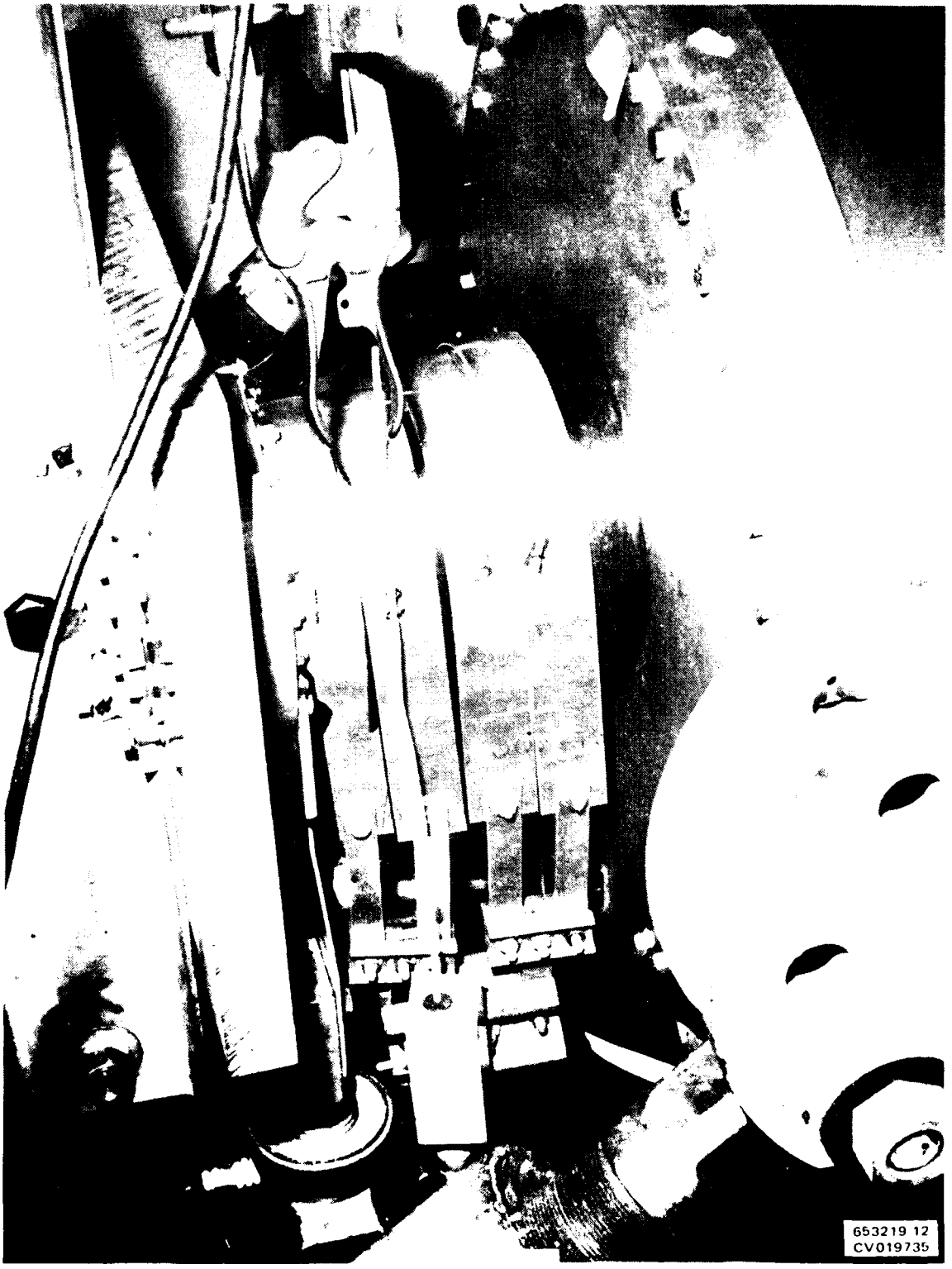

Figure 4-4. Combined Load Test (Closeup of Cone)

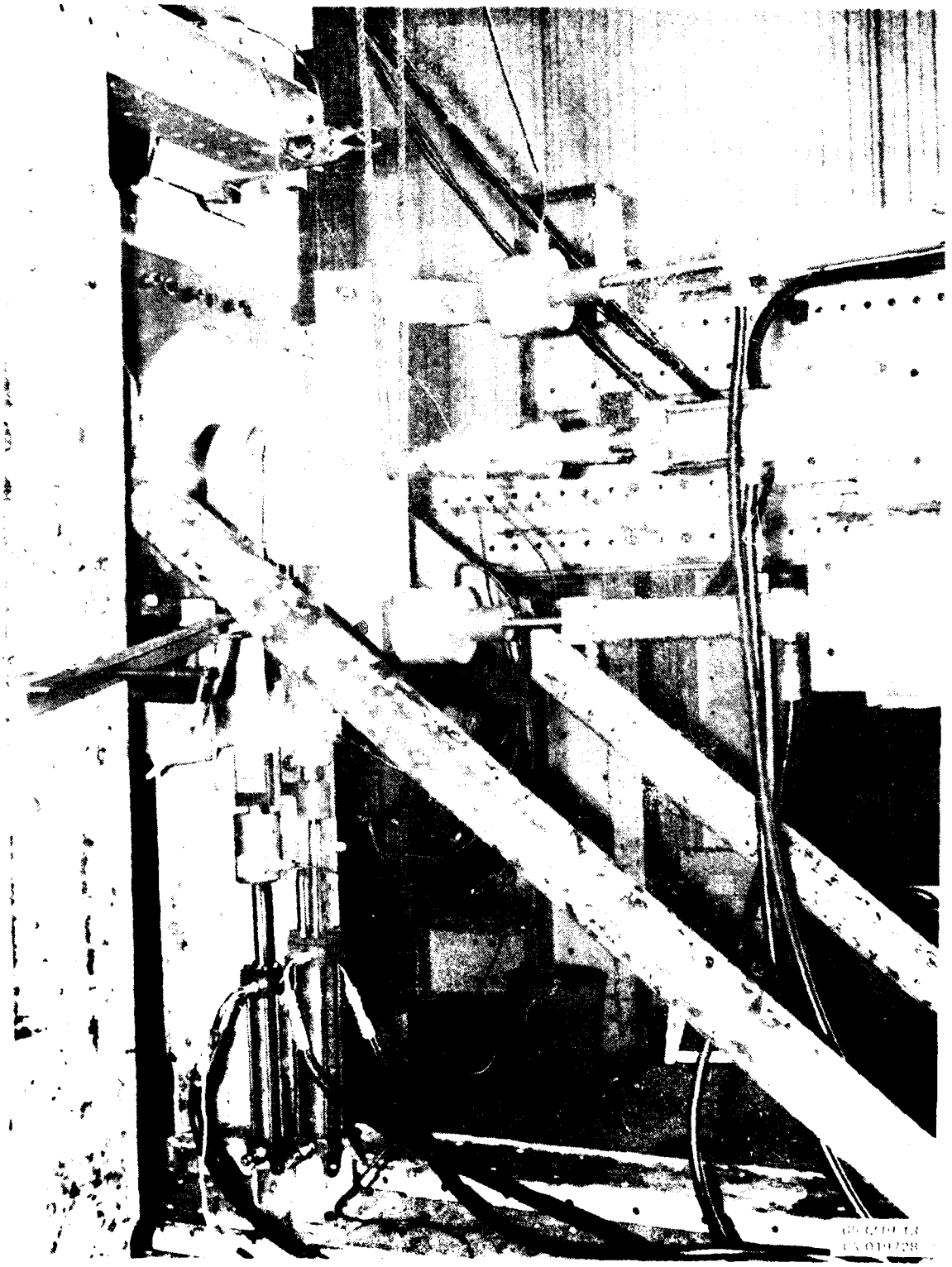

Figure 4-5. Combined Load Test Setup

```
ATI FRUSTA +RC      DATE:    2 /  14 /  79     TIME:   12 :  55 :  17

FILE:     4     RECORD:     3     CHANNELS  208  THROUGH  228

CHAN
 208 -13004. PD-1          +. DF-1          +. DF-2          +. DF-3
 212       +. DF-4       -838. SG-1       -843. SG-2       -843. SG-3
 216    -840. SG-4       -838. SG-5       -848. SG-6       -840. SG-7
 220    -840. SG-8       -845. SG-9       -838. SG-10      -840. SG-11
 224    -848. SG-12      -850. SG-13      -843. SG-14      -833. SG-15
 228    -838. SG-16
```

653219-14

Figure 4-6. Printout of Data

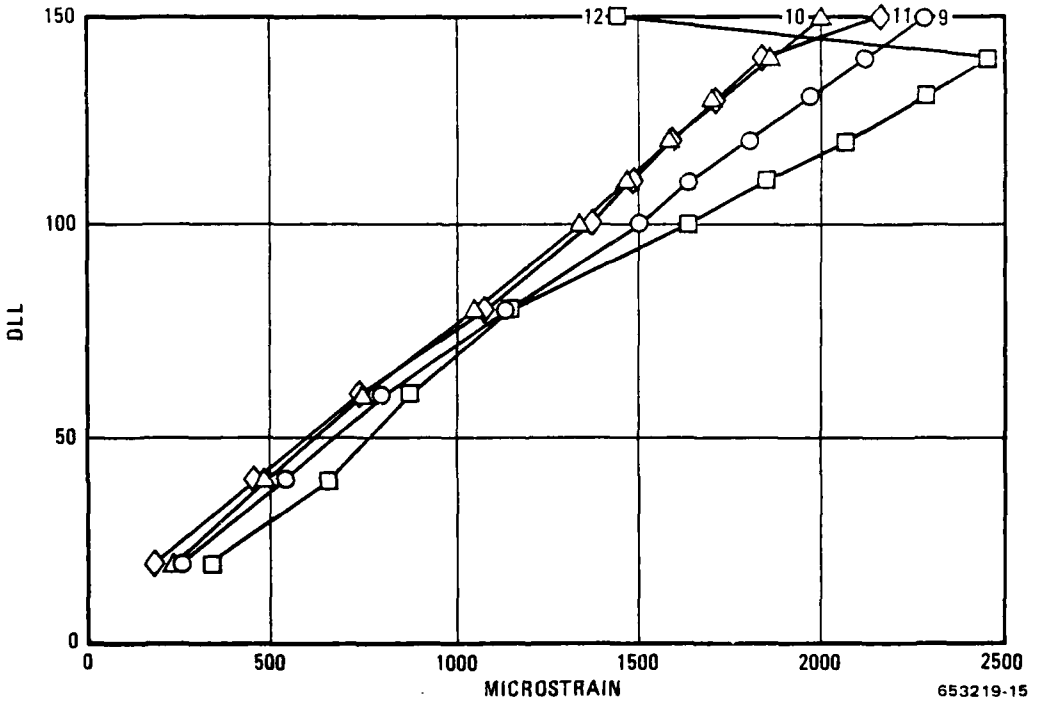

653219-15

Figure 4-7. ATI Frusta Test CI — Load Versus Strain Reading

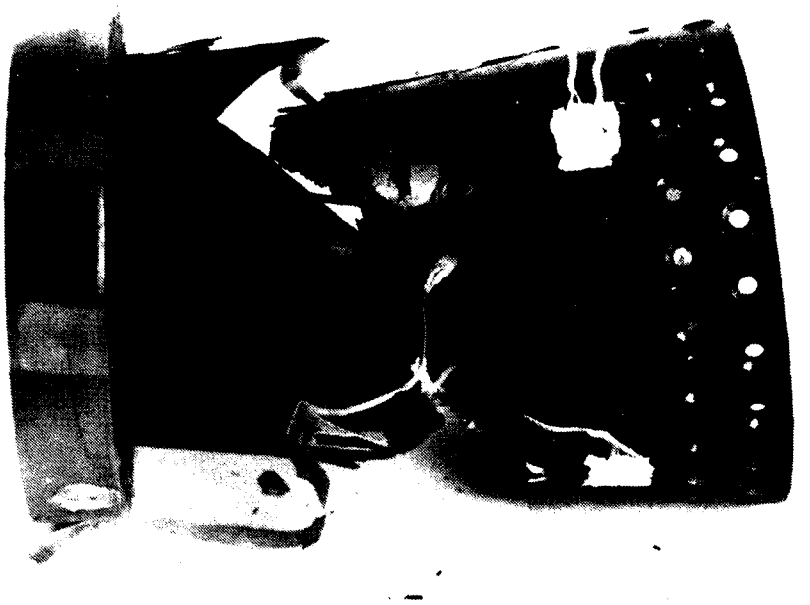

653219-16
CV079799

Figure 4-8. Failed Combined Load Test Specimen (Test C-3 S/N 12)

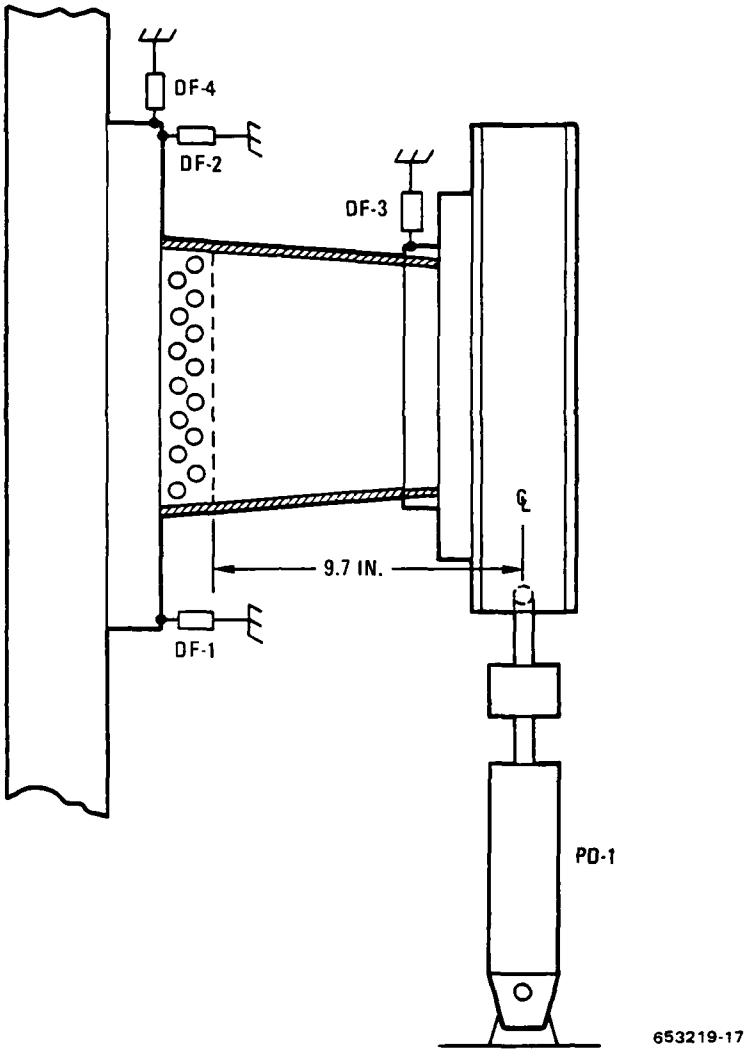

Figure 4-9. Shear/Bending — Test Orientation and Deflection Measurement Locations

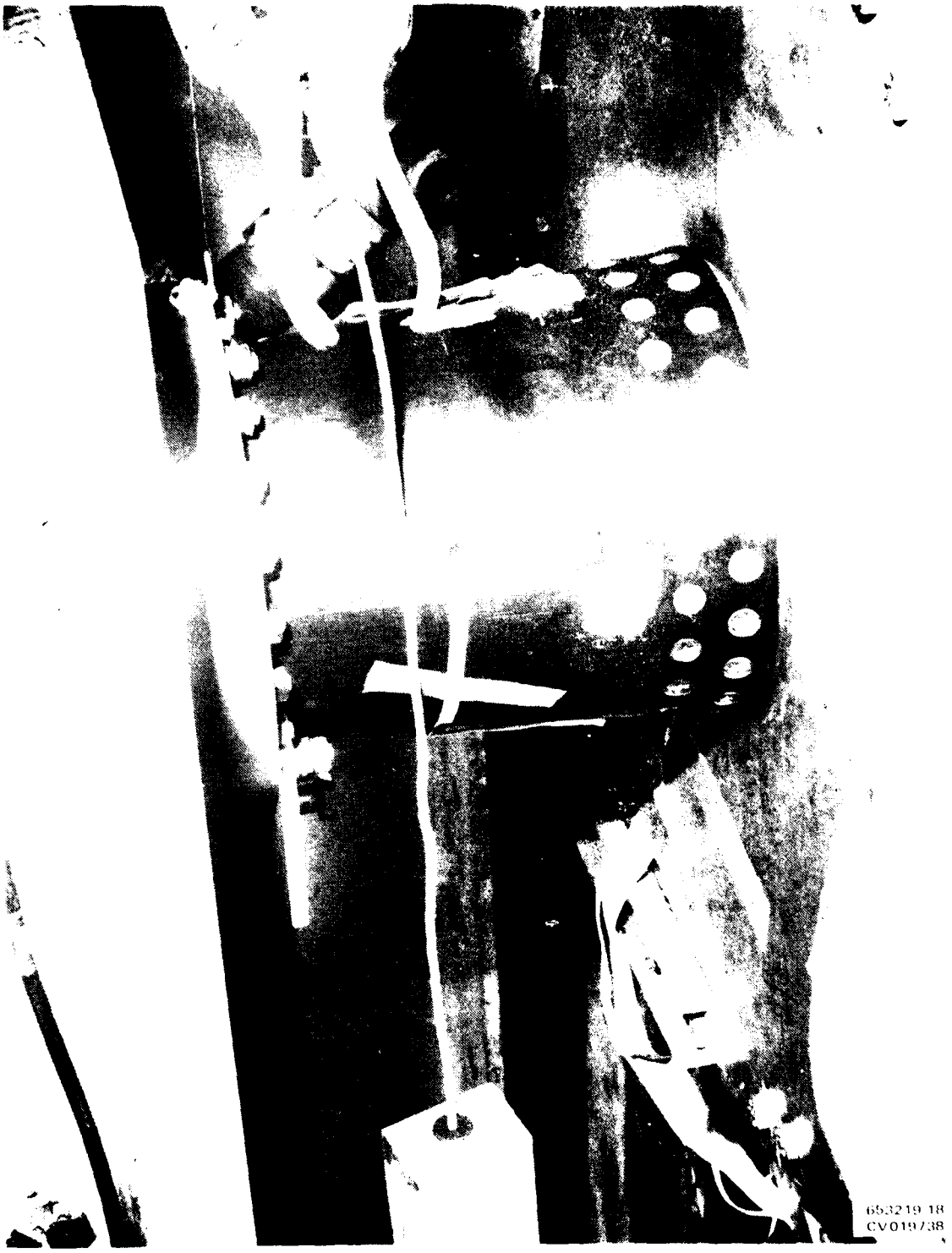

Figure 4-10. Shear Bending Test Setup

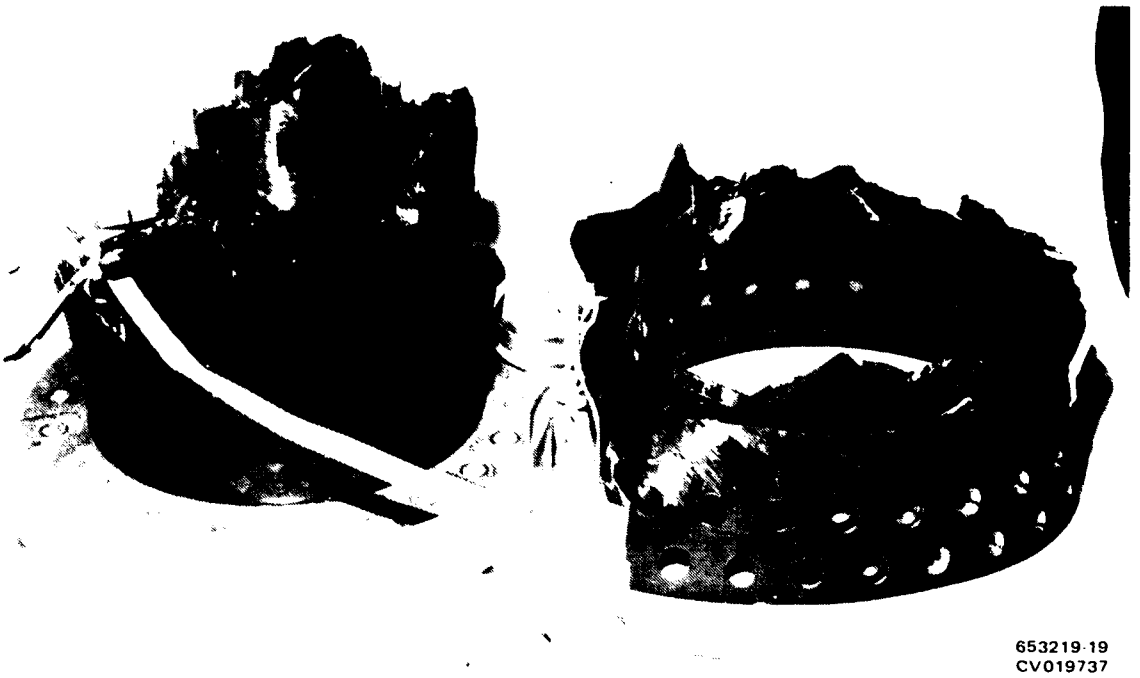

653219-19
CV019737

Figure 4-11. Failed Shear/Bending Specimen (Note Failure at the End of the Titanium Foils)

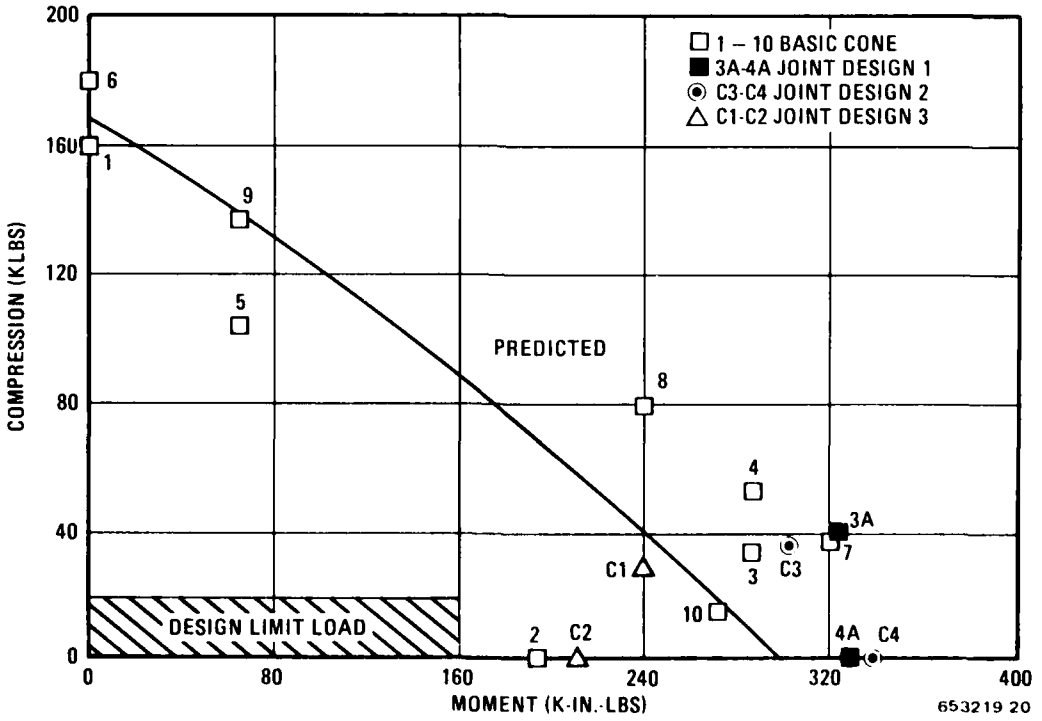

Figure 4-12. Load Interaction Diagram for GY70/934 Frusta

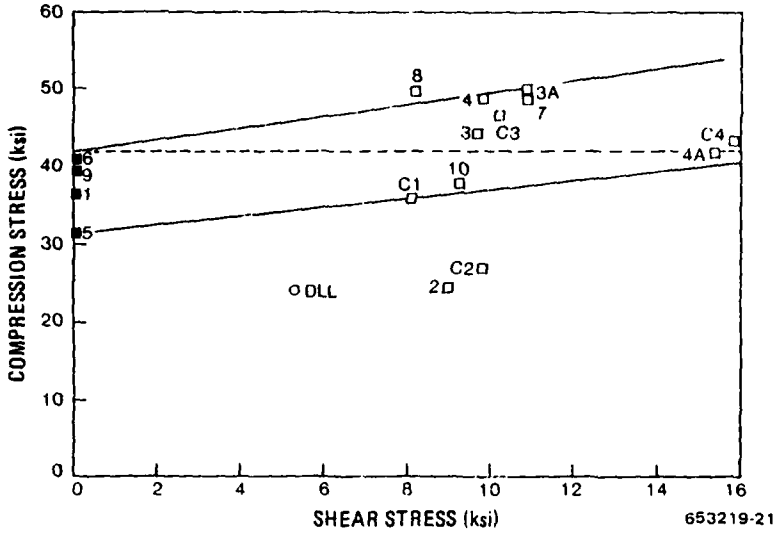

Figure 4-13. Strength Ratios for GY70/934 Frusta

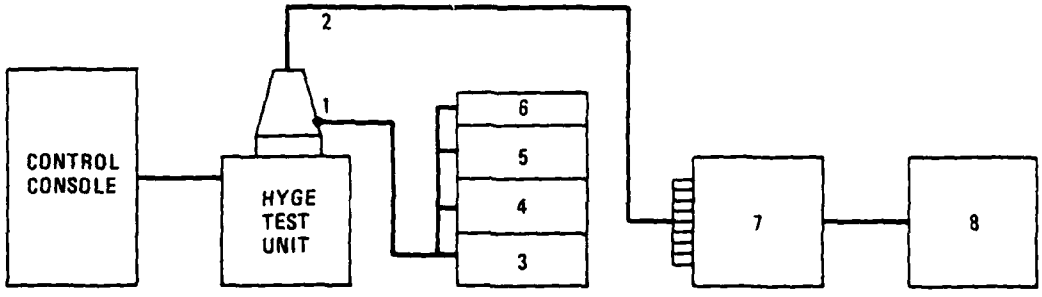

1. ACCELEROMETER – ENDEVCO MOD 2225
2. STRAIN GAGES – BLH FAE-25-12S0 (120Ω)
3. CHARGE AMPLIFIER – ENDEVCO MOD 2730
4. SPECTRUM ANALYZER – SPECTRAL DYNAMICS MOD SD 320A
5. X-Y PLOTTER – MOSELEY MOD 135A
6. OSCILLOSCOPE – HEWLETT PACKARD MOD 1205B
7. SIGNAL COND – UNHOLTZ – DICKIE MOD D22
8. TAPE RECORDER – AMPEX MOD FR 1300

653219-22

Figure 4-14. Schematic of Shock Test Setup

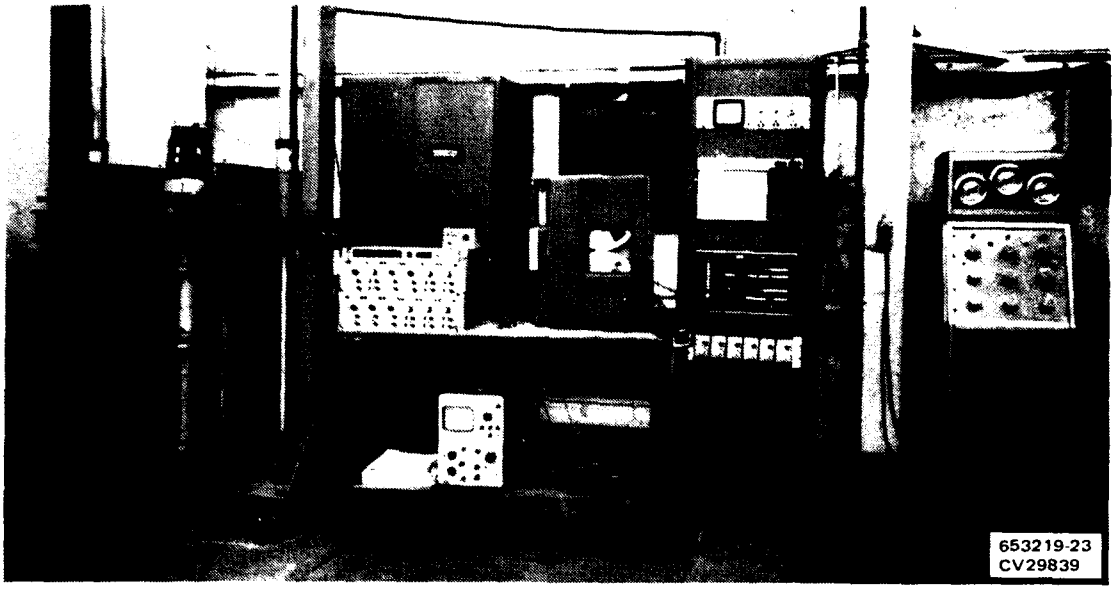

Figure 4-15. Shock Test Setup

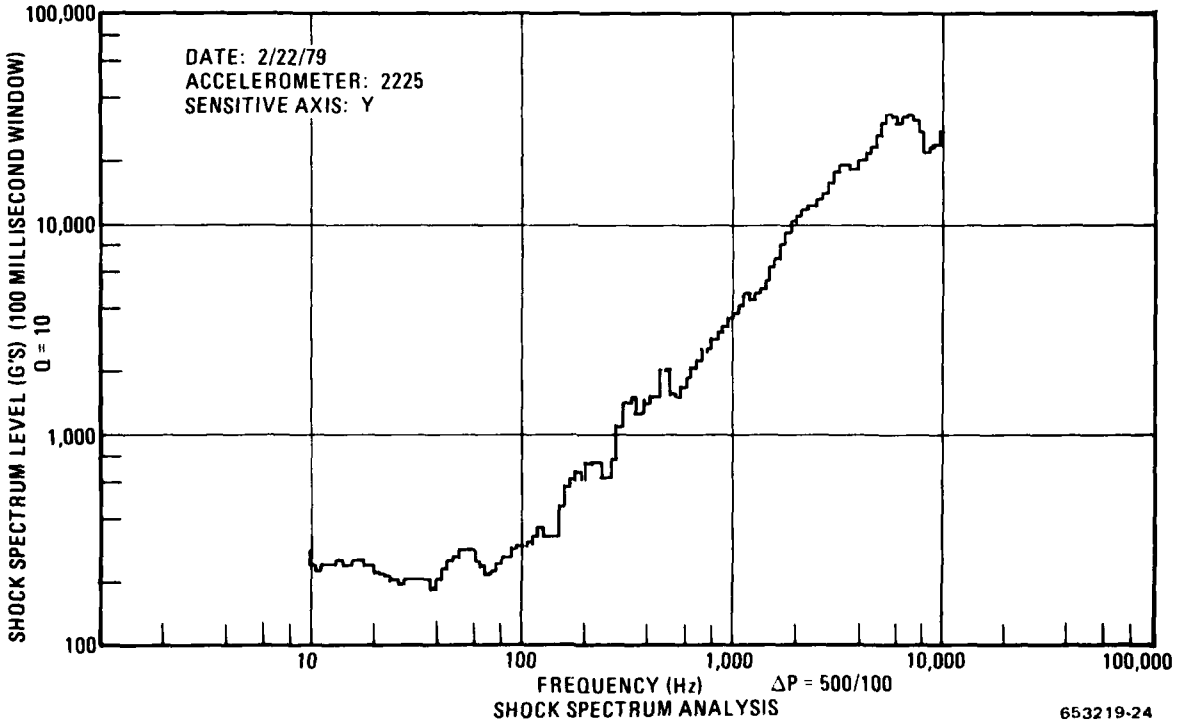

Figure 4-16. Typical Shock Spectrum

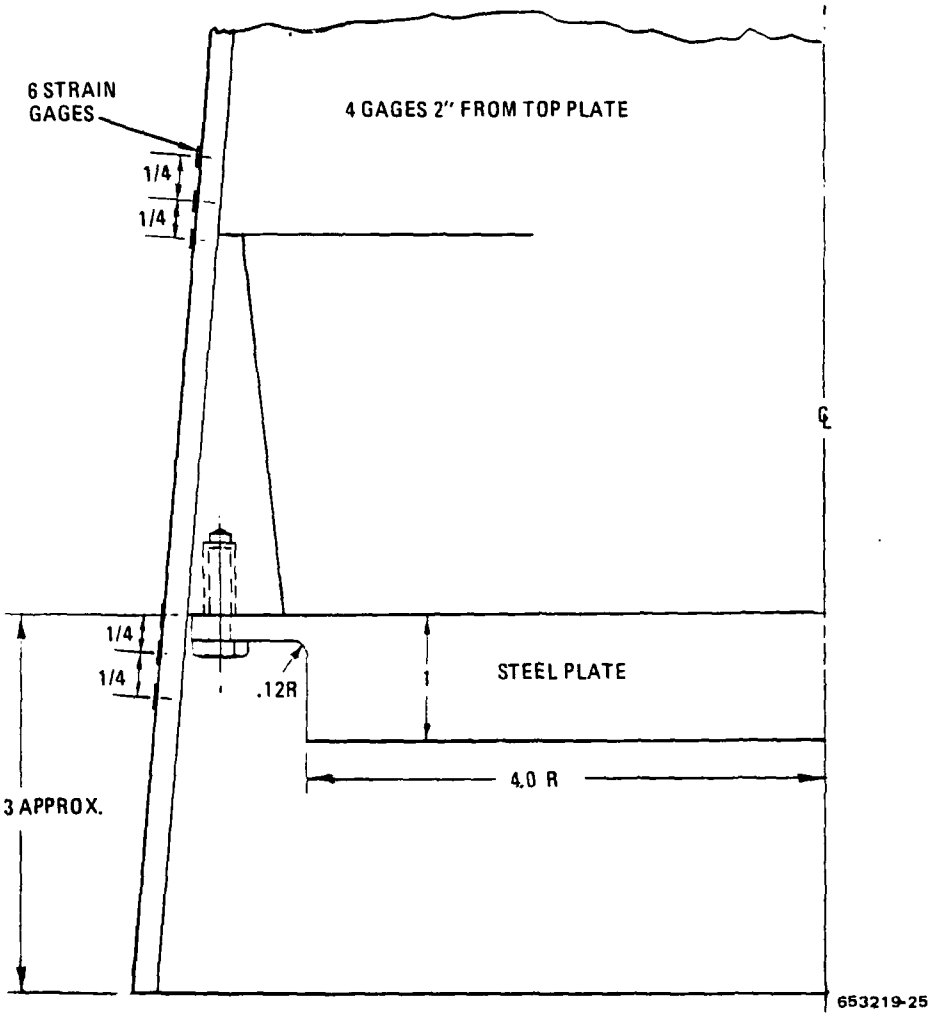

Figure 4-17. Strain Gage Position for Equipment Ring Tests

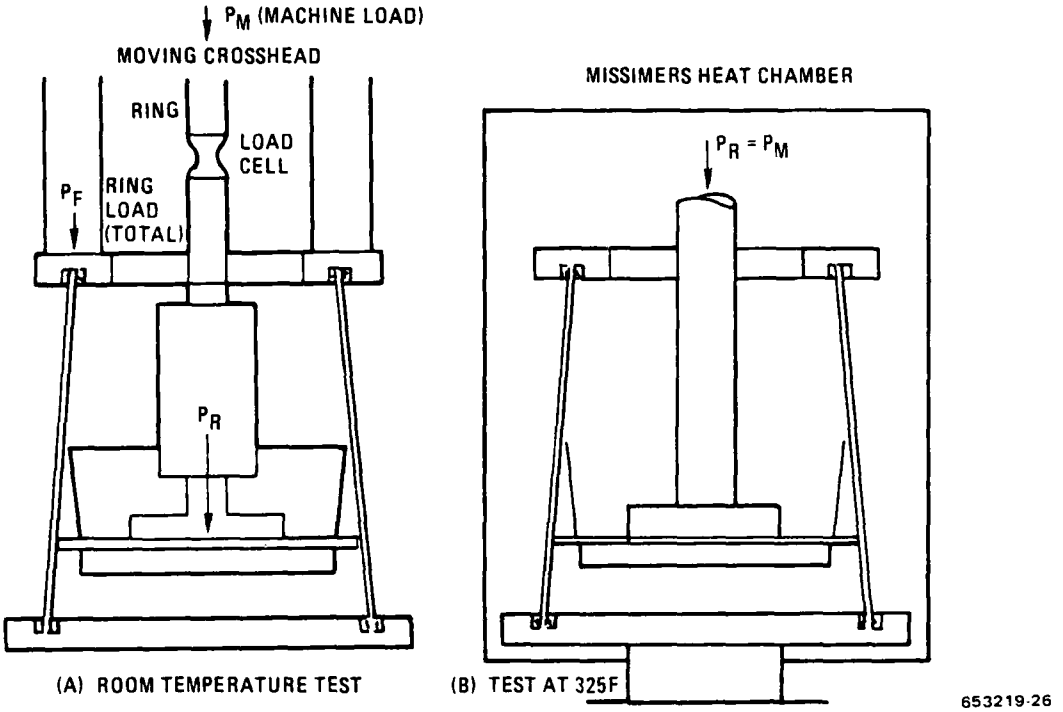

Figure 4-18. Sketch of Frustum Ring Tests

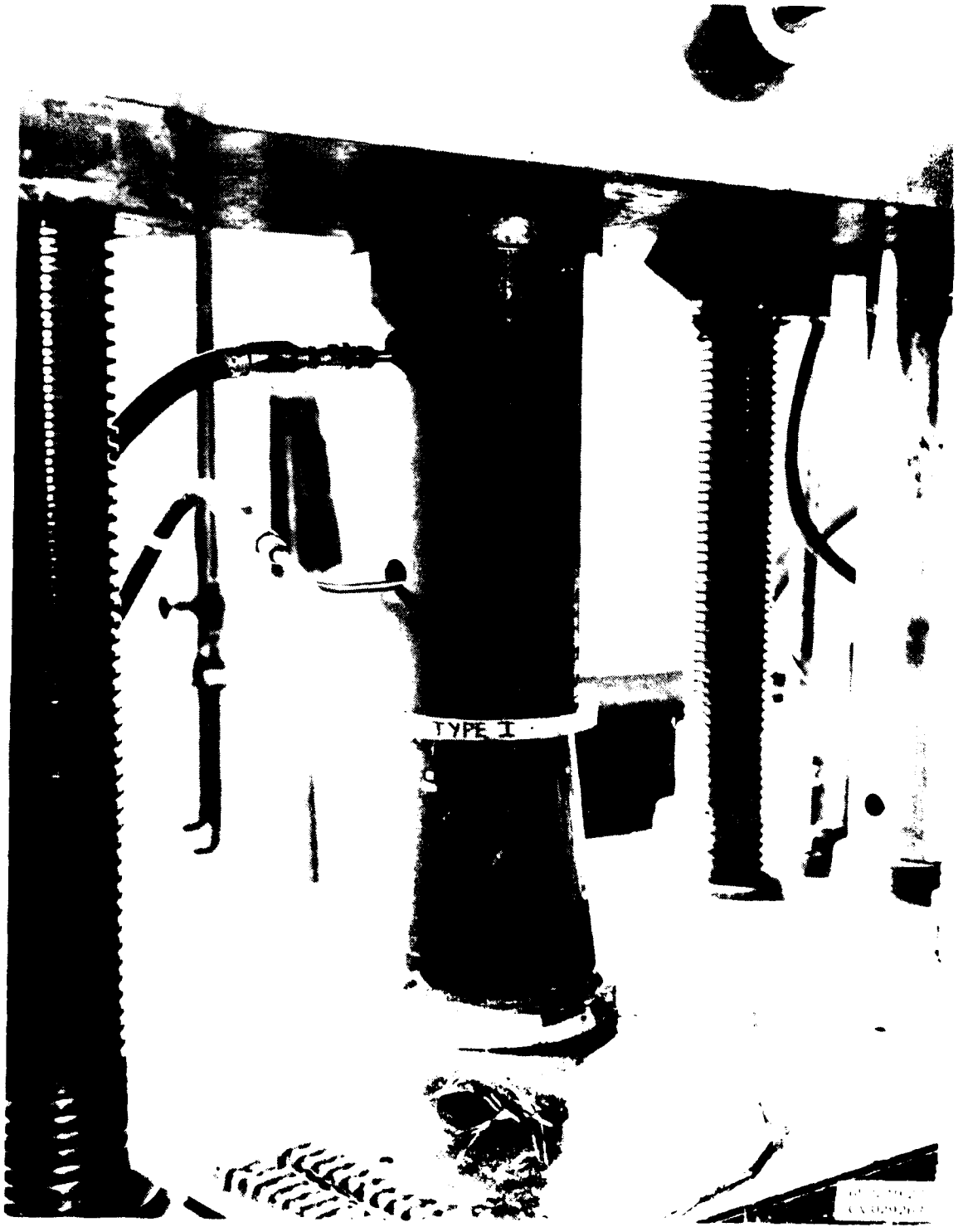

Figure 4-19. Equipment Ring Test Setup

653219-28
CV079796

Figure 4-20. Failed Titanium Equipment Ring Test

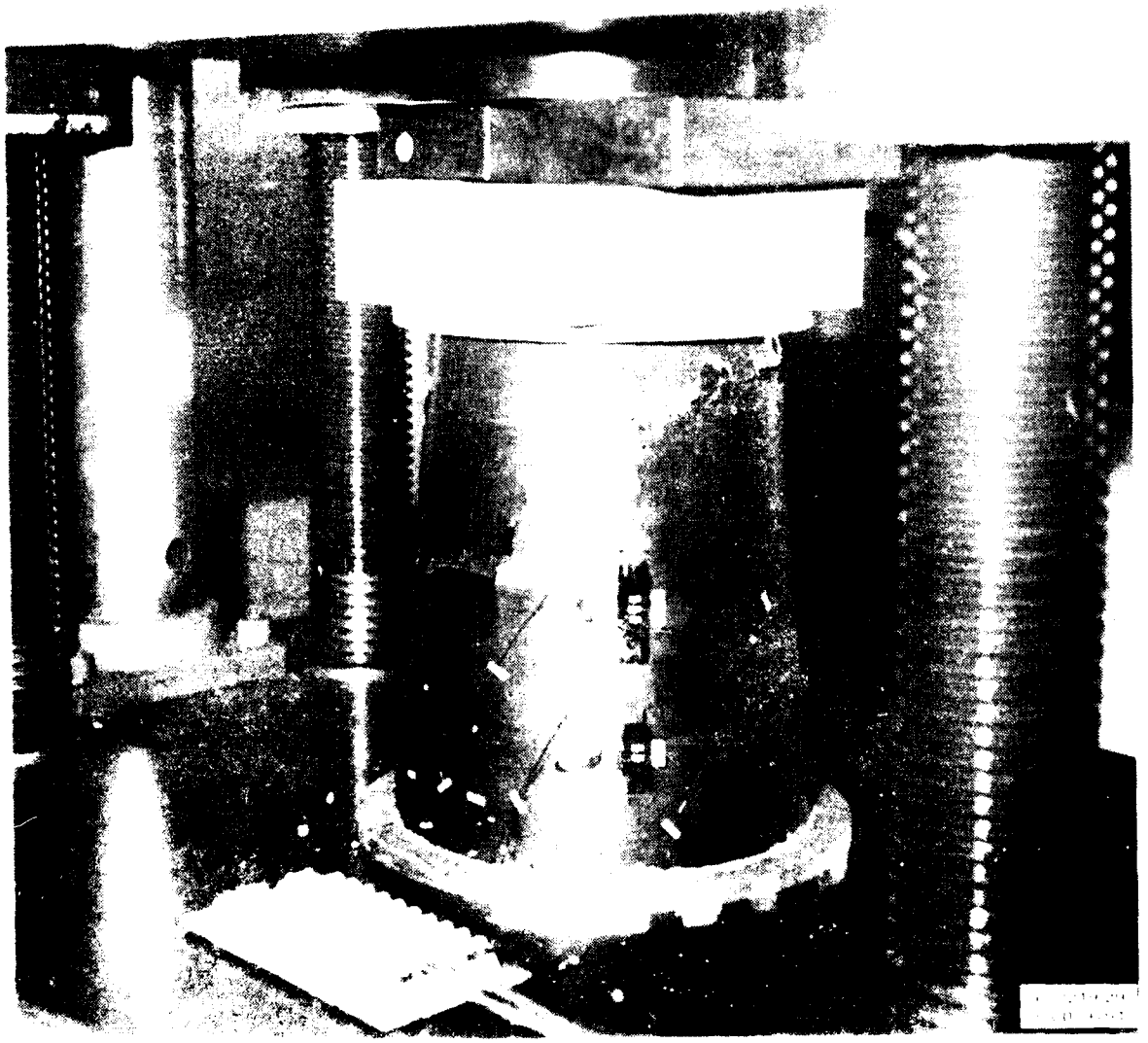

Figure 4-21. Failed Specimen LS-3

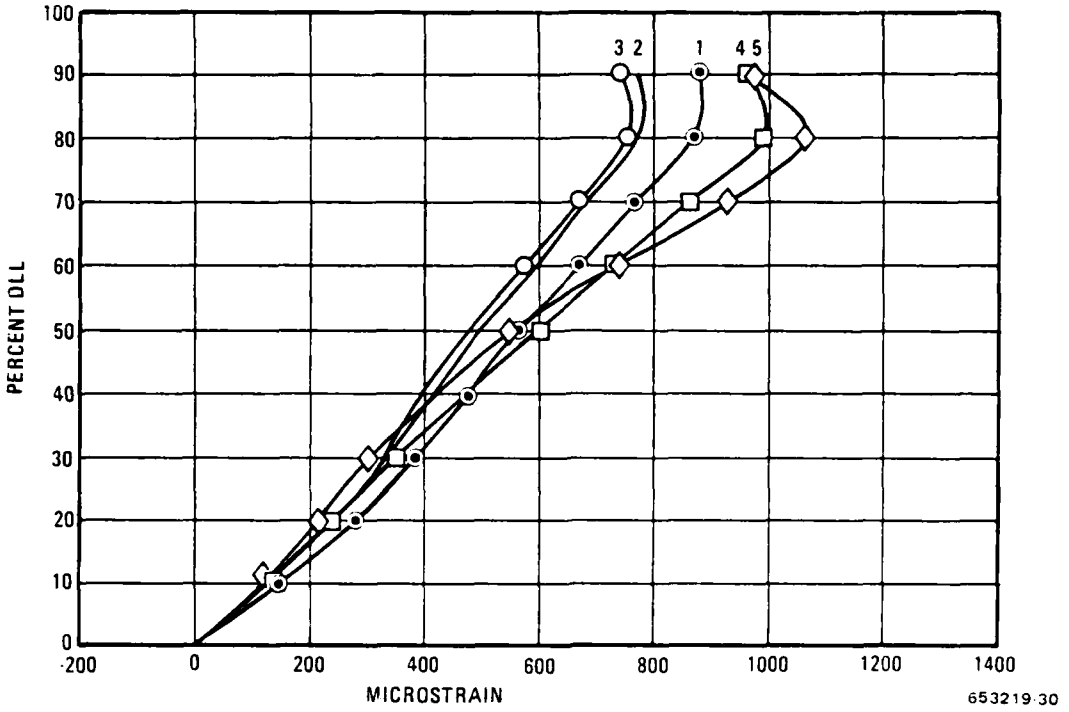

Figure 4-22. Load Strain Curves for LS-3

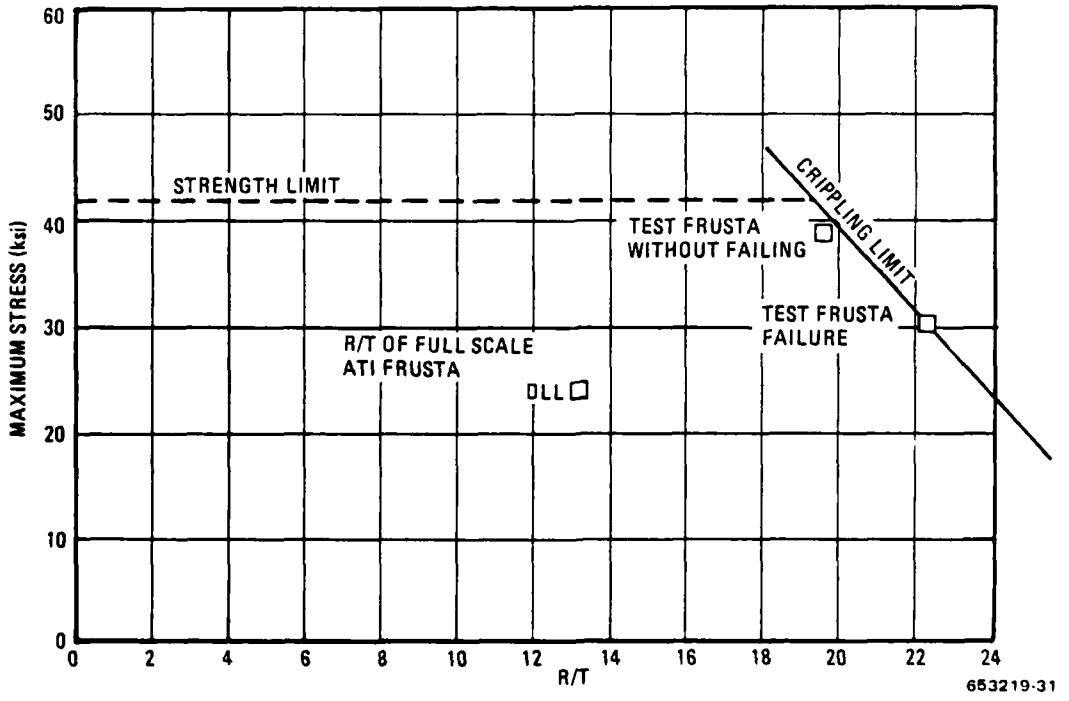

Figure 4-23. Crippling Curve for GY70/934

SECTION 5

SYSTEMS STUDY

5.1 INTRODUCTION

This study was undertaken by Prototype Development Associates (PDA) of Santa Ana, California. This section represents an unclassified summary of their work. The complete effort is reported in Reference 6.

Prior studies on the advanced terminal interceptor (ATI) have shown the requirement for high structural stiffness (Reference 7). Two materials, beryllium and ultra-high-modulus (UHM) graphite/epoxy (G/E), have been identified as leading material candidates to meet the stiffness requirement at a substantial weight saving over conventional aluminum structure or high-strength G/E. Beryllium offers the greatest weight-saving potential, but G/E enjoys a clear advantage in cost and availability.

The present study was designed to provide system analysis data to be used for design and evaluation of the G/E structure. Specific tasks included:

a. Define the baseline ATI configuration and trajectory.

b. Compute flight loads for the guidance section.

c. Design the heatshield for the G/E guidance section and compute structural temperatures.

d. Establish stiffness criteria for the guidance section structure to satisfy minimum frequency requirements.

5.2 FLIGHT LOADS

A baseline interceptor configuration was selected by AMMRC for use in the systems analysis tasks. It is configuration 4C from the ATI technology program (Reference 7).

All loads analysis were performed with PDA's BEAST computer code. For loads during boost, the two-stage missile was modeled by 80 beam elements and 19 discrete mass elements to represent internal components. For loads during second stage flight, 76 beam elements and 14 discrete masses were used. BEAST uses the Newtonian theory to compute aerodynamic loads for specified dynamic pressure and angle-of-attack. Effects of shadowing are included.

All loads presented in the following sections are limit loads. That is, they are maximum predicted loads with no safety factors applied for the full sized vehicle.

5.2.1 GUIDANCE SECTION SHELL LOADS. Lateral loads on the guidance section were evaluated for both steady turns and crossover maneuvers. Results show that the maximum lateral loads on the guidance section occur at first stage burnout. The loads over the guidance section are presented in Figures 5-1, 5-2, and 5-3. Configuration 4A loads (from Reference 1) are included since the guidance section composite frustum could be used for either configuration.

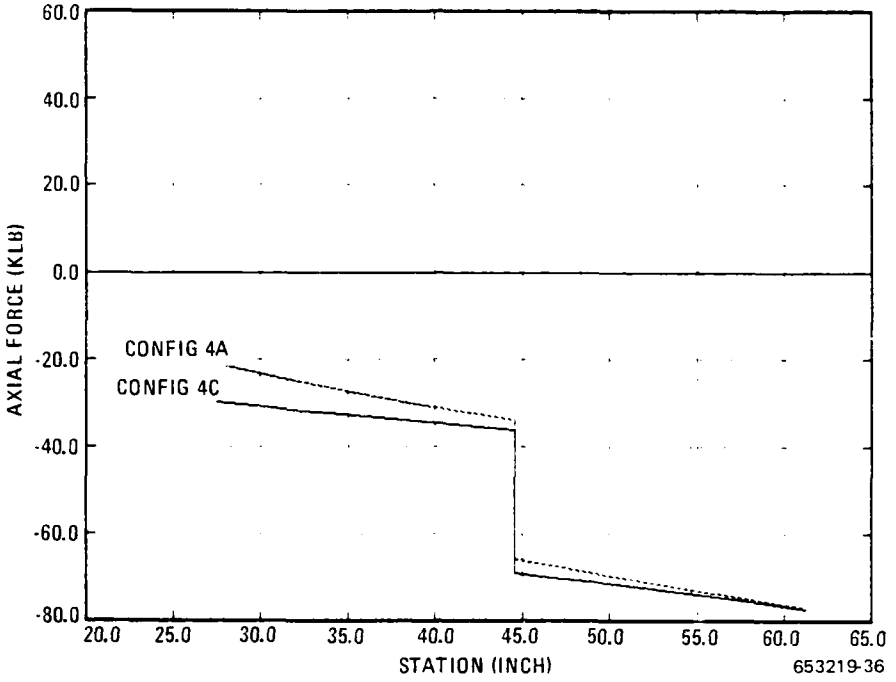

Figure 5-1. Guidance Section Axial Loads at Booster Burnout

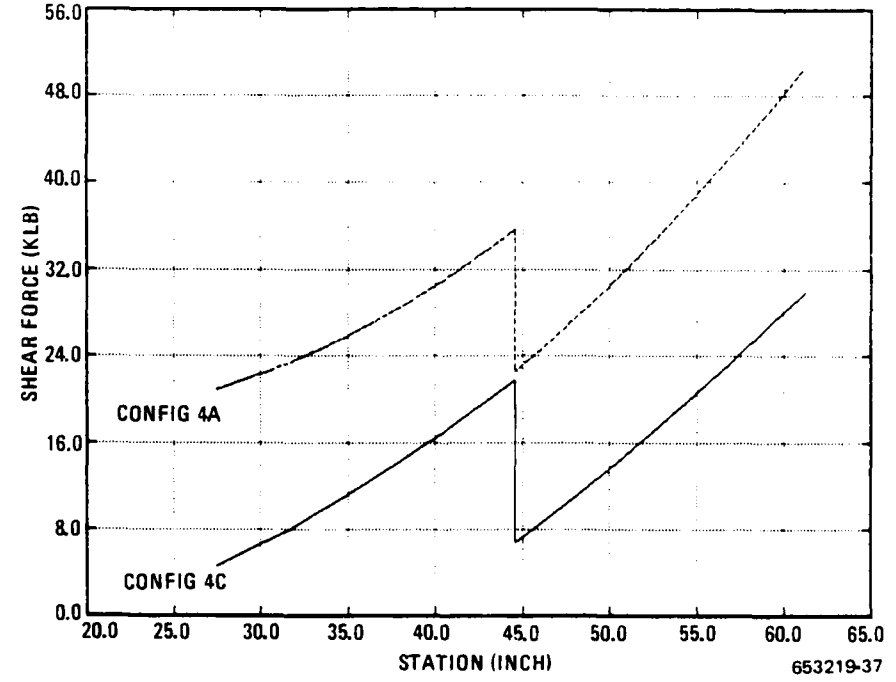

Figure 5-2. Guidance Section Shear Loads at Booster Burnout

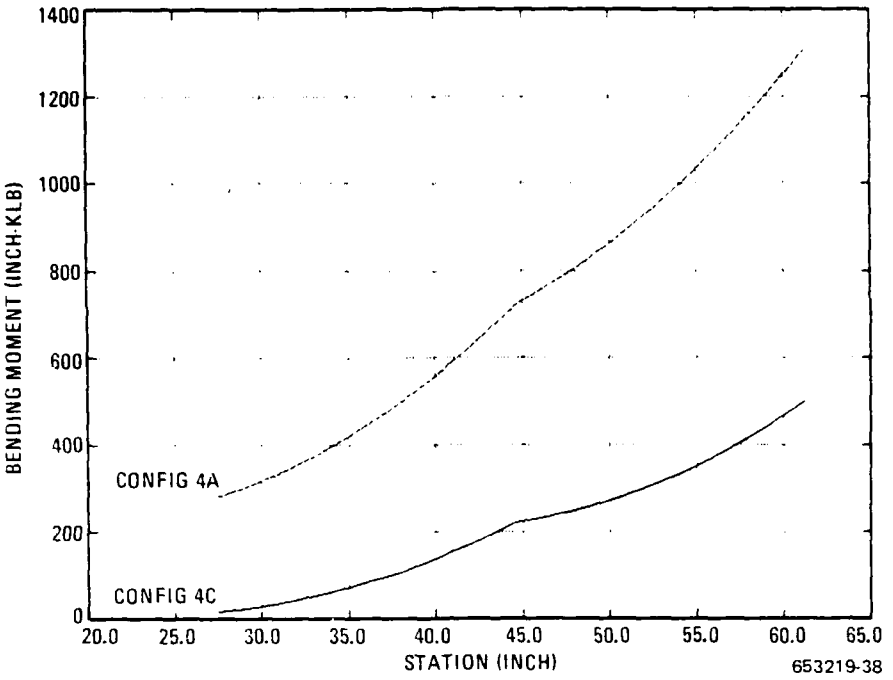

Figure 5-3. Guidance Section Bending Loads at Booster Burnout

Maximum shell loads for powered and unpowered flight occur at first stage burnout and maximum angle-of-attack, respectively. Guidance section end station loads at these times are listed in Table 5-1.

The loads at the maximum angle-of-attack are also given in Figure 5-4.

Table 5-1. Summary of Maximum Shell Loads For ATI Configuration 4C

Missile Body Forces[1][2] © LIMIT LOADS							
	Station 27.5			Station 61.2			Station 44.6
Load Condition	Axial (Klb)	Shear (Klb)	Moment (in-Klb)	Axial (Klb)	Shear (Klb)	Moment (in-Klb)	Moment (in-Klb)
First-Stage Burnout	−29.7	21.0[3]	282[3]	−77.1	50.7[3]	1306[3]	724
Max. Angle-of-Attack	−0.1	−6.9	205	−4.5	14.2	242	116

Notes:
(1) Trajectory 5-2
(2) Forces positive as shown:
(3) Configuration 4A (Reference 7)

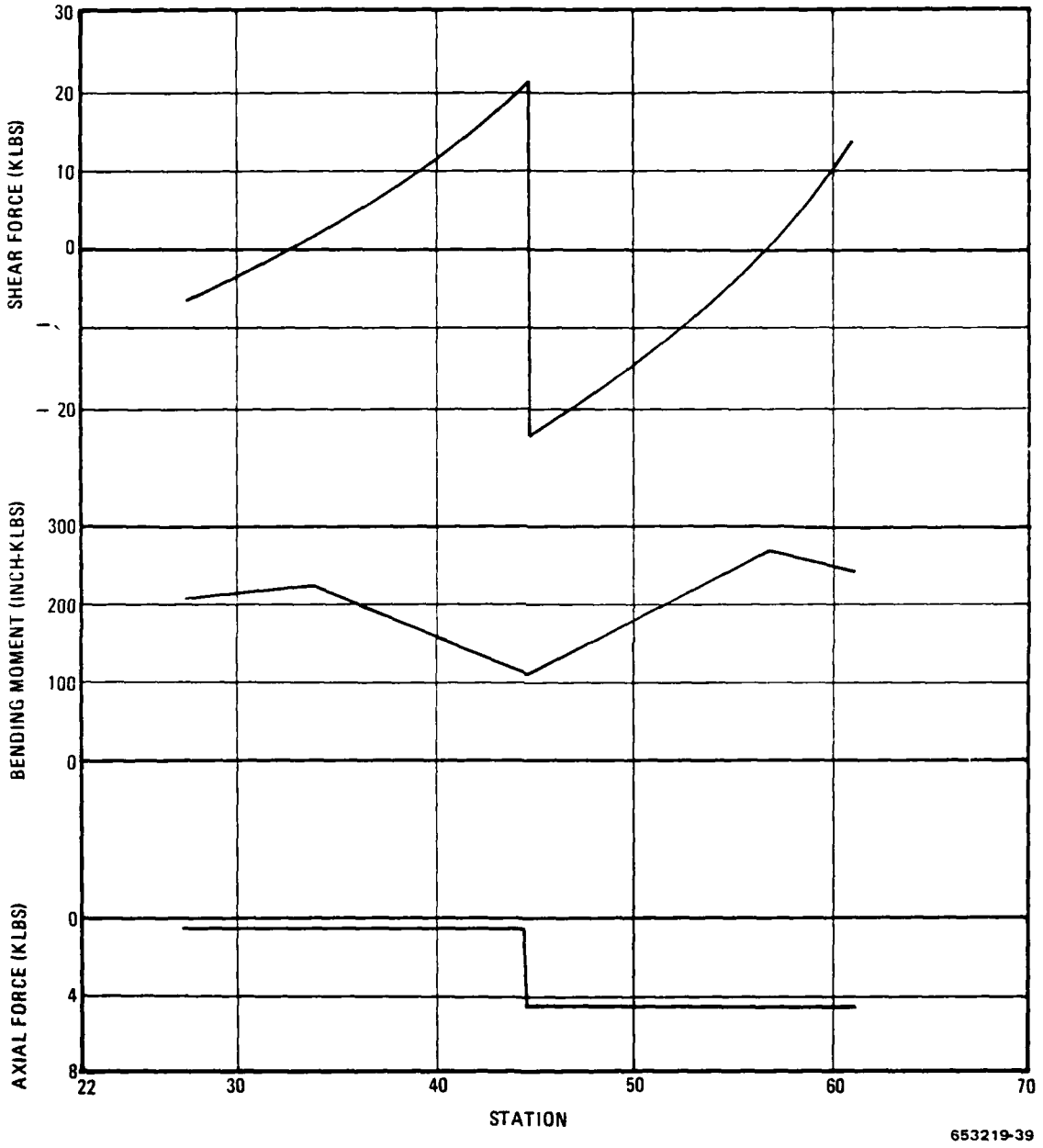

Figure 5-4. Guidance Section Loads at Maximum Angle-of-Attack

5.2.2 EQUIPMENT RING LOADS. The loads on the equipment ring (Sta 44.6) were found to be critical at two times in flight. The loads at these times are given in Table 5-2.

Table 5-2. Summary of Maximum Equipment Ring Loads

Load Condition	Equipment Ring Loads Station 44.6 Axial (Klb)	Shear (Klb)
Maximum Thrust[1]	36.4	12.7
Maximum Angle-of-Attack	−4.5	46.9

[1]Very near first-stage burnout and hence added at that point.

5.3 STIFFNESS REQUIREMENTS

A major design requirement for ATIs is that all structural frequencies must exceed 70 Hz during second stage flight. This ensures that all natural missile body frequencies are sufficiently above the control system frequency to avoid destabilizing structural deformations. In addition, it is necessary to achieve a fundamental torsional frequency at least 3 to 4 times higher than the fundamental bending frequency to avoid roll-pitch coupling.

Natural structural frequencies were computed for the baseline beryllium second stage and for UHM G/E second stages of various shell wall thicknesses. All frequency analyses were performed using the BEAST computer code. Each configuration analyzed was modeled with 76 Timoshenko beam finite elements plus 14 concentrated masses, representing internal components.

Bending frequencies were computed for the baseline beryllium second stage at ignition and at burnout to identify the critical time. The following results were obtained:

Time	Fundamental Bending Frequency
Second-Stage Ignition	77.0 Hz
Second-Stage Burnout	88.0 Hz

It is seen that ignition is the more critical time.

Four UHM G/E second-stage configurations were then analyzed for both bending and torsional frequencies at second-stage ignition. The purpose of these analyses was to obtain fundamental frequencies as functions of shell-wall rigidities. The four configurations had

graphite/epoxy guidance section wall thicknesses of 0.190, 0.285, 0.380, and 0.475 inch, respectively. G/E thicknesses used to replace other beryllium sections were calculated to obtain the same thickness ratio (G/E to Be) as in the guidance section. All G/E sections were protected by a 0.010-inch epoxy bondline and a heatshield of 0.150 inch. Representative values of meridional modulus of elasticity (E_x = 24.0 msi) and inplane shear modulus (G_{xy} = 3.8 msi) were used for G/E in all analyses.

Results of the parametric frequency analyses are presented in Figure 5-5. The experimental values of modulus, as well as the analytical value (Reference 1), was 26.7. Therefore, the extensional rigidity initially would be 10.1 (E_x =26.7 × 0.38 inches), which corresponds to a frequency of 76 Hz. This meets the design requirements. However, the joints can lower the frequency by up to 10 percent. This could reduce the frequency to just below the required value.

Figure 5-5 shows that adequate separation between bending and torsional frequencies can be achieved easily, provided a shear modulus around 3.7 msi is attained.

The predicted bending frequency of the baseline beryllium vehicle is also shown in Figure 5-5. The reason this point lies above the G/E curve is that, for the same shell wall extensional rigidity, the mean structural shell radius is greater for beryllium than for G/E because both the heatshield (0.080 inch) and the structure (0.200 inch) are thinner. This produces a higher bending moment of inertia for beryllium, leading in turn to a higher bending frequency. To achieve the same bending frequency as the beryllium vehicle, an UHM G/E shell requires an extensional rigidity of about 11.5 megapounds per inch.

5.4 THERMAL ANALYSIS

A thermal analysis was run to determine the quartz/phenolic heatshield response and thickness requirement for the trajectory designated 5-2. The analysis is a nominal, no-angle-of-attack, nonspinning, clear-air case.

The graphite/epoxy structure requires a secondary bond for retaining the quartz/phenolic heatshield, thus differing from the baseline configuration of Reference 7 that utilizes an 0.080-inch integral wrap and bond (IWB) silica/phenolic heatshield and an 0.20-inch beryllium structure. The quartz/phenolic heatshield thickness requirement is larger because of: 1) reduced heat capacitance of the graphite/epoxy in comparison to beryllium, and 2) the bondline-temperature requirement.

The G/E structure requires a bond to retain the quartz/phenolic heatshield. The present study assumed that the bond was Hysol EA934 epoxy adhesive. A heatshield design backface temperature criterion of 500F is based on EA934 thermogravimetric analysis (TGA) data that indicates nominal degradation of the bond at this threshold temperature level.

The heatshield thickness requirement is determined from a series of one-dimensional, charring ablator computer analyses of the quartz/phenolic, EA934 adhesive, and G/E combination. A fixed G/E structure thickness of 0.38-inch and a fixed bond thickness of 0.010-inch were assumed in all analyses, and the quartz/phenolic was varied between 0.080-inch and 0.200-inch thicknesses. Cross-plotting of the heatshield backface temperature at the final time, against

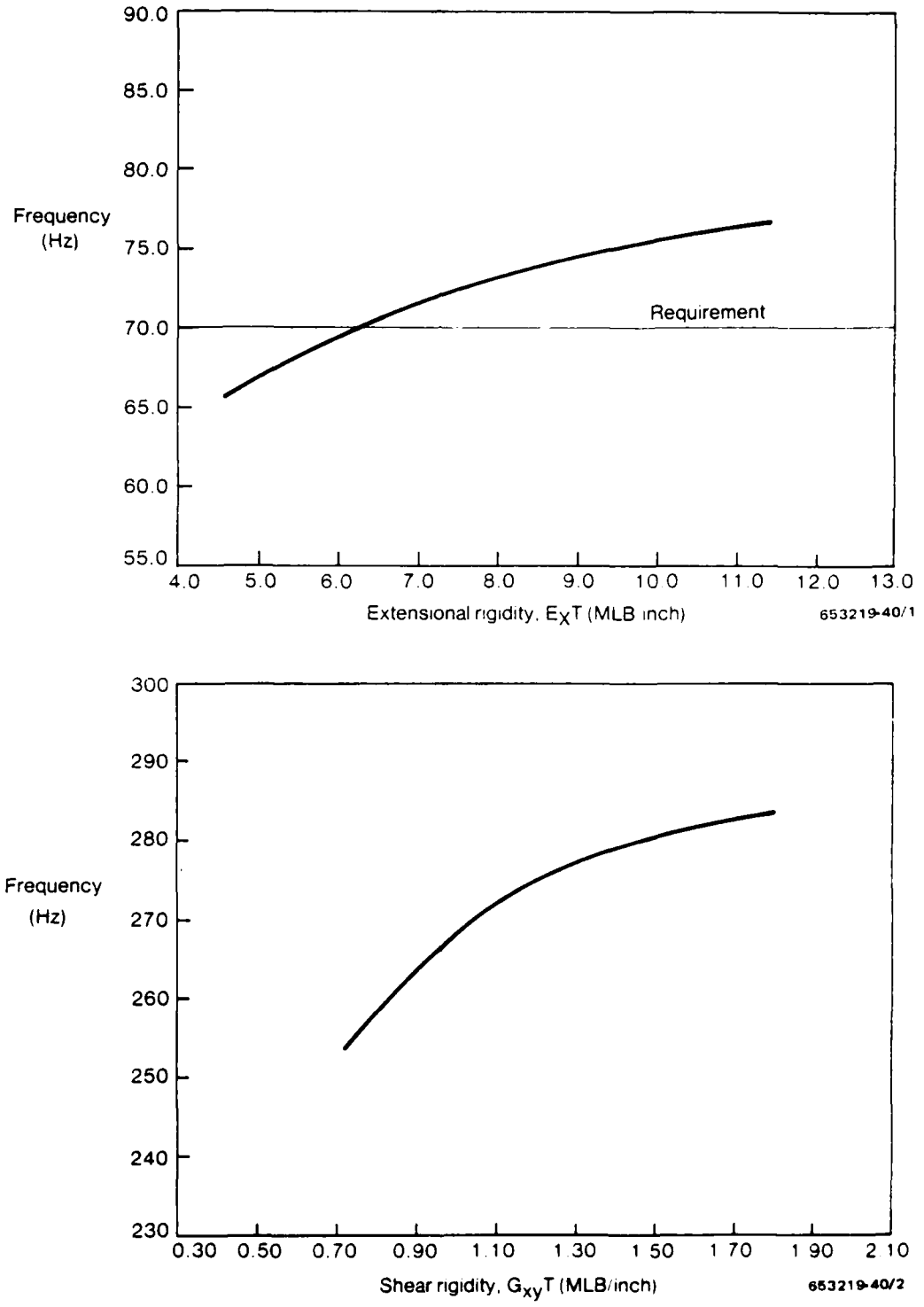

Figure 5-5. Parametric Bending and Torsional Frequencies at Second-Stage Ignition

the heatshield thickness generates a curve of thickness versus temperature and the 500F temperature limit determines the required heatshield thickness. Safety factors have not been incorporated in the results.

The PACE-calculated predictions are presented in Figures 5-6 and 5-7. The plots shown are for a 0.150-inch thick quartz/phenolic heatshield, which is required to meet the 500F heatshield backface criterion.

Figure 5-6 presents the temperature gradients at time = 2.4, 4.0, 6.0, and 10.0 seconds for the materials at Sta 28.56. The bulk of the substructure (G/E) remains at the initial temperature throughout the trajectory.

Figure 5-7 is an expanded scale presentation of the data of Figure 5-6. The focus is the bondline region and substructure gradients. The expanded scale should provide clarity for assessing the substructure thermostructural response.

The axial temperature gradients from stations 28.56 to 60.56 were less than 100F and hence would suggest heatshield thickness requirements at the aft 60.56 Sta of 0.143 inch.

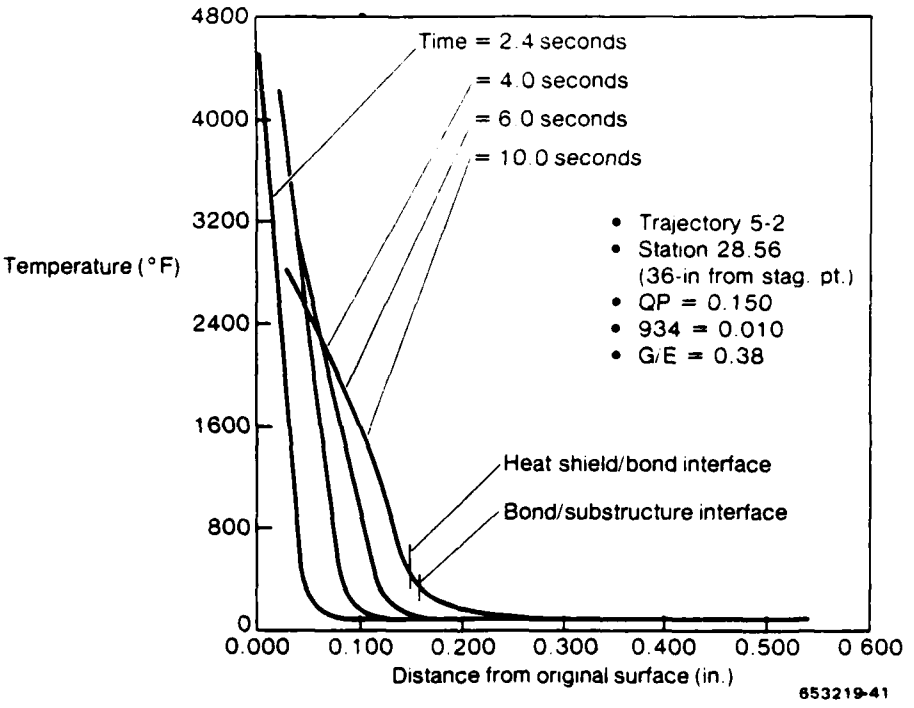

Figure 5-6. Temperature Profiles

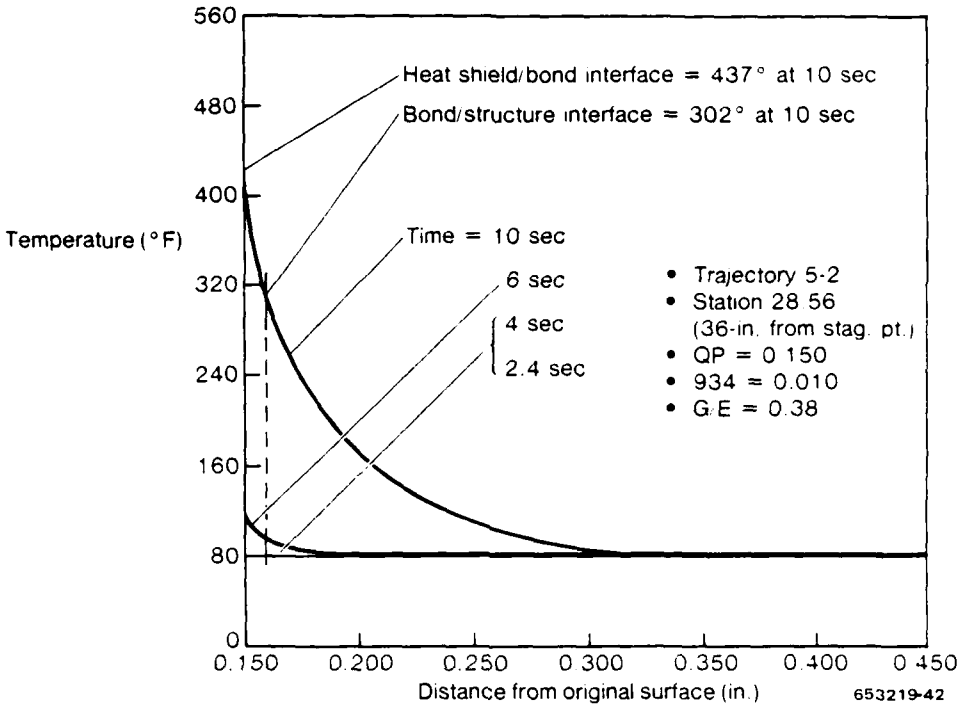

Figure 5-7. Temperature Profiles (Expanded Scale Presentation)

SECTION 6

PRELIMINARY FULL-SCALE DESIGN

6.1 OVERALL

The preliminary full-scale design of the guidance and control section (GCS) structure is based strictly on the results of analytical and experimental work previously accomplished and reported in References 1 and 2. Figure 6-1 illustrates the resultant design. An upsize version of Figure 6-1 is given in Appendix D.

The overall geometry is identical to that shown for the GCS in Reference 1. With respect to detail geometry, the three antenna cutouts are also located and sized to agree with the definition given in this reference. The pattern of reinforcement around the cutouts, however, is revised to integrate this with the reinforcement required for the bolted splice at Sta 27.5. The cross-sections of the three rings, which are shown semi-schematically in Reference 1, have also been changed during the evolution of the design.

For the full-scale shell structure, the basic laminate is scaled up from the half-scale laminate derived for compliance with stiffness requirements in Reference 1. This half-scale laminate was 0.19 inch thick and consisted of 38 plies of 0.005-inch graphite-epoxy with a generalized orientation of $(0_{11}/45_3/135_3/90_2)_S$. As scaled up for the full-size shell, the laminate is now 0.38-inch thick and the layup is $(0_{11}/45_3/135_3/90_2)_{S2}$. The actual stacking sequence is shown in Figure 6-2. Sequencing S2 in preference to 2S was selected to obtain the best distribution of zero plies for shell stability. The shell is designed for lay-up and cure in a female tool in manner identical to the technique used previously for the fabrication of the subscale frusta.

The following sections discuss the features of critical detail areas and the rationale used for design. Essentially, the rationale is an extrapolation from subscale test results to full-scale requirements. For this reason, the numerical values presented may not be in exact agreement with later, more refined analysis given in Section 7.

6.2 THE AFT SPLICE

The details of the splice are shown in Figure 6-1. It features the titanium interleave reinforcing concept Design No. 1, which was successfully tested as reported in References 1 and 2.

Design limit loads for this splice were taken from Table 5-1. These overall shell loads are:

Bending Moment (in-lb)	=	1,306,000
Axial Load (lb)	=	-77,100
Shear Load (lb)	=	50,700

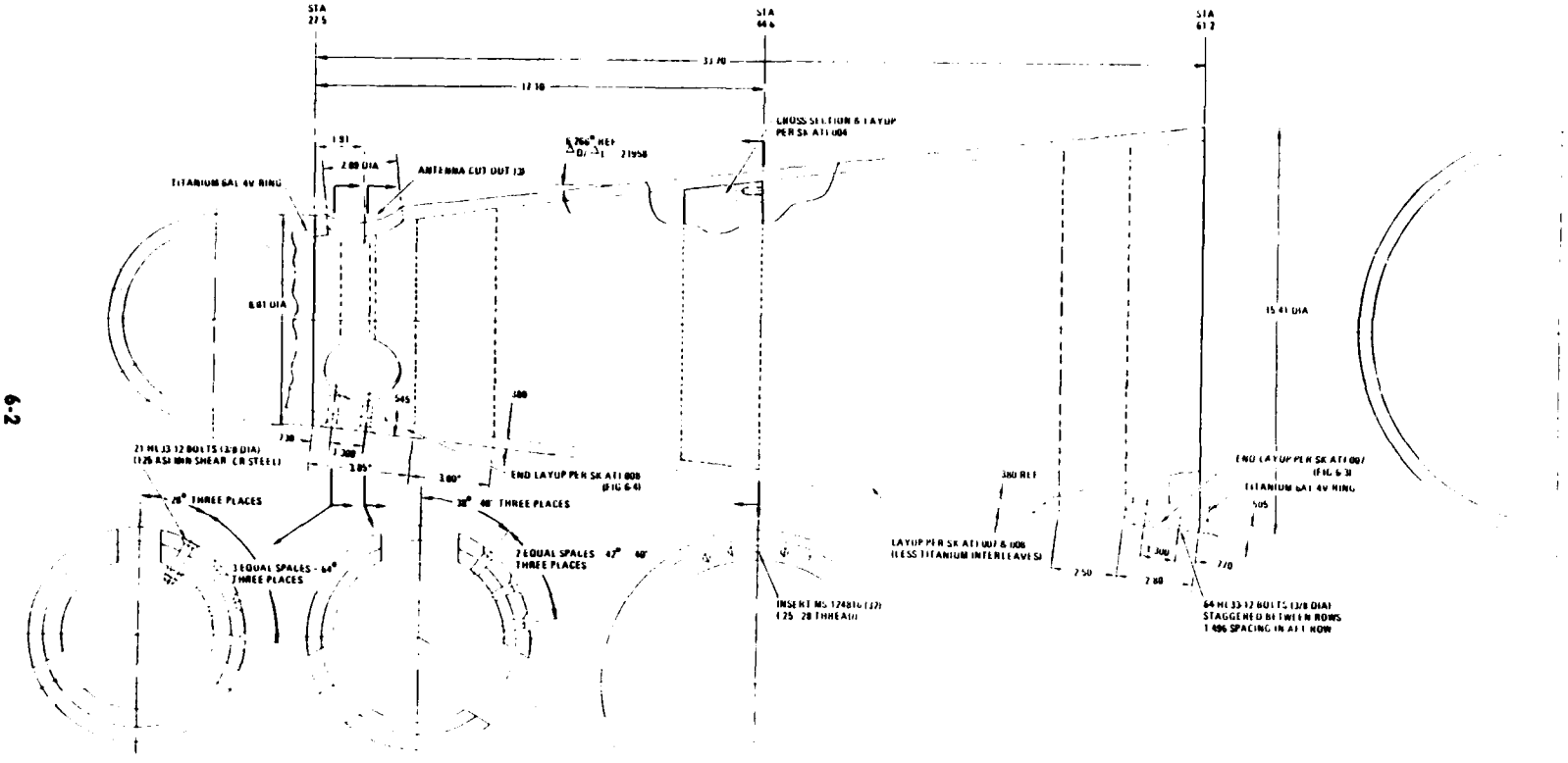

653219-43

Figure 6-1. Guidance and Control Section Full-Scale Composite Structure

Ply No.	Orientation	Ply No.	Orientation
1 (outside)	0	39	0
2	0	40	0
3	45	41	45
4	90	42	90
5	135	43	135
6	90	44	90
7	45	45	45
8	0	46	0
9	0	47	0
10	0	48	0
11	135	49	135
12	0	50	0
13	0	51	0
14	0	52	0
15	45	53	45
16	0	54	0
17	0	55	0
18	135	56	135
19	0	57	0
20	0	58	0
21	135	59	135
22	0	60	0
23	0	61	0
24	45	62	45
25	0	63	0
26	0	64	0
27	0	65	0
28	135	66	135
29	0	67	0
30	0	68	0
31	0	69	0
32	45	70	45
33	90	71	90
34	135	72	135
35	90	73	90
36	45	74	45
37	0	75	0
38	0	76 (inside)	0

Figure 6-2. Ply Orientation, Shell Laminate

Using an effective diameter of 14.2 inches for the shell/ring interface, the resultant section properties establish the following limit loads for the splice:

Peak Axial Tension (lb/in)	=	5,210
Peak Axial Compression (lb/in)	=	10,110
Peak Shear Flow (lb/in)	=	2,270

Applying a factor of safety of 1.5 as specified in Table 3-1 of Reference 1, gives the ultimate loads:

Peak Axial Tension (lb/in)	=	7,815
Peak Axial Compression (lb/in)	=	15,165
Peak Shear Flow (lb/in)	=	3,405

Analysis of the tests reported in Reference 1, concluded that the ultimate load for the half-scale Design No. 1 joint is 10,200 lb/in. For a full-scale ultimate load of 15,165 lb/in, a scale up factor of 1.5 would be appropriate. However, a direct scale-up in this proportion is not possible since the basic composite laminate is scaled up by a factor of 2.0. The approach taken was to factor the summation of the titanium interleaves by 1.5. This is conservative since, with the basic laminate thickness doubled, the total thickness at the joint is increased from the half scale by a factor of 1.88, a feature that will reduce the critical peak bearing stress. Another departure from direct scaling was introduced when, for procurement reasons, it was found necessary to accept 0.005-inch-thick material used for the Design No. 1 half-scale specimens. In the referenced tests, it had been shown that variation in the thickness of the foil down to 0.004 inch did not significantly affect bearing strength. In view of this finding, this change should not be of concern. It is considered also, that the overall approach adopted results in a design which generates an adequate degree of confidence for development test purposes. The layup and proportions of the titanium interleaved aft end laminate are shown in Figure 6-3.

The bolt size was established as 3/8-inch diameter by applying the basic scale-up factor of 1.5 to the 1/4-inch diameter bolts used in the test specimens. Spacing of the bolts was set to maintain the same bolt bearing width per inch as in the test specimens. These two features were necessary to maintain the validity of the previously described adjustments. HL 33-12 bolts (431 stainless steel) were selected on the basis of a shear-strength requirement of 11,400 lb/bolt and for corrosion resistance in a G/E application.

6.3 FORWARD SPLICE

The design of this splice is complicated by the proximity of the three relatively large antenna cutouts. These cause three portions of the periphery to be ineffective for splicing and require consideration of the interaction of the splice reinforcement with the reinforcement around the cutout. It was found that the interaction could be readily accomplished by extending the titanium interleaves past the cutouts. The resultant configuration of the forward end is shown in Figures 6-1 and 6-4.

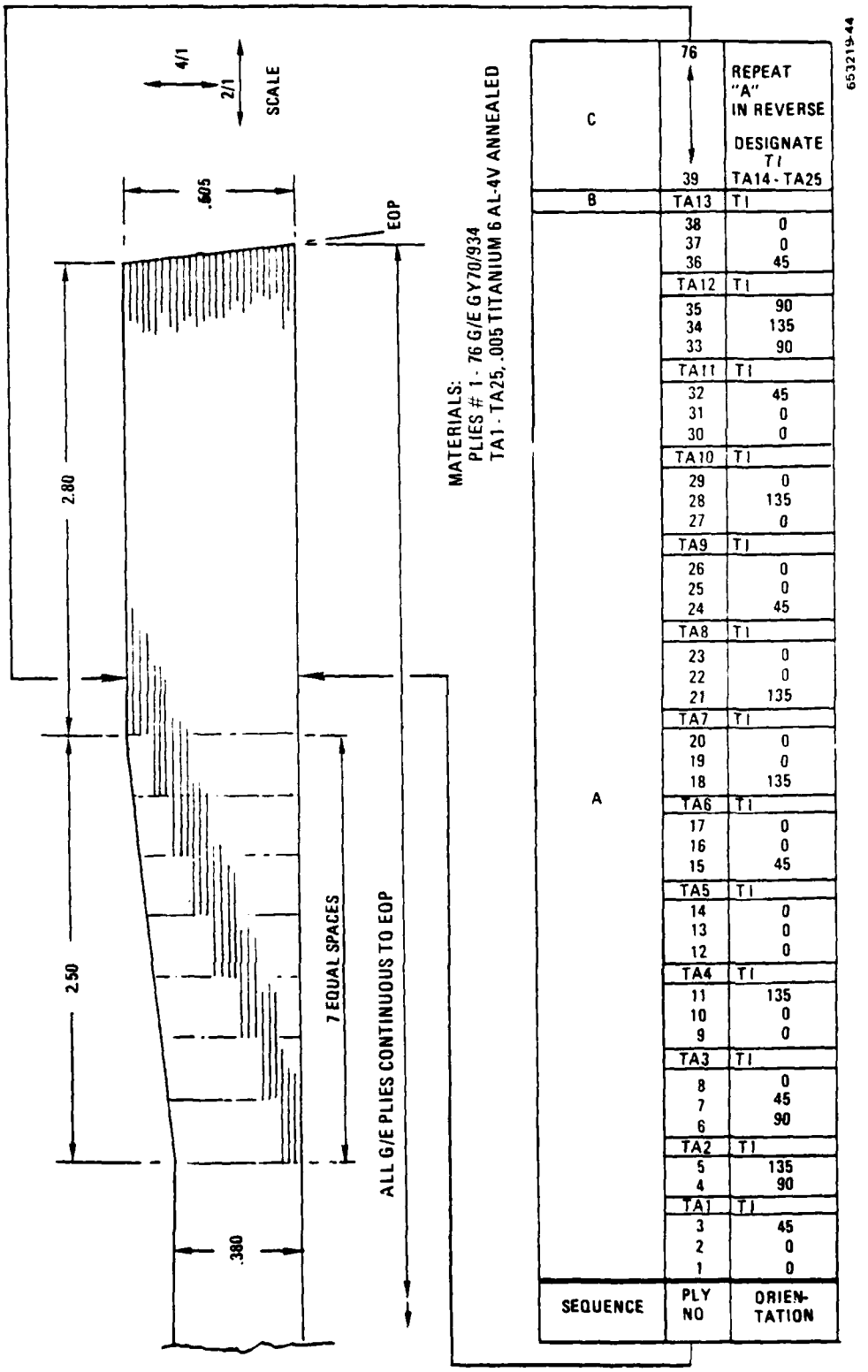

SEQUENCE	PLY NO	ORIENTATION
C	76 ↕ 39	REPEAT "A" IN REVERSE DESIGNATE T1 TA14 - TA25
B	TA13	T1
A	38	0
	37	0
	36	45
	TA12	T1
	35	90
	34	135
	33	90
	TA11	T1
	32	45
	31	0
	30	0
	TA10	T1
	29	0
	28	135
	27	0
	TA9	T1
	26	0
	25	0
	24	45
	TA8	T1
	23	0
	22	0
	21	135
	TA7	T1
	20	0
	19	0
	18	135
	TA6	T1
	17	0
	16	0
	15	45
	TA5	T1
	14	0
	13	0
	12	0
	TA4	T1
	11	135
	10	0
	9	0
	TA3	T1
	8	0
	7	45
	6	90
	TA2	T1
	5	135
	4	90
	TA1	T1
	3	45
	2	0
	1	0

Figure 6-3. Aft End Splice Lamination

Table 5-1 gives the following external limit loads for this splice station:

Bending Moment (in-lb)	=	282,000
Axial Load (lb)	=	-29,700
Shear Load (lb)	=	21,000

Due to the interruption of the splice bolt pattern by the cutouts, a high-peaking effect is introduced on the splice running load adjacent to the cutouts. This requires that the splice be designed for the most critical bolt.

The first task in the design of the splice was to determine the optimum pattern, size, and number of bolts, similar to the previously tested arrangements, that could be accommodated between the antenna cutouts. This was established to be the seven 3/8-inch bolt staggered pattern depicted in Figure 6-1.

From the moment of inertia, area, and center of gravity of this bolt pattern, the peak bolt load for the above external loads is 9,100 pounds limit or 13,600 pounds ultimate. This load can apply to any of the three bolts centered between the cutouts, depending on the plane of the external bending moment.

As noted in Section 6.2, the ultimate load exhibited by the 1/4-inch diameter bolt pattern described in Reference 1 was 10,200 lb/in, or 5,100 lb/bolt. From this, a full scale-up to 1/2-inch diameter bolts and twice the laminate thickness should give 20,400 lb/bolt, ultimate. For the 3/8-inch diameter bolt actually selected, the load should reduce approximately according to the ratio of bolt bearing areas. This would give a value of 15,300 lb/bolt compared with the requirement of 13,600 pounds. From the standpoint of shear strength, the strength of the selected bolt is 13,800 pounds compared with the above requirement of 13,600 pounds shear.

From this rationale, the design evolved to feature a 0.545 inch-thick titanium interleaved laminate twice the thickness of the sub-scale test laminate, and with the pattern of 3/8-inch diameter bolts shown in Figure 6-1. The basic end laminate is shown in Figure 6-4.

6.4 EQUIPMENT RING

The overall configuration of this ring is depicted in Figure 6-1, and the layup is defined by Figure 3-6. The cross-section, layup and material are similar to those used in the test ring reported in Section 4.3 and in Reference 2. T-300/934 high-strength G/E was selected for the material in contrast to the UHM GY-70/934 material used for the stiffness critical-shell structure. This selection was made since there is no stiffness requirement for the ring. T-300/934 is much lower in cost, and the higher interlaminar strength is beneficial. Attachment to the outer shell, as in the case of the test ring, is made with EA934 room temperature curing adhesive. Provision is made for mounting the equipment package by 32 1/4-inch diameter helicoil inserts in the aft face of the ring.

The anticipated failure modes are:

a. Shear of the ring/shell bond.

b. Pullout of the helicoil inserts.

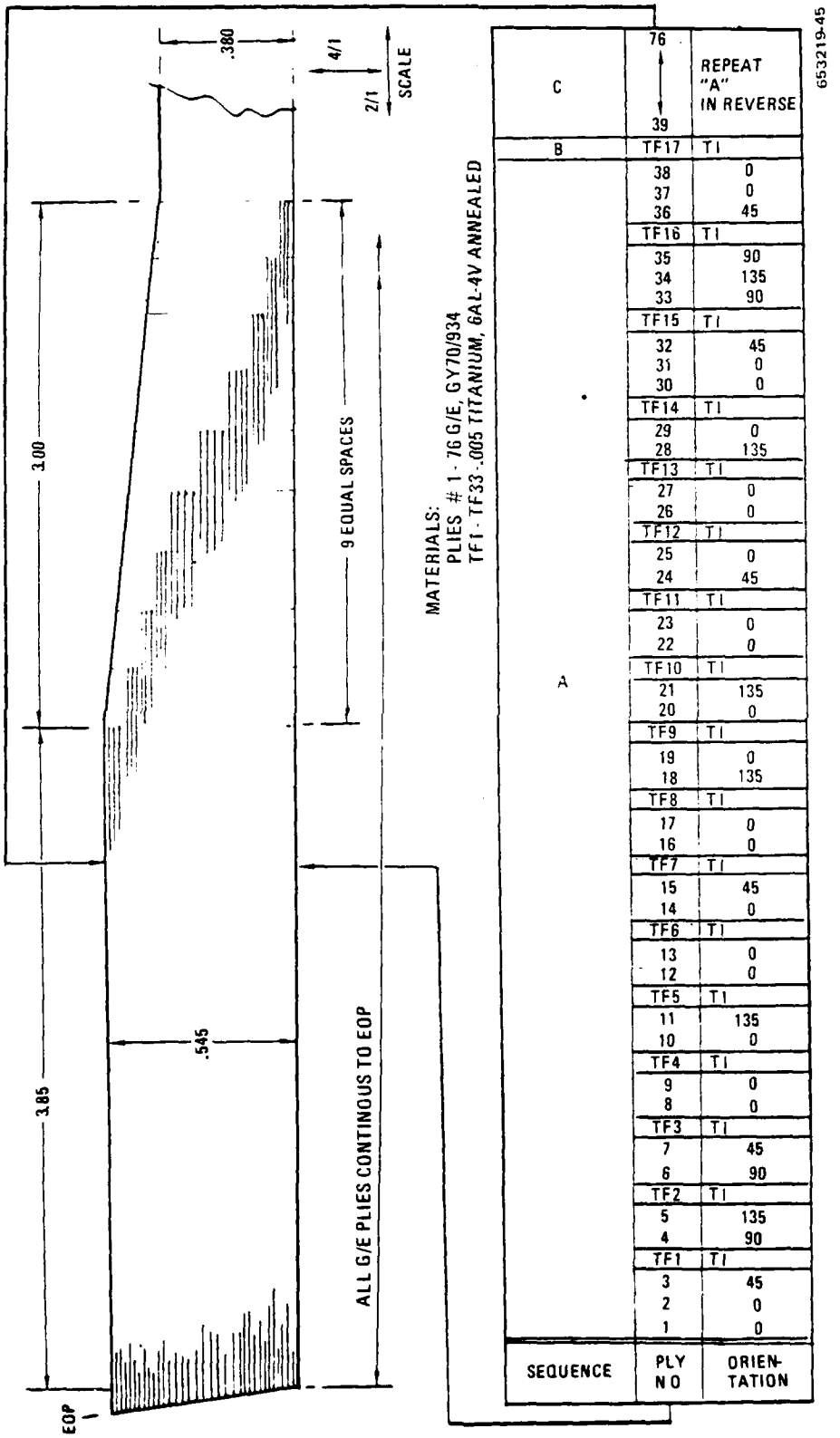

SEQUENCE	PLY NO	ORIENTATION
C	76 ↕ 39	REPEAT "A" IN REVERSE
B	TF17	T I
A	38	0
	37	0
	36	45
	TF16	T I
	35	90
	34	135
	33	90
	TF15	T I
	32	45
	31	0
	30	0
	TF14	T I
	29	0
	28	135
	TF13	T I
	27	0
	26	0
	TF12	T I
	25	0
	24	45
	TF11	T I
	23	0
	22	0
	TF10	T I
	21	135
	20	0
	TF9	T I
	19	0
	18	135
	TF8	T I
	17	0
	16	0
	TF7	T I
	15	45
	14	0
	TF6	T I
	13	0
	12	0
	TF5	T I
	11	135
	10	0
	TF4	T I
	9	0
	8	0
	TF3	T I
	7	45
	6	90
	TF2	T I
	5	135
	4	90
	TF1	T I
	3	45
	2	0
	1	0

Figure 6-4. Forward End Splice Lamination

The inertia loads applied to the ring are given by the discontinuities in the axial load and shear load curves in Figures 5-1 and 5-2. These are:

	Limit	Ultimate
Axial Load (lb)	36,000	54,600
In-Plane Load (lb)	12,700	13,250

These requirements were compared to the ring test results reported in Reference 2. The test ring was actually only slightly smaller than full size, 9.75 versus 11.00 inches diameter, thus a direct comparison of the test load with the design ultimate load could be made on a conservative basis.

Failure occurred in the ring test at 49,300 pounds at ambient temperature. A test at 325F with a load of 12,100 pounds did not cause failure. The failure mode for the 49,300-pound-load was pullout of the helicoil inserts. To improve this, the size of the helicoil for the current design has been increased from 3/16 to 1/4-inch diameter. Assuming that pullout strength varies directly with diameter, this change should increase the failure load for this mode to approximately 66,000 pounds. There was no indication of ring/shell bond failure in the test, so the ratio of test to full-scale diameters indicates that the current design is good for at least 55,000 pounds. This compares to an equivalent load of 57,900 pounds for the combined design axial and in plane ultimate loads, and since failure did not occur in the test, is considered sufficiently close for development purposes.

In this circumstance, the basic size and essentially the same cross-section used for the test ring were retained for the current design. The ply orientation and the layup sequence are also identical, as is the EA934 attachment to the shell. The previously discussed increase in the size of the helicoil inserts is essentially the only difference which has been introduced.

6.5 MASS PROPERTIES

6.5.1 BASIC-WEIGHT ESTIMATE. The following estimate was made for the current design configuration as defined on Drawing SK-ATI-009 (Figure 6-1).

Item	Weight (lb)
Basic Shell	28.71
Aft Titanium Interleaves	3.79
End Titamium Interleaves	3.58
Less Antenna Cutouts	−0.97
Less 85 Bolt Holes	−0.42
Equipment Ring	4.16
Equipment Ring Bond	0.07
Total Section	38.92

6.5.2 WEIGHT OF EQUIVALENT ALUMINUM STRUCTURE. For this stiffness critical structure, a close estimate of the minimum weight for an equivalent aluminum structure can be obtained from:

a. Determination of the aluminum shell thickness by using the same shell stiffness parameter. This parameter is the EI product where E is the modulus of elasticity of the shell material and I is the area moment of inertia of the shell cross-section.

b. In the absence of a stiffness requirement for the equipment ring, vary the weight of this item linearly with the density of the material. For a conservative comparison, assume that this ring is integrally machined in the aluminum structure.

6.5.2.1 Aluminum Shell Thickness. The effect of thickening the shell to compensate for the lower modulus of aluminum will vary along the length of a cone. To allow for this, the required inside diameter was determined at five stations and assumed to vary linearly between these points.

$$E_{GR} = 26.1 \text{ msi} \qquad E_{AL} = 10.4 \text{ msi}$$

$$I_{AL} = I_{GR} \frac{E_{GR}}{E_{AL}} = 2.51\, I_{GR}$$

$$I = \frac{\pi}{64} (D_0^4 - D_1^4)$$

Calculating the internal diameter for aluminum at each end and at 25 percent intervals of length between:

Sta No.	Graphite			Aluminum				Thickness (Ref)
	D_0	D_1	I_{GR}	I_{AL}	D_0^4	$D_0^4 - \frac{64}{\pi} I_{AL}$	D_1	
1	8.01	7.25*	66.47	166.84	4,117	718.17	5.18	1.42
2	9.86	9.10	127.36	319.67	9,452	2,939.74	7.36	1.25
3	11.71	10.95	214.70	538.90	18,803	7,824.62	9.41	1.15
4	13.56	12.80	341.97	859.34	33,810	16,303.67	11.29	1.13
5	15.41	14.65*	506.98	1272.52	56,391	30,476.44	13.21	1.10

Dimensions in inches.
*Not including effect of titanium interleaves.

It is noteworthy that the aluminum shell thickness required for equal stiffness is greater than the thickness of the graphite/epoxy shell multiplied by the ratios of the moduli (0.38 × 2.51 = 0.95).

Determine aluminum shell interval volume:

Sta No.	D_I	A_I	L	L_T	L_F	$L_T A_A$	$L_F A_F$	Segment Volume
1	5.18	21.07						
			8.425	28.445	20.02	1210.05	421.82	262.74
2	7.36	42.54						
			8.425	38.675	30.25	2689.46	1286.84	467.54
3	9.41	69.54						
			8.425	50.715	42.29	5077.08	2840.84	712.07
4	11.29	100.11						
			8.425	57.965	49.54	7944.68	4959.44	995.08
5	13.21	137.06						

Internal Volume =	2437.43 in^3
Total Volume =	3750.56
Shell-Wall Volume =	1313.13

6.5.2.2 Summary

Aluminum Shell Weight	132.63
Equipment Ring	6.99
Less Antenna Cutouts	−2.69
Less Bolt Holes	−1.68
Total Aluminum Version	135.25 lb

This value for this aluminum version should be considered as an approximation when compared with the realistic weight of 38.92 pounds for the graphite/epoxy shell. Several factors need to be considered apart from the direct maintenance of the EI product. Firstly, the 1.42 thickness at the forward end of the aluminum shell probably could not be spliced with the simple bolted arrangement used for the composite shell. Secondly, the same frequency might be attained more efficiently by decreasing the aluminum thickness at the forward end and increasing the aft-end thickness. Any such gain in efficiency, however, would to some degree be offset or perhaps negated by the effects on the frequency of the increased mass of the aluminum as compared with the composite shell.

SECTION 7

STRUCTURAL ANALYSIS

7.1 ANALYSIS OF TEST RESULTS

The composite ATI structure is shown in Figure 6-1, where the ends are attached to metal rings of the adjacent structures. The forward end shows three cutouts for antenna supports, which results in high-stress concentrations. Accordingly, titanium interleaves in a thickened section are provided to support the direct stresses and the high-bearing loads from the countersunk fasteners. The use of titanium interleaves was proven successful earlier (References 1 and 2) for high-bearing loads from countersunk fasteners. Titanium interleaves are also necessary for the countersunk fastener loads in the aft end.

A test program was performed by General Dynamics Convair Division and Martin Marietta Corporation on one-half scale G/E frusta with three different end joint design concepts for countersunk fasteners. The shell-specimen and end-joint concepts are shown in Figure 3-1. The test failure loads at the large end are presented in Table 4-1. The wall stresses in the half-scale specimens are equivalent to those that will be seen in the full size frustum. Accordingly, the test program has verified the strength integrity of the full-size basic shell wall. The frustum is shown in Figure 4-2 with two rows of ¼-inch diameter countersunk holes. Figure 4-10 shows a specimen-mounted in the test fixture for the shear/bending test. Figure 4-4 shows a specimen ready for the combined loading test. A view of the inside of the fixture at the large end (Figure 7-1) shows the nuts attached to the countersunk fasteners.

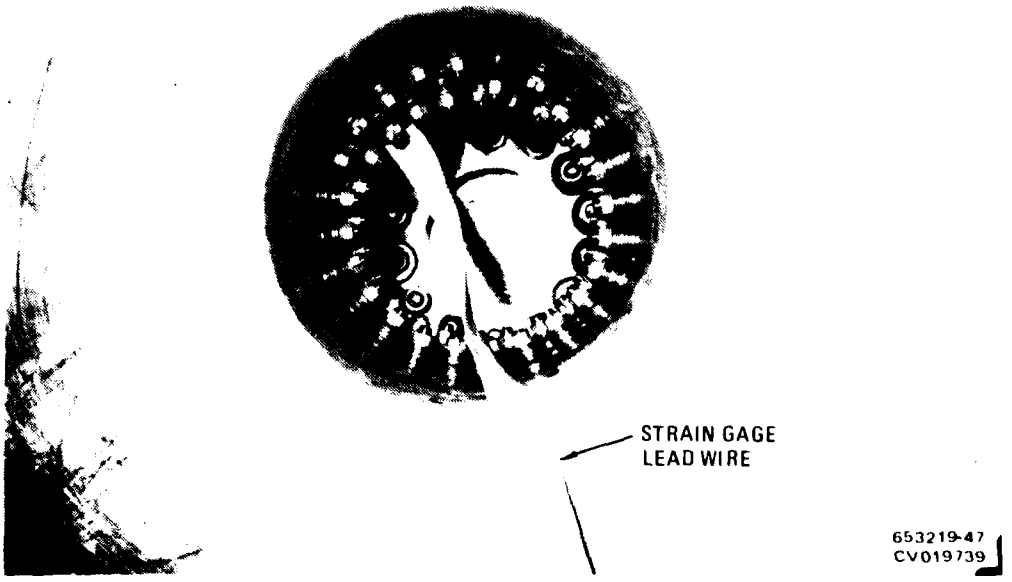

Figure 7-1. End View of Frustum Showing Countersunk Fasteners

The results of the foregoing tests are used to provide approximate design allowables for the full size structure, including the bearing allowables for the countersunk fasteners in the titanium interleaved G/E.

7.1.1 BEARING ALLOWABLE

Inside diameter of frustum at fasteners —

$$D_i \approx 7.58^* - 0.02 - (2 \times 0.270)$$
$$\approx 7.02 \text{ in. } (R_i = 3.51 \text{ in.})$$

*Calculated from dimensions in Figure 3-1

Inside circumference —

$$C_i \approx \pi D_i = 22.054 \text{ in.}$$

Circular distance (pitch) between fasteners —

$$d = C_i/24 = 22.054/24 = 0.9189 \text{ in.}$$

Maximum fastener shear on compression side for test specimen C3:

$$N^c_{max} = \frac{F^c}{C_1} + \frac{M}{\pi R_i^2} = \frac{35,900}{22.05} + \frac{302,000}{\pi \times 3.51^2} = 9431 \text{ lb/in}$$

$$P^s_{max} = \frac{N^c_{max} d}{2} = \frac{9431 \times 0.919}{2} = 4334 \text{ lb}$$

Maximum fastener shear for test specimen C4:

$$N_{max} = \frac{M}{\pi R_i^2} = \frac{340,000}{\pi \times 3.51^2} = 8784 \text{ lb/in (less critical)}$$

7.1.2 BEARING AREA. The fastener/nut clampup and the load carried in the countersink region was ignored. Random measurements were made on the depths of ¼-inch holes exclusive of countersink for one test specimen. The values varied from a minimum of 0.170 inch to a maximum of 0.194 inch. The mean measurement was 0.178 inch. Therefore, the bearing area is assumed to be about

$$A_{br} = 0.25 \times 0.178 = 0.0445 \text{ in}^2$$

Maximum ultimate allowable bearing stress:

$$F^{bru} = P^{s}_{max}/A_{br} = 4334/0.0445 = 97,390 \text{ psi (excludes countersink)}$$

7.1.3 EQUIPMENT RING. A test of a bonded intermediate ring was performed and a sketch is shown in Figure 7-2. The helicoils pulled out at a total load of 69,700 pounds (refer to Table 4-4). Thus, a lower bound allowable average shear stress for the adhesive bond over a 3-inch length may be found by

$$\tau^{a}_{avg} = \frac{69,000}{2\pi R \ell} = \frac{69,700}{2\pi \times 4.75 \times 3} = 770 \text{ psi}$$

which also includes some undetermined interlaminar tension at the small end.

There are 32 helicoils supporting the tension load of the fasteners. Thus, the allowable load of the helicoils in the present application is

$$P^{a}_{helicoil} = 69,000/32 = 2156 \text{ lb}$$

7.2 ANALYSIS OF PRELIMINARY DESIGN

7.2.1 FORWARD STRUCTURAL JOINT. A view of the forward-joint area is shown in Figure 7-2, and Sections A-A and B-B indicate the two lines of fasteners. Section B-B is shown in Figure 7-3 where the shear planes for the fasteners are indicated by the symbol (O). In addition, the shear planes for the fasterners of Section A-A are indicated by the symbol (□). It has been found that bending about the neutral axis shown is critical for obtaining the maximum shear load on a fastener.

For expediency, it is assumed that the two rows of fasteners are in the same plane. The critical limit loads found in Section 5 at Sta 27.5 (refer to Table 5-4) are

$$\left.\begin{aligned} P^{c} &= 29,700 \text{ lb} \\ S &= 21,000 \text{ lb} \\ M &= 282,000 \text{ in-lb} \end{aligned}\right\} \text{ Limit Loads}$$

The maximum shear load is on fastener 1B in Figure 7-3, and is found by the expression

$$S_{1B} = \frac{P^{c}}{N} + \frac{MC_{1B}}{\Sigma C_i^2}$$

where

N = total number of fasteners

C = distance of fastener shear plane from neutral axis (NA)

N = 21

C_{1B} = 3.70 in.

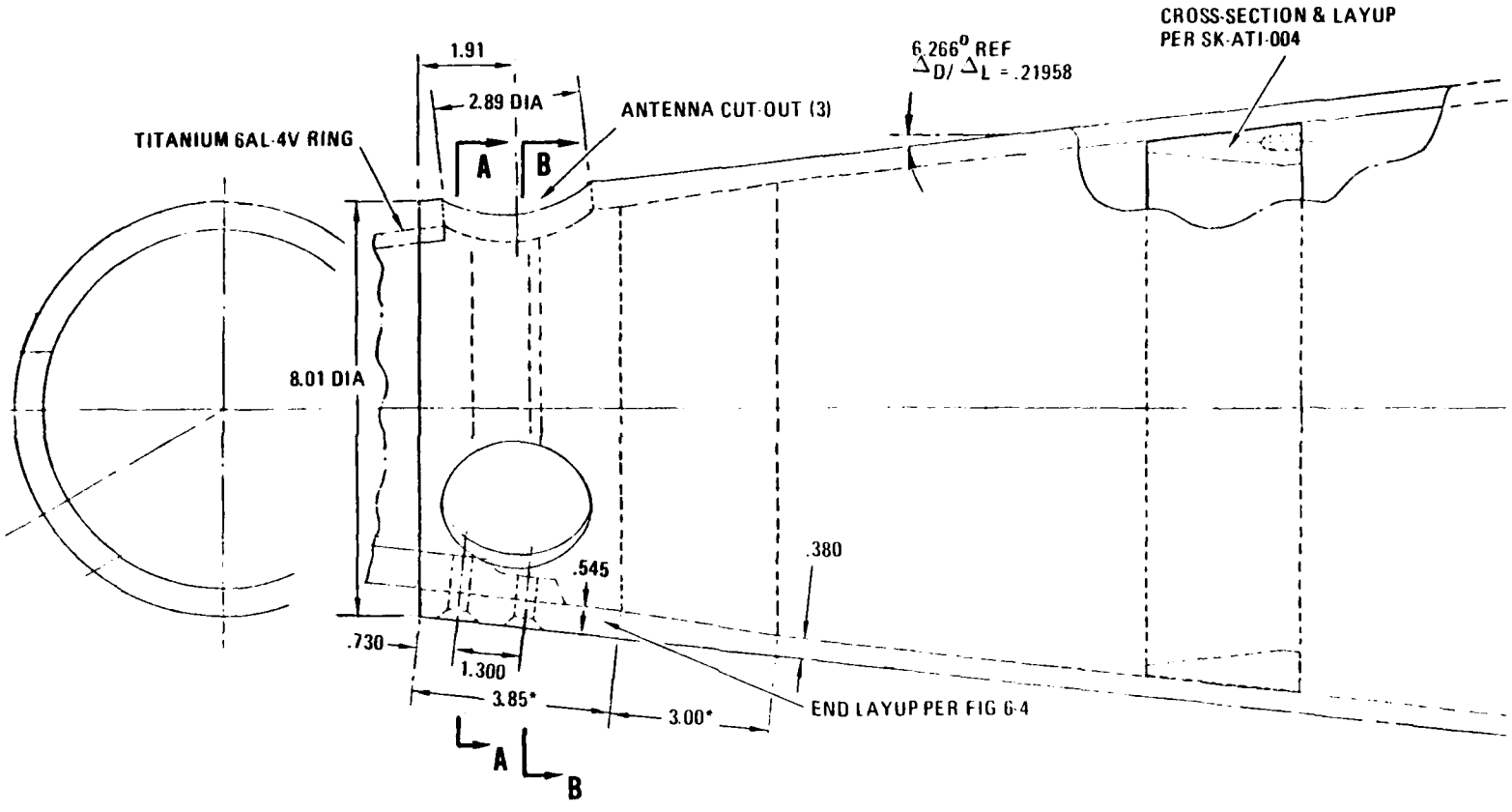

Figure 7-2. Forward End Joint of Frustum

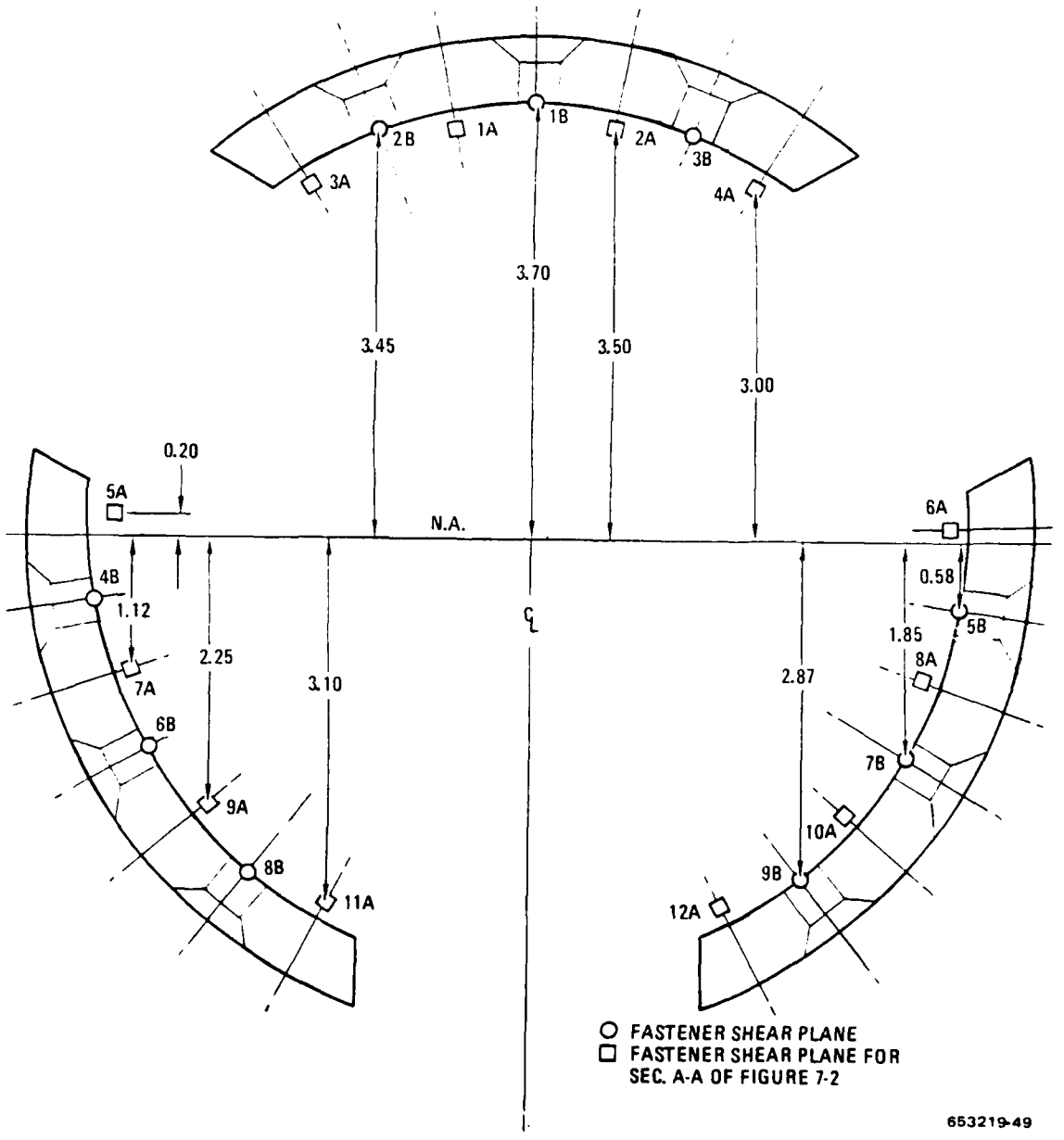

Figure 7-3. Section B-B of Figure 7-2

$$\Sigma C_i^2 = 3.70^2 + 2 \times 3.45^2 + 2 \times 3.50^2 + 2 \times 3.00^2 + 2 \times 0.20^2$$
$$+ 2 \times 1.12^2 + 2 \times 0.58^2 + 2 \times 1.85^2 + 2 \times 2.25^2$$
$$+ 2 \times 2.87^2 + 2 \times 3.10^2 = 135.9 \text{ in}^2$$

$$S_{1B}^{lim} = \frac{29,700}{21} + \frac{282,000 \times 3.70}{135.9} = 1414 + 7678 = 9092 \text{ lb}$$

$$S_{1B}^{ult} = 1.5 \times 9092 = 13,638 \text{ lb}$$

The approximate length of straight shank in bearing for the 3/8-inch diameter countersunk fastener is 0.35 inch. Accordingly, the approximate maximum bearing stress is

$$F_{ult,max}^{br} = S_{1B}^{ult} / (0.375 \times 0.35) = 13,638 / (0.375 \times 0.35) = 103,910 \text{ psi}$$

The margin of safety in bearing is

$$M.S.^{br} = \frac{97,390}{103,910} - 1 = -0.062*$$

The fasteners are heat treated steel HL33, where the allowable shear load is

$$S^a = 13,810 \text{ lb}$$

The margin of safety for the fastener in shear is

$$M.S.^{s} = \frac{13,810}{13,017} - 1 = 0.060$$

*This negative margin will disappear with just a slight hole elongation, whereby the fasteners on either side will pick up a greater share of the load. Then, the margin in this fastener will become positive.

7.2.2 AFT STRUCTURAL JOINT. The aft end is shown in Figure 6-1, where two rows of fasteners are required to carry the load. For expediency, assume the load is equally divided between the two rows. The critical limit loads found in Section 5 at Sta 61.2 (refer to Table 5-4) are

$$\left.\begin{aligned} P^c &= 77,100 \text{ lb} \\ S &= 50,700 \text{ lb} \\ M &= 1,306 \text{ in-klb} \end{aligned}\right\} \text{Limit Loads}$$

The maximum shear load on a fastener is found by the expression

$$S = \frac{P^c}{2N} + \frac{Mp}{2\pi R^2}$$

where

N = total number of fasteners per row

p = pitch of fasteners

P = mean radius of shear planes of the two rows

R = 7.04 in.

N = 32 (per row)

p = 1.38 in. (mean pitch)

$$S^{lim} = \frac{77,100}{2 \times 32} + \frac{1,306,000 \cdot 1.38}{2\pi \times 7.04^2} = 1205 + 5787 = 6992 \text{ lb}$$

$$S^{ult} = 1.5 \times 6992 = 10,488 \text{ lb}$$

$$\sigma^{br}_{ult} = S^{ult}/(0.375 \times 0.375 \cdot 0.35) = 79,915 \text{ psi (not critical)}$$

7.2.3 EQUIPMENT RING. The equipment ring in the full-size frustum is similar to the test ring shown in Figure 3-6 except for the respective cone angles. The cone angle for the test ring was 4.67 degrees, while the angle on the actual structure is 6.27 degrees. Because of the very small difference in these cone angles, the test result may be used in the analysis of the preliminary design. Also, since the shell wall of the test was one-half the thickness of the preliminary design, the use of the test data would be conservative.

The loads on the equipment ring at Sta 44.6 are presented in Section 6, and the critical design limit loads (refer to Table 5-2) are

P^t = 36,400 lb
S = 12,700 lb
} Limit Loads

The inside radius of the shell at the large end of the ring is

R = 5.50 in.

The average axial shear stress in the bondline is equal to

$$\tau^{axial}_{avg} = \frac{P^t}{2\pi R \times 3} = \frac{36,400}{2\pi \times 5.5 \times 3} = 351 \text{ psi lim}$$

$$\tau^{axial}_{ult,avg} = 1.5 \times 351 = 527 \text{ psi}$$

The maximum hoop shear stress on the bondline is equal to

$$\tau^{hoop}_{max} = \frac{S}{\pi R \times 3} = \frac{12,700}{\pi \times 5.5 \times 3} = 245 \text{ psi lim}$$

$$\tau^{hoop}_{ult,max} = 1.5 \times 245 = 368 \text{ psi}$$

The maximum ultimate resultant shear stress in the bondline is equal to

$$\tau_{ult,max} = \sqrt{\left(\tau^{axial}_{ult,avg}\right)^2 + \left(\tau^{hoop}_{ult,max}\right)^2} = \sqrt{527^2 + 368^2} = 643 \text{ psi}$$

$$\tau^{a}_{avg} = 770 \text{ psi (refer to Section 7.1)}$$

The axial shear on the bondline results in much higher peak stresses than those due to transverse shear loads. Accordingly, the margin of safety for the maximum bondline shear stress may be expressed in the form

$$\text{M.S.} > \frac{\tau^{a}_{avg}}{\tau_{ult,max}} - 1 > \frac{770}{643} - 1 > 0.19$$

SECTION 8

MANUFACTURING STUDY

A manufacturing analysis was conducted concurrent with the full-scale section definition. The need to facilitate rate production along with functionality was emphasized during the design of the ATI composite structure. The manufacturing analysis was based on the following groundrules:

a. A production rate of 1,000 units per year (four per day).

b. Materials and processes identical to those used in fabrication of conical frusta under this program and the prior contract, DAAG46-76-C-0008.

c. Production based on formally reviewed and released standard planning emanating from approved materials and process specifications.

d. Tools manufactured to formally reviewed and released tool design drawings.

e. All production work accomplished on a standard 40-hour week, three-shift basis.

The preliminary full-scale design is producible on a rate production basis. Production experience gained at General Dynamics Convair Division on a similar size and shaped part, the Standard ARM radome, was applied where applicable in arriving at our proposed manufacturing cycle. The radome was manufactured using fabric reinforced polyimide, gore patterns, female tools, autoclave curing, and approximately the same production rate as groundruled for this study.

The GY-70/934 prepreg used to date in making the subscale conical frusta was all standard prepreg. GY-70 prepreg is unique in a sense from other graphite prepregs in that the starting material provided by Celanese is a 3-inch wide tape of 304 parallel yarns woven with a light carbonized filling yarn (2 picks/inch) to help maintain the GY-70 yarn collimation. Because of this unique form of starting material, the prepregger is generally limited to nominal 3-inch wide tape for the final prepreg. In recent years, some companies have taken the fiber tape form supplied by Celanese, cut the filling yarns, and respooled the GY-70 as single end yarn. The latter has been available to prepreggers at approximately a 36 percent increase in fiber price. This latter form could be used for prepregging wider tapes and possibly for tape laying large sheets. Since this latter form has not been used in the program to date, the manufacturing study was conducted with the conventional tape form as a baseline. Potential cost savings from material changes or process changes are discussed in a later section.

The baseline form limits mechanization to gore cutting. The initial layup of sheets and layup of gores into female tools would still be done manually. Compaction of single-ply sheet stock would be accomplished on vacuum-augmented layup benches. Curing four or more full-scale conical sections as well as numerous equipment rings in a single autoclave run minimizing cycle time per part.

8.1 FABRICATION TECHNIQUES

8.1.1 CONE LAYUP AND CURE. Each batch of graphite/epoxy prepreg and perforated titanium foil will be acceptance-tested per pertinent material specification requirements prior to storage for use. The graphite/epoxy prepreg rolls will be stored in the original moisture-proof bags at 0F. When fabrication is ready to begin, the rolls will be thawed to within 10 degrees of ambient temperature prior to removal from their sealed moisture-proof bags. The tape will be laid onto large caul plates that have been covered with perforated Teflon-coated glass fabric. The tape will be laid down to form large rectangular sheets of single-ply prepreg of predetermined dimensions. The prepreg sheets will be covered with a ply of perforated Teflon-coated glass fabric. The entire operation will be conducted on a vacuum table that will have a reusable rubber bag and a quick, reusable edge-seal design. The single-ply sheets will be compacted on the vacuum table to stabilize them prior to die cutting them into the proper gore configurations. The size of sheets and cutting layout plan will be optimized to minimize material scrappage. After compaction, the graphite/epoxy prepreg sandwiched between release films will be die cut using an automatic steel-rule die press with nested dies. This press will also be used to trim bleeder materials.

There will be twelve unidirectional gores, each with a segment wrap angle of 30°, for every 0° ply. There will be four angled gores, each with a segment wrap angle of 90°, for every off-axis ply (+45°, 90°, or −45°). Sufficient gores to make a single ply will be kitted in sealed plastic bags and identified. The kits will then be returned to 0F storage.

Perforated titanium foil, which will act as inserts for both forward and aft flange areas, will also be die cut into gore segments. These gores will be cleaned, acid-etched, and then assembled and kitted in plastic bags in a similar manner to the graphite epoxy gores.

When ready to proceed with cone layup, the bulk graphite tool will be Frekoted and subjected to a typical graphite/epoxy cure cycle. The kits of prepreg will be thawed and prepreg layup will proceed per drawing requirements and planning instructions. Layers of titanium foil will be placed in the forward and aft areas as specified. Preplying and precompaction steps will occur at intervals in the layup as specified on the drawing. Preformed rubber bags will be used for these operations as well as during the final cure operation. Preplying is conducted at room temperature under vacuum-bag pressure, while precompaction is accomplished in an autoclave. The latter is accomplished using vacuum bag plus 50 psig autoclave pressure and a maximum temperature of 160F. Alternating layup and compaction steps will continue until the layup is complete. Then the part is to be bagged and cured in an autoclave with maximum temperature and pressure of 350F and 100 psig, respectively. Sufficient parts are included in each cure cyle to meet the required production rate. Layup and cure of equipment rings is accomplished in a similar manner.

After the parts are cured, they are debagged and removed from the tools. The cones and rings will be machine trimmed, and the antenna cutouts will be machined. End-ring attach holes will also be drilled into the cone at this point. Fixtures will be provided to ensure machining accuracy at a minimum of elapsed time.

8.1.2 EQUIPMENT RING BONDING. Assembly tools will be provided for bonding the equipment rings into the cones. Provision will be made for correct axial and rotational location. Each

equipment ring and cone will have their mating surfaces abraded and solvent cleaned prior to the adhesive application. Hysol EA-934 will be used for the adhesive bonding and a minimum cure of 24 hours at room temperature will be specified prior to further cone processing. Wire shims will be used in the bonding operation to control bonding thickness. Ring drilling and helicoil installation can be accomplished before or after bonding. If it was accomplished prior to bonding, the antenna cutouts and end joint attach holes would be done as the final operation. The trim and drill fixtures would be designed to assure proper relationship of the helicoils in the equipment ring with the antenna cutouts and end-joint attach holes.

8.2 OTHER DESIGN CONCEPTS

Two other material and design concepts for the equipment ring were considered during the course of this study. The two materials studied, bulk graphite and titanium, need more conventional ring designs (refer to Sections 3.3.1 and 3.3.2). The bulk graphite is subject to impact damage and is marginal in its ability to meet load requirements. The bulk graphite design was a solid ring with a quadrilateral cross section. The titanium-ring design had a primarily rectangular cross section that then tapered sharply at the outer diameter in both directions to a much wider section. The tapered design has been used successfully in the past to reduce peak load stresses at the edges of the joint. Although the titanium equipment ring concept was tested and found to successfully carry the loads, it was decided to go with the wedge-shaped graphite/epoxy ring design as baseline. This material results in a closer thermal expansion match between cone and ring and would minimize thermal stresses arising during flight heating. It would allow the use of elevated temperature curing adhesives should that prove necessary at some later date.

Graphite/polyimide systems were also considered during the design phase for possible use in future versions of the conical shell. Although the present thermal requirements do not require or justify the use of polyimide systems, the manufacturing approach would not change should we go to bismaleimide-type resins. Resins such as Hexcel F-178 and U.S. Polymeric V-378A could be used in place of the epoxy with no change in layup, preplying, or precompaction procedures. The final cure conditions, 350F and 100 psig, would remain the same although heatup rates and hold times would vary from those used with the Fiberite 934 epoxy. A postcure would be required, dependent on desired maximum use temperature.

8.3 FACILITY AND TOOLING REQUIREMENTS

8.3.1 FACILITIES. The assumed production rate of 1,000 units per year warrants the setup of a stationized line to fabricate the ATI composite structures. Prior to production go-ahead, a trade study should be conducted to determine the optimum form for the graphite/epoxy prepreg. This study would evaluate the baseline 2.75-inch wide preimpregnated GY-70/934 versus unidirectional GY-70/934 broadgoods made from GY-70 single yarns. In either event, two vacuum-layup (press) tables, approximately 3 ft. by 8 ft. would be required to compact sufficient single-ply sheet stock to support the material requirements of a single frustum per day. This assumes 76 plies of prepreg per frustum and a scrappage cutting factor of 25 percent. Assuming a useful layup area of approximately 22 ft^2 for the table, one arrives at a requirement for 35 runs/day/cone. We anticipate 20 runs/day for a three-shift operation, and therefore, to support the production of four cones per day we would require seven vacuum-layup tables.

The stock would be taken off the vacuum layup tables in the form of large unidirectional sheet sandwiched between layers of porous Teflon-coated glass cloth. These would be fed through an automatic press having a 20-ft-long bed of steel-rule dies. This would allow the die cutting of two sheets per press closing. One press could accommodate the daily output of seven layup tables. The single-ply gores would be kitted in sealed polyethylene bags, identified, and stored in a walk-in freezer awaiting layup in the bulk-graphite female tools.

All titanium gores would also be die cut on a press. This would require a second press with its own permanent setup of steel-rule dies. The titanium gores would be acid etched in a dedicated process line prior to being kitted and sealed for storage.

All operations that involve the uncured graphite/epoxy would be conducted in a temperature/humidity/particle-size controlled room. Periodically, during the layup process, the parts would be bagged and preplied at room temperature and precompacted in a small autoclave at elevated temperature and pressure. A minimum of 12 female tools would be required, since the total part layup and cure time is approximately three days. An additional six tools would be required as backup to replace damaged tools while they are being repaired. A second, larger autoclave would be required for daily curing of cones and equipment rings.

Gore sections and female tools are used in the manufacture of equipment rings in a manner similar to that used in the layup of the conical shells. The primary difference is the use of 8-ply modules rather than individual plies for the layup.

Standard machining equipment could be used to machine and drill the conical shells and equipment rings. High-speed steel or carbide tools would be used to machine the titanium interleaved graphite/epoxy composite. For drilling pure graphite/epoxy such as the holes on the wedge-type equipment rings, we would use diamond-coated drill bits. Fixtures would be required to support end trimming, machining of antenna cutouts, and drilling of holes in the shell-joint areas.

The layout of a facility which would support the manufacture of a 1,000 units per year is shown in Figure 8-1. This type of layout facilitates linear work and task stationization.

8.3.2 TOOLING. The family of tools listed herein was selected to minimize labor using a state-of-the-art approach. Steel-rule dies nested on a common board minimize material scrappage and trim labor. The female molds will be supported on rollers on a cart to facilitate layup and tool movement. A sketch of the cone mold is shown in Figure 8-2. Provision would be made on the molds to simplify the use of silicone rubber bags for debulking and curing. For all machining operations, fixtures would be fabricated to ensure accuracy while minimizing setup labor. Where practical, machining operations would be numerically controlled.

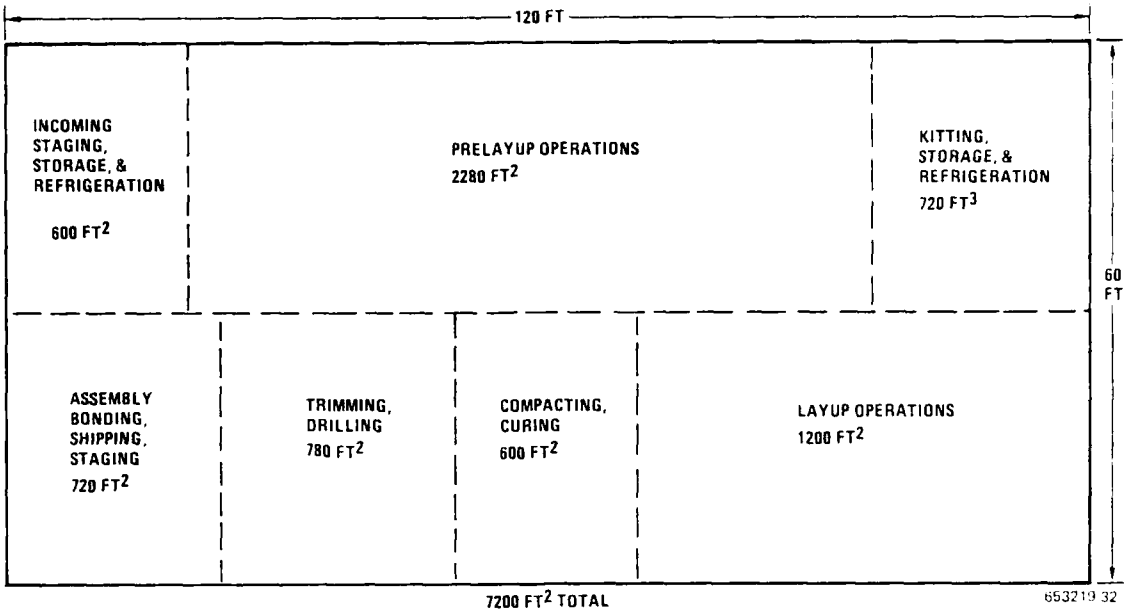

Figure 8-1. Typical Production Area Requirements

TOOL LIST

Cone

- Steel-rule dies for graphite/epoxy (G/E) gores
- Steel-rule dies for titanium gores
- Cure mold, bulk graphite, female
- Fixture for milling cone aft end
- Fixture for milling cone forward end
- Fixture to hold and index cone for machining antenna cutouts

Equipment Ring

- Steel-rule dies for G/E gores
- Cure mold, bulk graphite, female
- Fixture for milling ring aft and forward ends
- Insert hole drill fixture

Assembly

- Assembly bond tool — cone and equipment ring
- Fixture for drilling for the forward and aft ring attach bolts

8.3.3 STARTUP PLAN. Prior to any start-up activities, a manufacturing plan will be prepared utilizing the experience of manufacturing engineering and production personnel gained on the

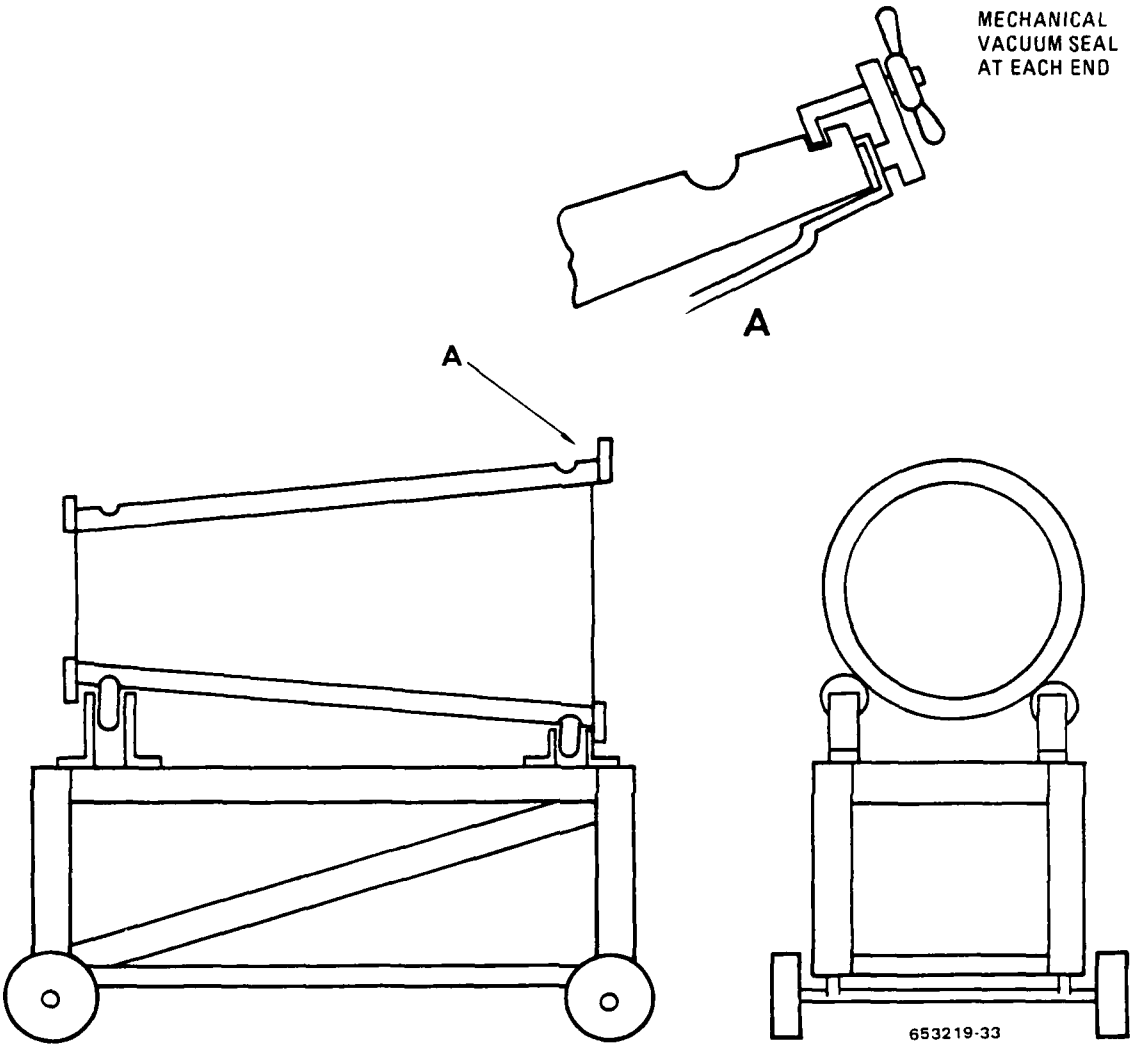

Figure 8-2. Production Cure Mold Concept

successful Standard ARM radome program. Many features developed in tooling, shop aids, and facilities to decrease labor and increase reliability are directly applicable.

In the interest of reaching rate production early, General Dynamics Convair Division would initiate production in the general composite fabrication area as soon as tooling becomes available. When the individual facility items become operational, they would be installed and used. The fabrication tasks would gradually be moved to the dedicated production area, until finally all work would be done there. Figure 8-3 shows the anticipated schedule for production start-up.

To achieve this schedule, it would be necessary to initiate tooling and facility tasks at the earliest possible point in time. The bulk-graphite female tools for curing of shells can be obtained

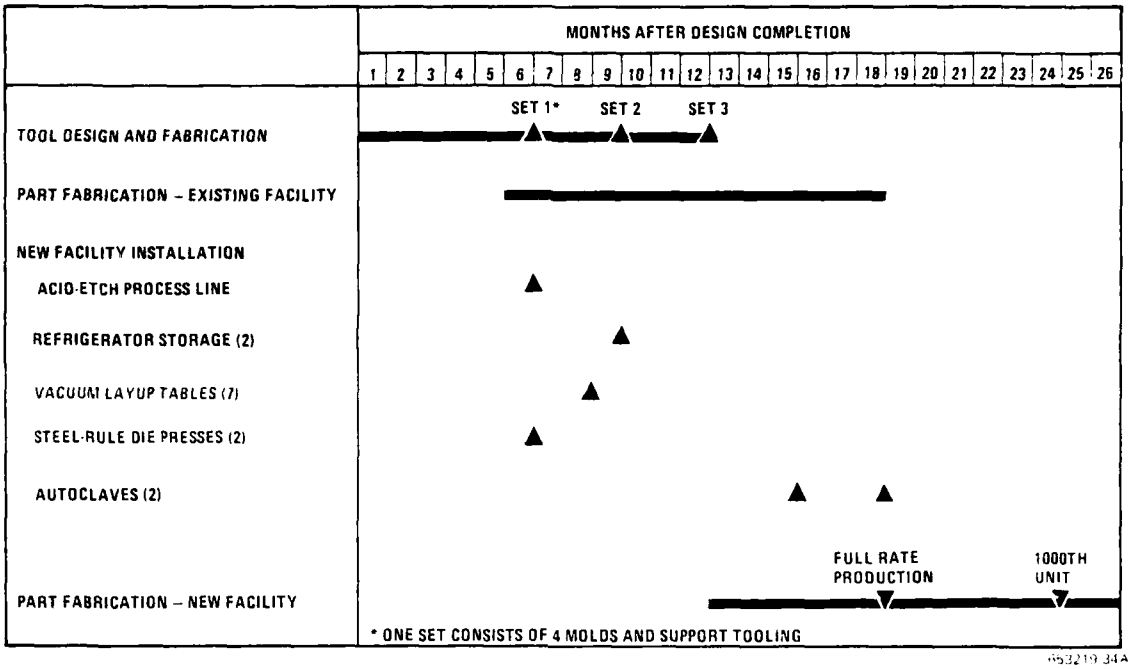

Figure 8-3. Projected Production Startup Schedule

prior to design completion since the outer contour of the cone would be known. The autoclaves, vacuum benches, automatic stamping presses, and steel-rule dies are also items that could be ordered early.

8.4 COST STUDY

The average unit cost of an ATI composite structure (cone and equipment ring assembly), based on a production quantity of 1,000, was parametrically estimated to be $57,000. This figure, in 1979 dollars, is for recurring cost only and does not include design, tooling, or facilities. It assumes that the G/E will be obtained in tape form and hand laid up into sheet stock. The fabrication techniques described in Section 8.1 and the facility and tooling requirements described in Section 8.3 were used as an estimating baseline.

Of the approximately 600 manhours (unit average) estimated, 482 manhours are fabrication hours. The remaining 128 manhours are for other direct hourly charges, including quality assurance. An 82 percent learning curve was used because this rate of efficiency increase was experienced on the Standard Arm Radome during volume production. Utilizing this curve, the $1{,}000^{th}$ unit would drop to 430 manhours, total.

Table 8-1 shows the labor distribution between fabrication operations for three different circumstances. The first column contains an estimate of the hours that would be required by the technicians in the engineering laboratory. They are highly skilled and have the benefit of having fabricated many similar structures. The second column is an estimate of the hours that

Table 8-1. Fabrication Manhour Estimate Comparisons

Operation	Lab. Fab. Unit 32 (Hours)	Production Unit 32 (Hours)	Production Unit 250 (Hours)
Cone			
Preplying	38	56	24
Gore Cutting	38	62	20
Kitting	24	24	8
Ti Foil Preparation	64	70	30
Mold Preparation	4	4	4
Lay-Up	128	210	128
Cure	20	14	12
Trim	100	120	90
Subtotal	416	560	316
Equipment Ring			
Preplying	20	26	18
Gore Cutting	30	48	12
Mold Preparation	4	4	4
Lay-Up	70	110	70
Cure	16	12	10
Trim/Drill/Inserts	40	70	24
Subtotal	180	270	138
Assembly			
Fixture Setup	4	8	2
Install Ring	8	16	8
Cure	8	16	18
Subtotal	20	40	28
Total	606	870	482

would be required by the plastics shop personnel on the 32nd unit. Generally, these hours are higher than the laboratory hours, reflecting early learning on production tooling and worker training. An exception is the time required for curing. The lower shop hours result from curing four parts at a time, whereas the laboratory would cure one part at a time. The third column is an estimate of the hours that would be expended at the average cost level (unit 250). These hours reflect familiarity with the production tooling. At the 250 unit, lay-up hours have reached the efficiency level of the engineering laboratory personnel. Preplying, gore cutting, and curing,

because of improved material handling and mechanization, have surpassed laboratory efficiency. It is expected that the fabrication hours for unit 1000 would drop from the unit 250 total of 482 hours to 324 hours.

8.5 POTENTIAL COST REDUCTIONS

During this program, we have continuously reviewed the materials and manufacturing cycle to identify potential areas for cost reductions. Several areas in the type and form of graphite/epoxy prepreg material have potential for cost reduction. In the area of GY-70/934 unidirectional tape, we are presently limited to 2.75-inch-wide tape. Although single end GY-70 fiber is presently 36 percent more costly per pound than the Celanese continuous 3-inch-wide lightly woven tape, Fiberite has been working on a technique of slitting the tape and respooling the single yarns that may prove cost effective from a prepreg-price standpoint. Present projections indicate that prepreg made from the respooled single yarns will cost 65 percent more per pound than existing GY-70/934 tape. The advantage to using respooled yarns is that it would then be possible to produce uniform 12-inch wide continuous GY-70/934 tape. This would save approximately 75 percent of the hand layup costs prior to gore cutting, since each strip being layed down would be equivalent to 4.36 strips of presently available tape. There would also be some secondary advantages such as easier inventory control.

A second potential cost reduction can be accomplished by replacing the GY-70/934 with the new P-75S/934. The P-75S is a relatively new pitch-based UHM graphite fiber manufactured by Union Carbide. Some typical General Dynamics data obtained recently on unidirectional laminates is as follows:

Ultimate Tensile Strength	87.1 ksi
Ultimate Tensile Modulus	48.1 msi
Ultimate Flexural Strength	101 ksi
Ultimate Flexural Modulus	45.5 msi
Horizontal Shear Strength	10.3 ksi
Fiber Volume	65%
Specific Gravity	1.73

Present costs for mid-size quantities of GY-70/934 and P-75S/934 are $303 and $138 per pound, respectively. On a straight substitution basis, one would save approximately 54 percent in frustum material costs (approximately $8,000*). However, the P-75S prepreg tape can presently be made 12 inches wide or wider. This would then present a 75 percent layup cost reduction in addition to the lowered material cost. In large quantities, such as that needed for a 1,000 ATI units per year, it is envisioned that P-75S/934 costs could approach $100 per pound. This would raise the potential material cost savings to approximately 67 percent.

A third potential for cost savings is to layup multiple stacks of unidirectional layers of prepreg each sandwiched between two layers of porous Teflon-coated glass cloth. These multiple stacks could then be fed through the automatic presses and die cut as multiples. The number

*Based on a scrap factor of 50 percent.

of multiples that could be cut in this fashion would have to be determined experimentally.

A fourth technique to reduce costs would be to change gore size on all 0° plies. At present, the 0° plies all have a wrap angle of 30°. By going to a wrap angle of 90° we could minimize the costs of laying the material in the tools. This change would also reduce handling costs in kitting and tooling costs for steel-rule dies. The effect of larger gores on the structural properties of the cones would have to be evaluated analytically and/or experimentally.

SECTION 9

CONCLUSIONS

The following conclusions are drawn as a result of this program:

a. A preliminary full-scale frustum design has been completed.

b. Analysis of this design show that the full-scale graphite/epoxy frustum will meet all design requirements. A full scale test plan has been prepared that would demonstrate viability of the design.

c. The graphite/epoxy frustum would weigh 38.92 lb vs 135.25 lb for an aluminum frustum (a 71 percent weight savings).

d. Manufacturing studies have shown that the General Dynamics Convair Division could produce the ATI guidance and control section at 1,000 articles/year.

e. Thermal analysis of an ATI concept showed that there is no internal heating of the graphite/epoxy substructure.

f. The graphite/epoxy and titanium concepts of equipment rings have proven successful in carrying the required loads. The graphite/epoxy ring was selected for the full-scale development because it minimizes thermal expansion stresses.

g. Two of the reinforced joint concepts met and exceeded the design requirements. The failures of these reinforced joint specimen were in the basic shell, not the joint.

SECTION 10

RECOMMENDATIONS

General Dynamics Convair Division recommends that this successful program be continued to the successful demonstration of full-scale hardware. Specific recommendations are:

a. At least two frusta sections representing the forward-end of a full-scale frusta should be built and tested to demonstrate the design concept.

b. A limited number of coupons of the full-thickness joints should be tested to demonstrate scale-up techniques.

c. At least two complete full-size frusta should be built using concepts developed in this and earlier programs.

d. These two frusta should be drilled and fitted the same as would be done on a production article.

e. These two frusta should be tested as outlined in the full-scale test plan prepared as part of this report and given in Appendix E.

f. Further articles should be made and tested on a full-scale test bed when one becomes available.

SECTION 11

REFERENCES

1. Koo, F.H. and Seinberg, J.P., "Subscale Development of Advanced ABM Graphite Epoxy Composite Structure," Martin-Marietta Corp., Report No. AMMRC TR 78-4, January 1978.

2. Hertz, J., "Ultra-High-Modulus Graphite/Epoxy Conical Shell Development," General Dynamics Corp., Report No. AMMRC TR 78-38, April 1978.

3. Hertz, J., "Ultra-High-Modulus Graphite/Epoxy Conical Shell Development," General Dynamics Corp., Report No. AMMRC TR 78-38 Supplement, August 1978.

4. Holmes, R.D. and Haskins, J.F., "Advanced Composites Design Data for Spacecraft Structural Applications," General Dynamics Convair, Report No. CASD-AFS-78-006, May 1979.

5. Forest, J.D., Fujimoto, A.F., and Foelsch, G.F., "Advanced Composite Applications for Spacecraft and Missiles, Phase I Final Report," General Dynamics Convair, Report No. AFML-TR-71-186 Volume I, March 1972.

6. Harrington, N.M. and Miyazawa, E.T., "Systems Analysis for Development of ATI Full-Scale Composite Frustum," Prototype Development Associates, Inc., Report No. PDA TR-5431-00-03, July 1979.

7. "Advanced Terminal Interceptor Technology Program, Volume 7: SPRINT Derivative Program Plan," Martin-Marietta, Report No. OR-12,393-7, April 1973.

APPENDIX A

TEST PLAN

Development of Advanced Interceptor Substructural Materials

DAAG-46-78-C-0056

Test Plan

30 October 1978

by

N. R. Adsit

GENERAL DYNAMICS
Convair Division

1.0 INTRODUCTION

Previous work on contracts DAAG46-76-C-0008 and DAAG46-75-C-0097 have shown that graphite/epoxy cones can be manufactured and tested that meet the Advanced Terminal Interceptor (ATI) required loads. This series of tests is to expand that initial effort and test other elements. The work includes tests of the base joint on four (4) cones (i.e., joint reinforcement specimens). These will be tested with one each, of two designs, tested in (1) combined axial load and bending load, and (2) shear load. Specimens will be fully instrumented to allow a comparison with previous tests.

The second set of tests will use the remaining four (4) base joint cones fitted with two configurations of equipment rings. One each of these specimens will be tested in shock loading and one each will be static tested.

The third set of tests will involve the testing of two new 13.4 inch long cones fabricated on this contract and fitted with the best design(s) for the equipment ring. These specimens will be tested statically.

2.0 BASE JOINT TESTS

This series of tests will evaluate the two untested designs of base joint reinforcement. We will use the same test conditions as were used for the previous test of joint reinforcement type I. These are (1) a combined axial and bending test, and (2) a shear/bending test. As in the previous tests the design limit loads for the combined tests are:

P (axial compression) = 19,000 lb

V (shear at fixed end) = 12,000 lb

M (bending moment at fixed end)= 158,000 in-lb

The design limit shear load is 30,000 lb for the shear-bending test. A total of sixteen (16) single element strain gages (FAE 25-12S0) will be installed on the shell specimen. The locations of these gages are shown in Figure 1. Along with the strain gages, four (4) deflection gages will be installed to measure the joint displacement and rotation.

The test cone will be attached to the test fixture by means of the forty-eight 1/4 inch screws at the reinforced end and by thirty-six 5/16 bolts at the loading end. The schematic of this test set-up is shown in Figures 2 and 3.

After the test cone is installed in the loading fixture, photographs of the test set-up will be made and all instruments will be adjusted to zero for the start of the test. The loads will be increased simultaneously in increments of 10% of Design Limit Load (DLL). Readings of all instrumentation will be made while the load is constant. After failure, the cone will be unloaded and the failure area examined.

3.0 CONES WITH EQUIPMENT RINGS

Work completed on contract DAAG46-76-C-0008 showed that an all graphite/epoxy cone and equipment ring far exceeded the design requirements. The work here will be to test two other concepts of equipment rings and determine their adequacy.

3.1 Static Tests of Half Size Cones

Two static tests will be run with two different design concepts of the equipment ring. Each graphite/epoxy cone will be instrumented with ten (10) strain gages. Six will be installed near the equipment ring and the other four will be at the top of the cone. An elevated temperature curing epoxy adhesive (M-bond 600) will be used. This adhesive cures at 200 F which is substantially below the cure temperature of the cone. The use of such an adhesive will allow us to obtain data from an elevated temperature test as well as an ambient temperature test.

The cones and equipment rings will be tested in axial compression only as was done previously. A sketch of the test set-up is shown in Figure 4. Tests will be conducted in the sequence given in Table I. Each specimen will be incrementally loaded during each test. Increments will be 10% of the DLL and the strain will be recorded on a digital strain indicator/recorder.

AD-A090 127 GENERAL DYNAMICS SAN DIEGO CA CONVAIR DIV F/G 11/4
DEVELOPMENT OF ADVANCED INTERCEPTOR SUBSTRUCTURAL MATERIAL(U)
AUG 80 J HERTZ, N R ADSIT DAAG46-78-C-0056

UNCLASSIFIED AMMRC-TR-80-44 NL

2 OF 2
AD A 090127

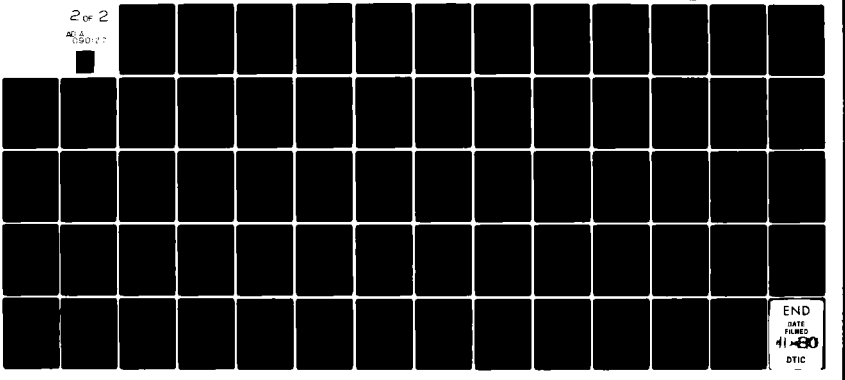

END
DATE FILMED
11-80
DTIC

3.2 Shock tests of half scale cones

Two cones will be used for this part of the study. Each will have twelve axial type strain gages (FAE-25-12S0) installed. The placement will be as shown in Figure 5. The strain measurements will be recorded on magnetic tape during the testing.

One accelerometer will be mounted on the base of the test fixture to measure the acceleration level of the input pulse. The data will be used in the shock spectrum analyzer.

The graphite/epoxy frustum will be bolted to a test fixture through the 48 countersunk holes. The test fixture will be fastened to the shock machine at its base. The smaller end of the frustum stands free. The test fixture is designed such that the loads are transmitted to the frustum through the 48 radial screws. Figure 6 shows the frustum and test fixture in relation to the shock machine.

The shock machine (HYGE) will simulate as closely as possible the specimen shock environments shown in Figure 7. In order to determine the fragility level of the reinforced joint, the acceleration magnitudes of the test environment will be increased on successive shock pulses. The shock machine will be calibrated so that the increments in acceleration magnitudes correspond to those shown in the shock spectra (Figure 7) as closely as possible.

3.3 Static tests of subscale frustum cone

The effort in this phase of the test program is to evaluate the three previous equipment ring tests. From these data we will fabricate and test the most promising design(s) of equipment ring.

The test set-up and procedure will be similar to that discussed above in section 3.1. As above, and in our previous tests, ten strain gages will be installed to measure the strain in the shell around the attachment point of the equipment ring.

The same loading sequence given in Table I will be used but the magnitude of the loads will be increased to

$$P_F = 129,500 \text{ lb}$$

$$P_R = 12,600$$

$$P_e = 10,080$$

At the conclusion of the tests we will examine the failure mode of the equipment ring shell to determine the adequacy of the design.

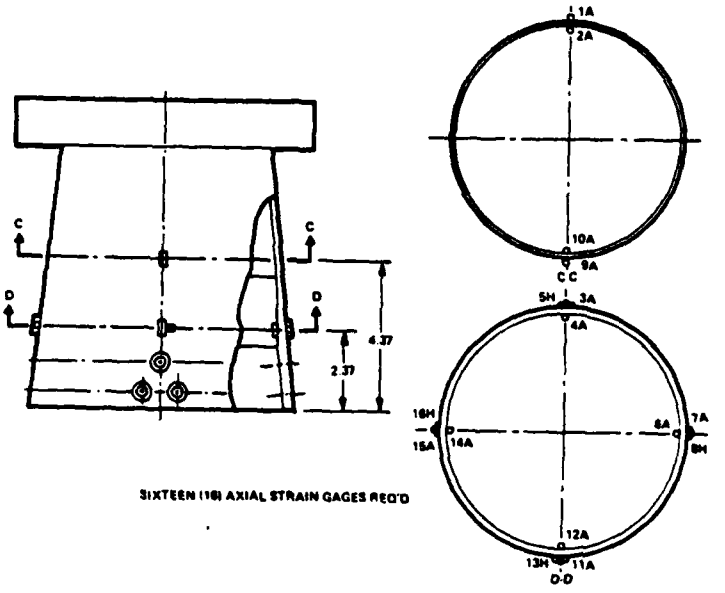

Figure 1. Strain Gage Location - Static Tests

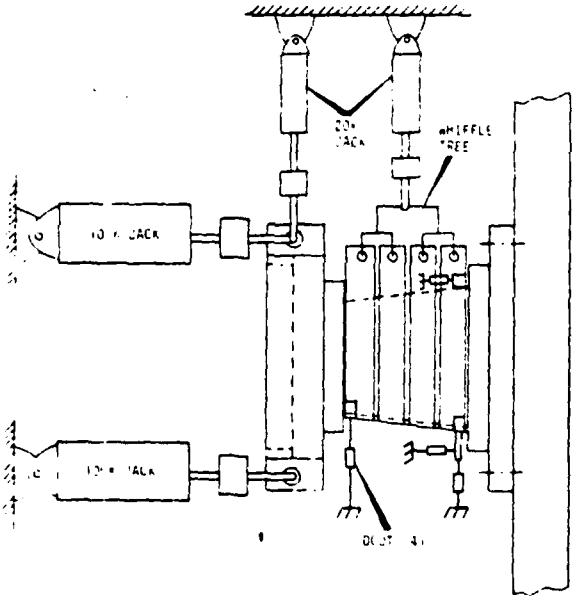

Figure 2. Test Set-Up

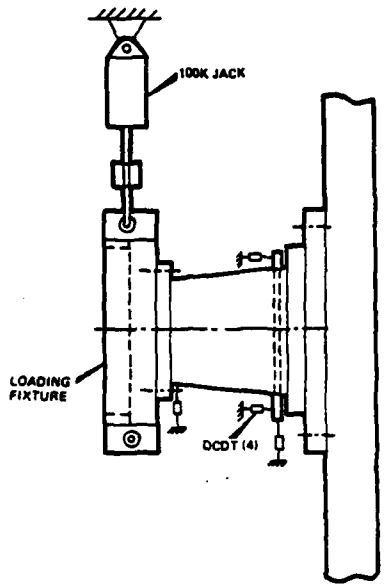

Figure 3. Test Set-Up Shear/Bending Test

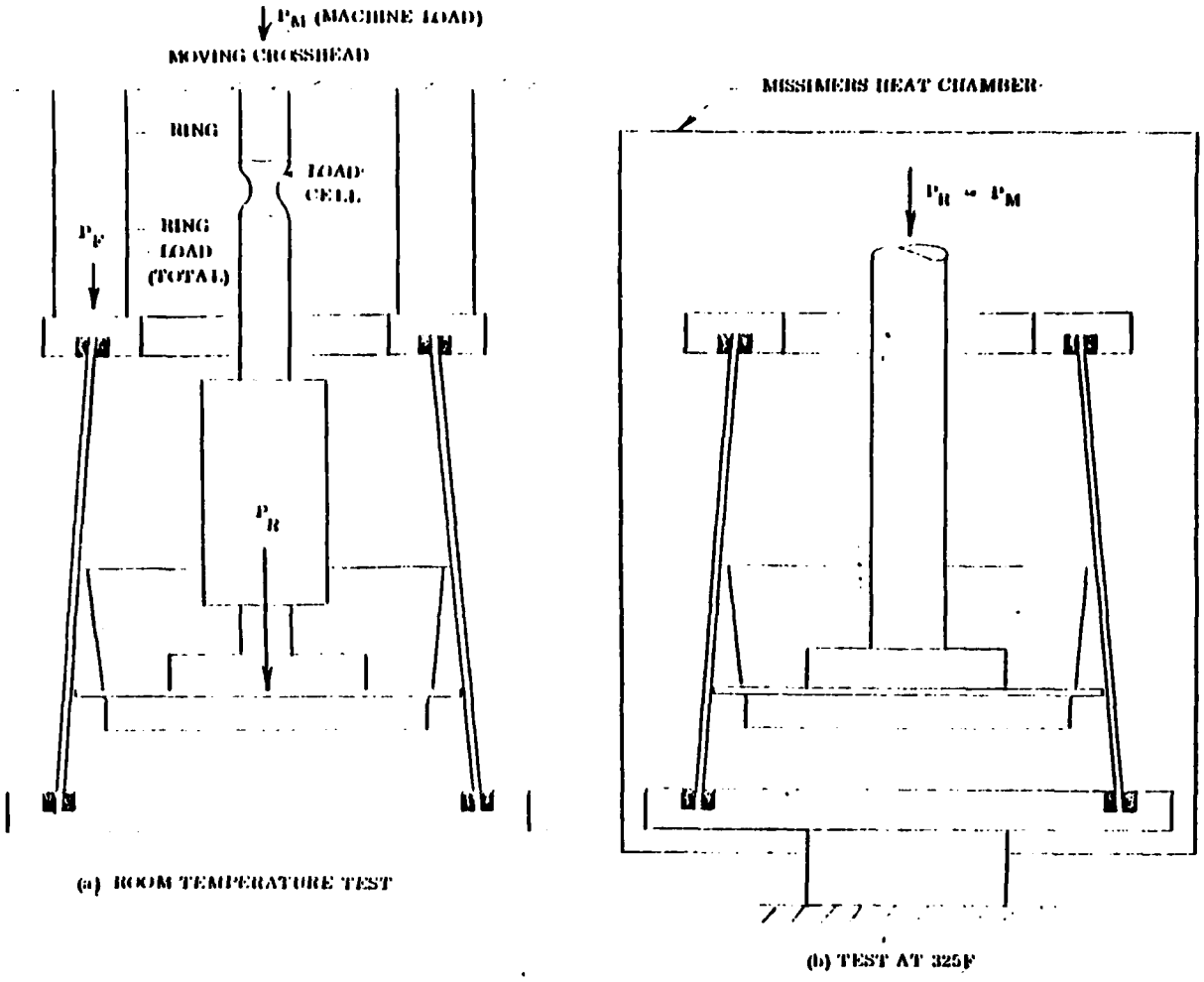

Figure 4. Sketch of Frustum Ring Tests

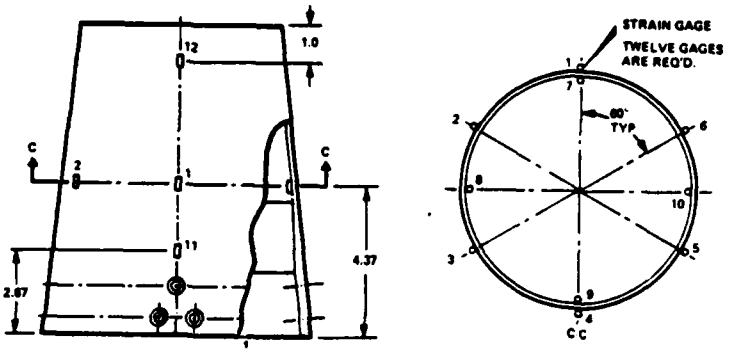

Figure 5. Strain Gage Locations - Shock Tests

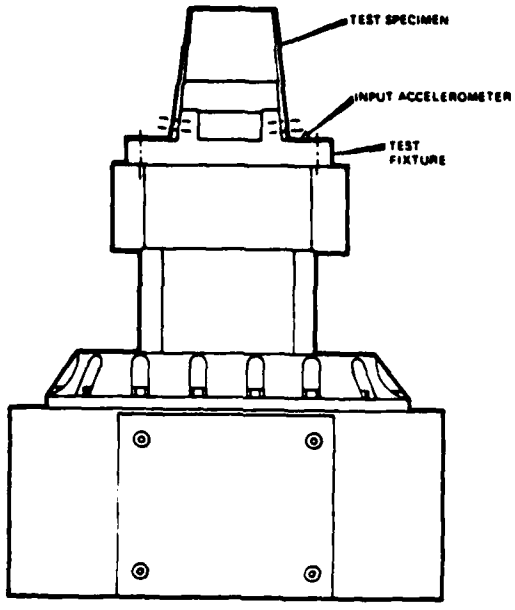

Figure 6. HYGE Shock Machine With Frustrum in Test Mode

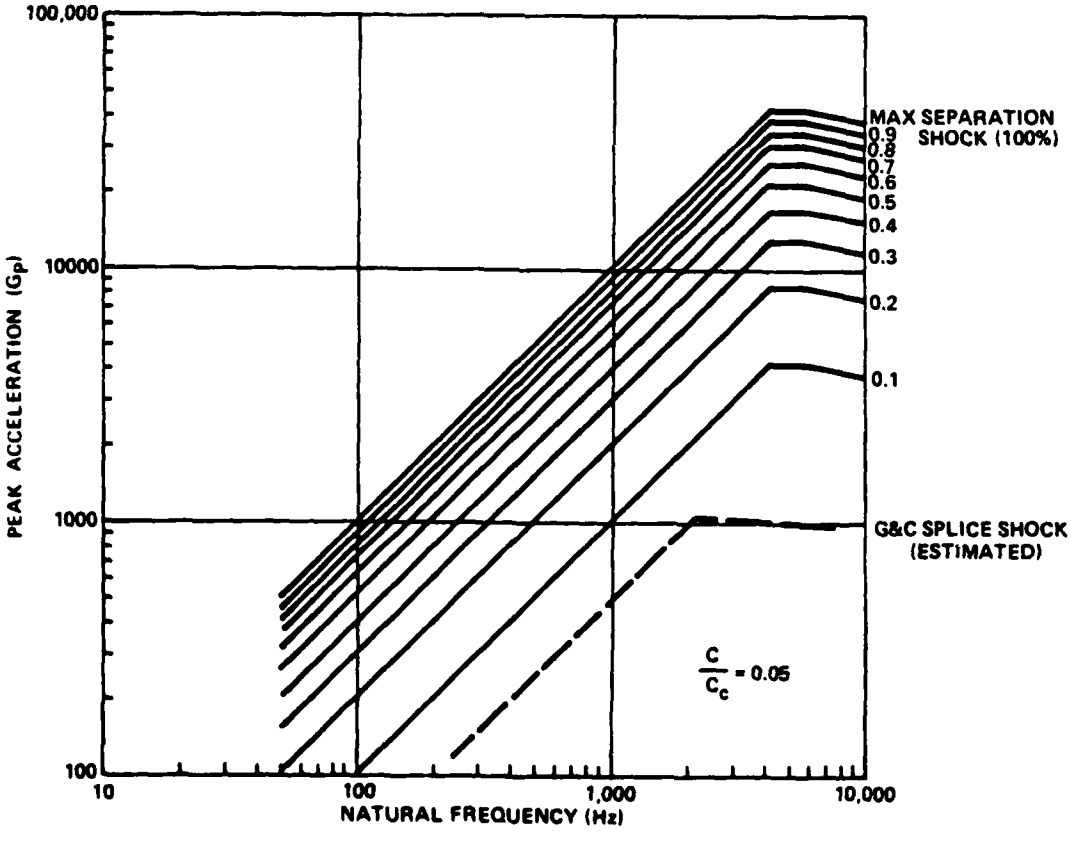

Figure 7. Shock Spectra Simulating Stage Separation Shock

Table I. Static Test Sequence for Cones
With Equipment Rings

Test Number	Temp.	Loading	DLL
1	Amb.	Cone & Eq. Ring	P_F = 72,200 lb P_R = 7,010 lb
2	Amb.	Eq. Ring	P_R = 7,010 lb
3	El. Temp.	"	P_e = 5,668 lb
4	Amb.	"	to failure

APPENDIX B

LOAD-STRAIN AND LOAD-DEFLECTION CURVES

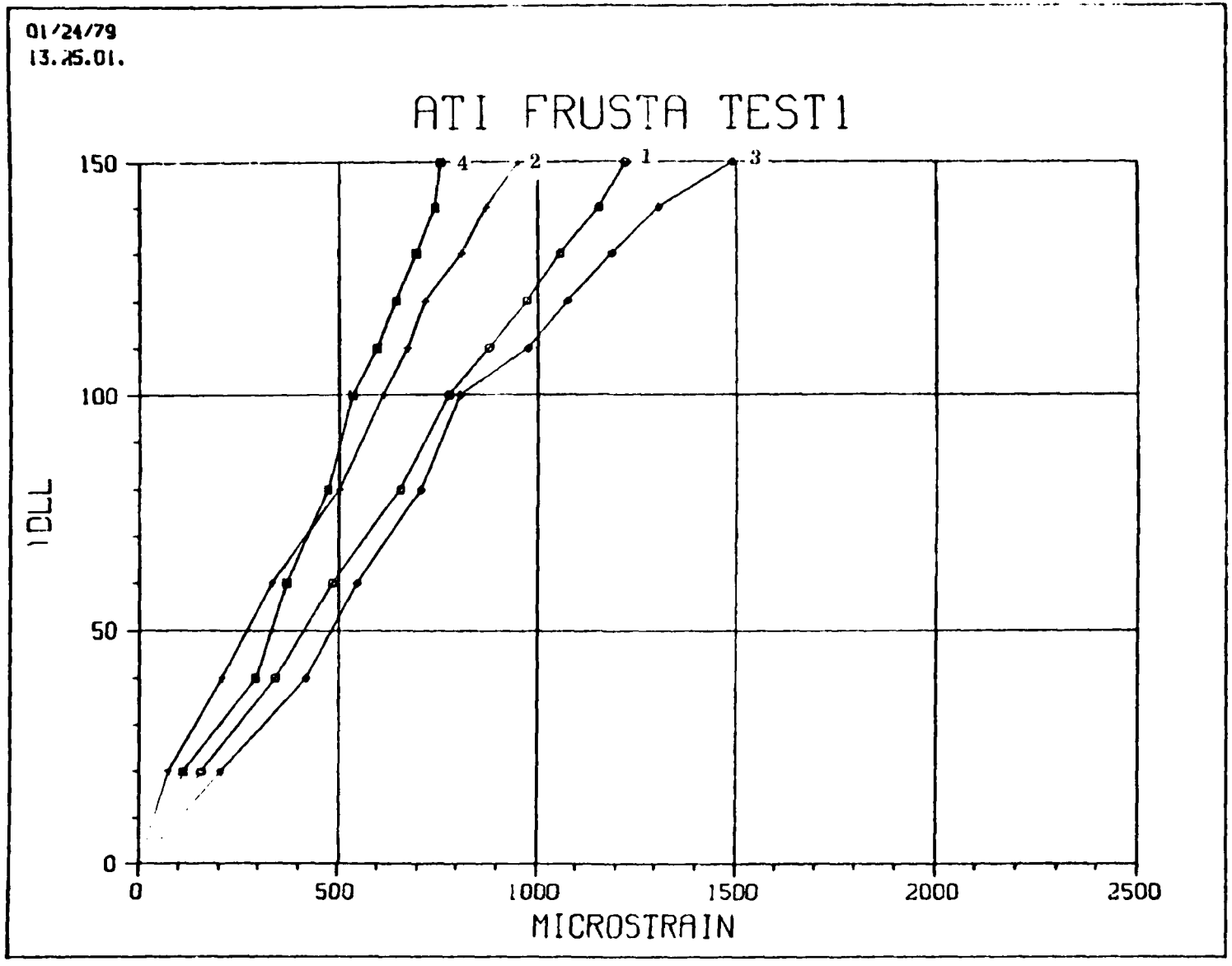

FIGURE B-1. Load vs Strain Data for GAGES 1, 2, 3 and 4 on Half Scale Frustum No. 8 Tested in Combined Loads.

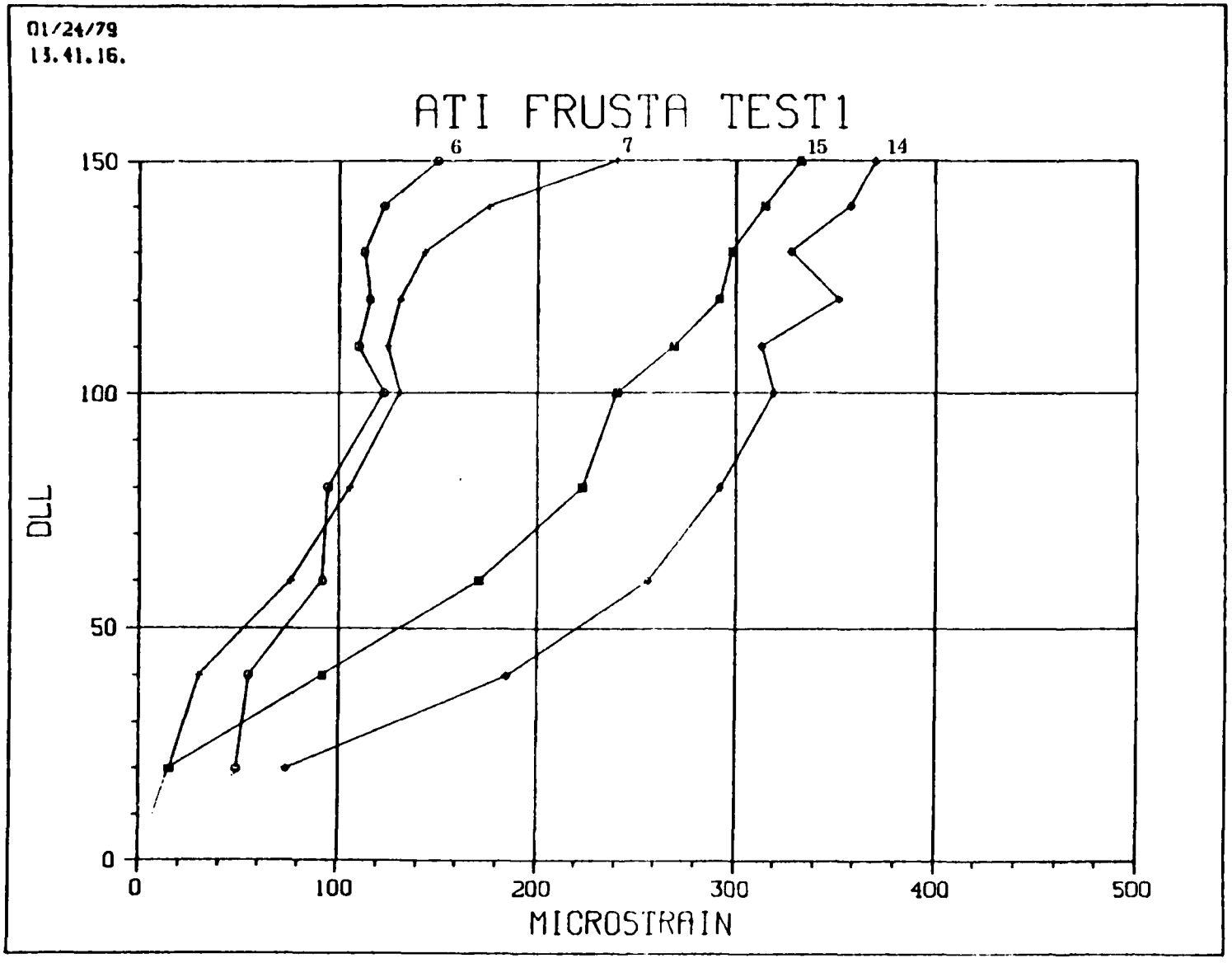

FIGURE B-2. Load vs Strain Data for Gages 6, 7, 14, and 15 on Half Scale Frusta No. 8 Tested in Combined Loads.

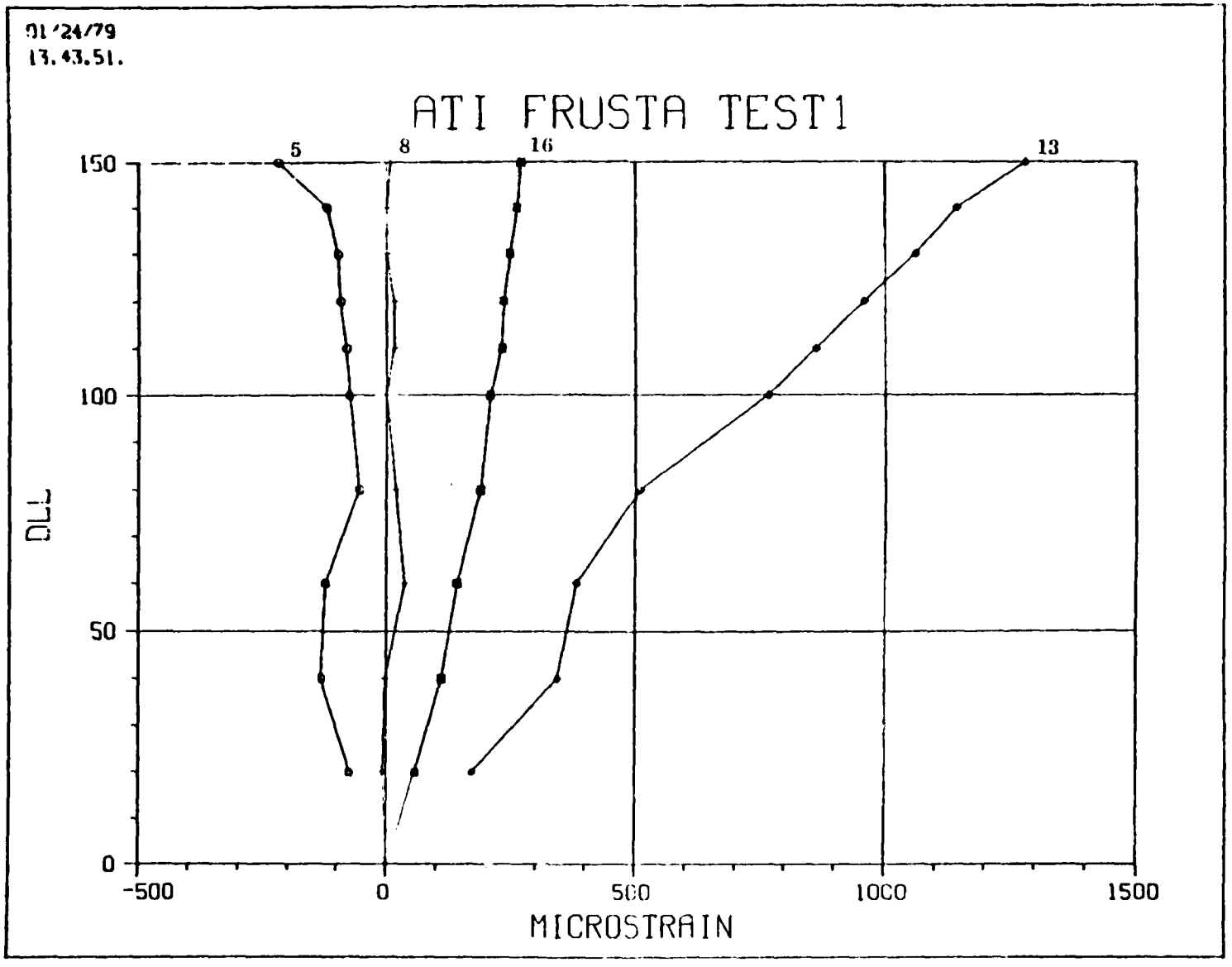

FIGURE B-3. Load vs Strain Data for Gages 5, 8, 16, and 13 on Half Scale Frustum No. 8 Tested in Combined Loads.

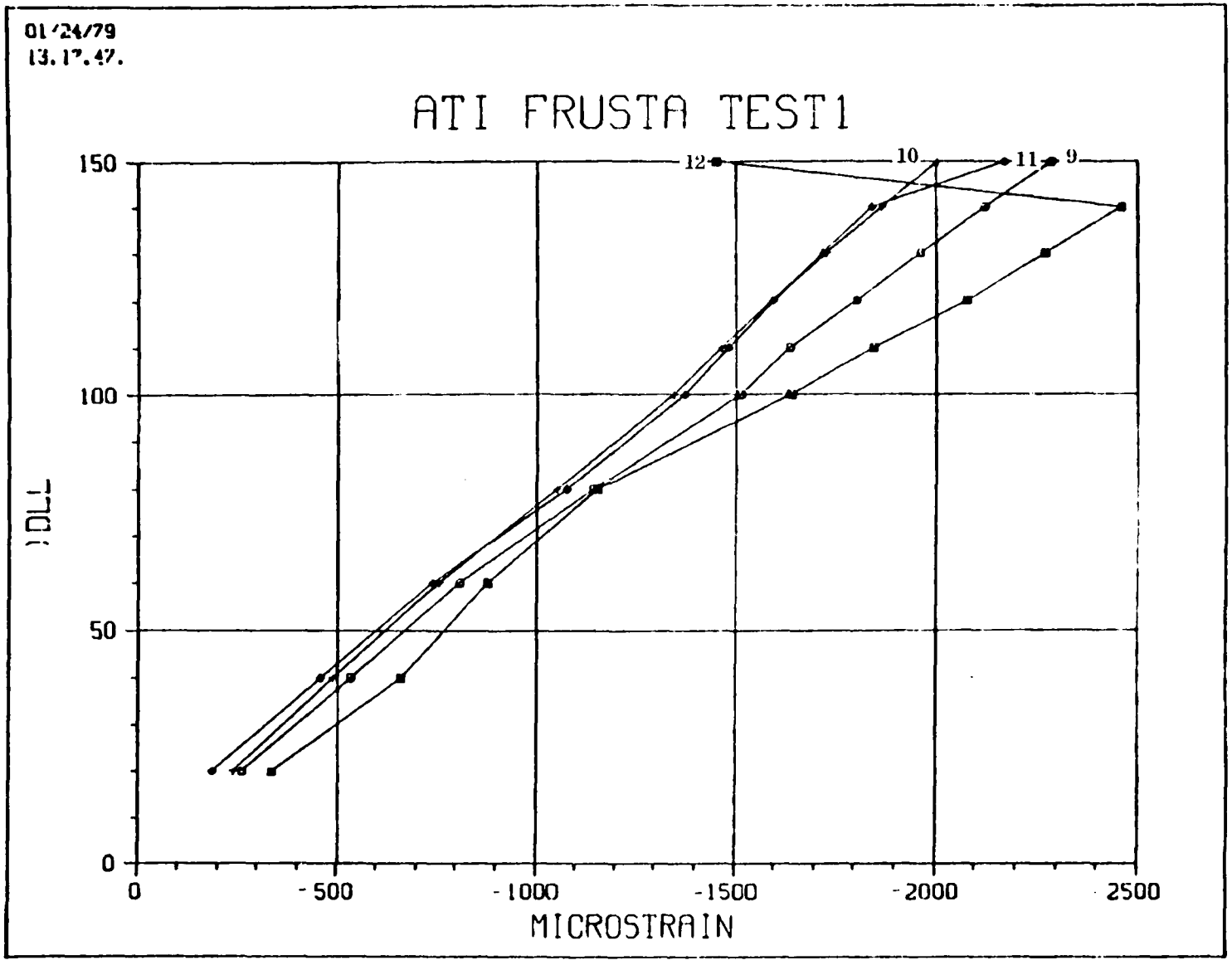

FIGURE B-4. Load vs Strain Data for Gages 9, 10, 11 and 12 on Half Scale Frustum No. 8 Tested in Combined Loads.

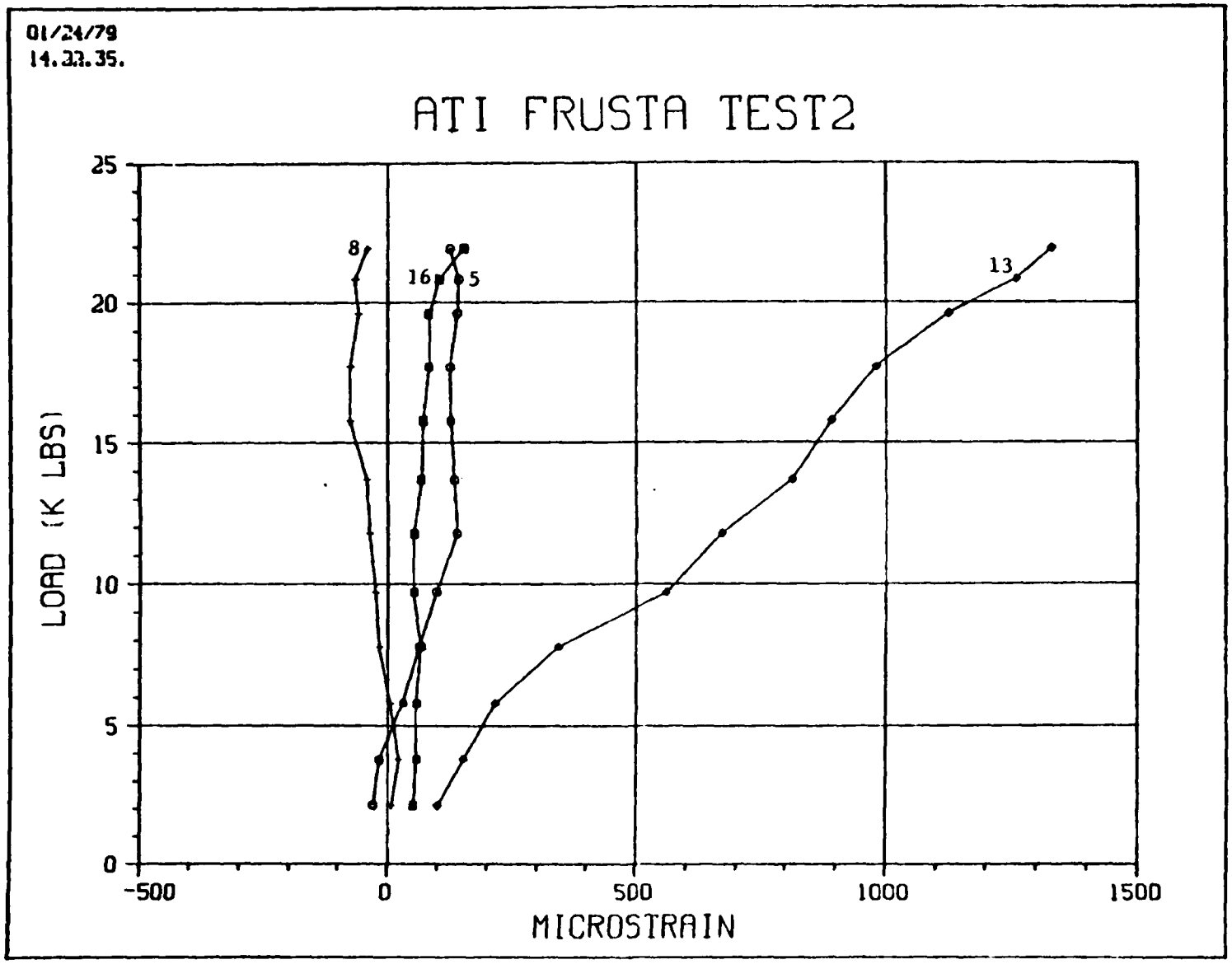

FIGURE B-5. Load vs Strain Data for Gages 5, 8, 13, and 16 on Half Scale Frustum No. 9 Tested in Shear/Bending.

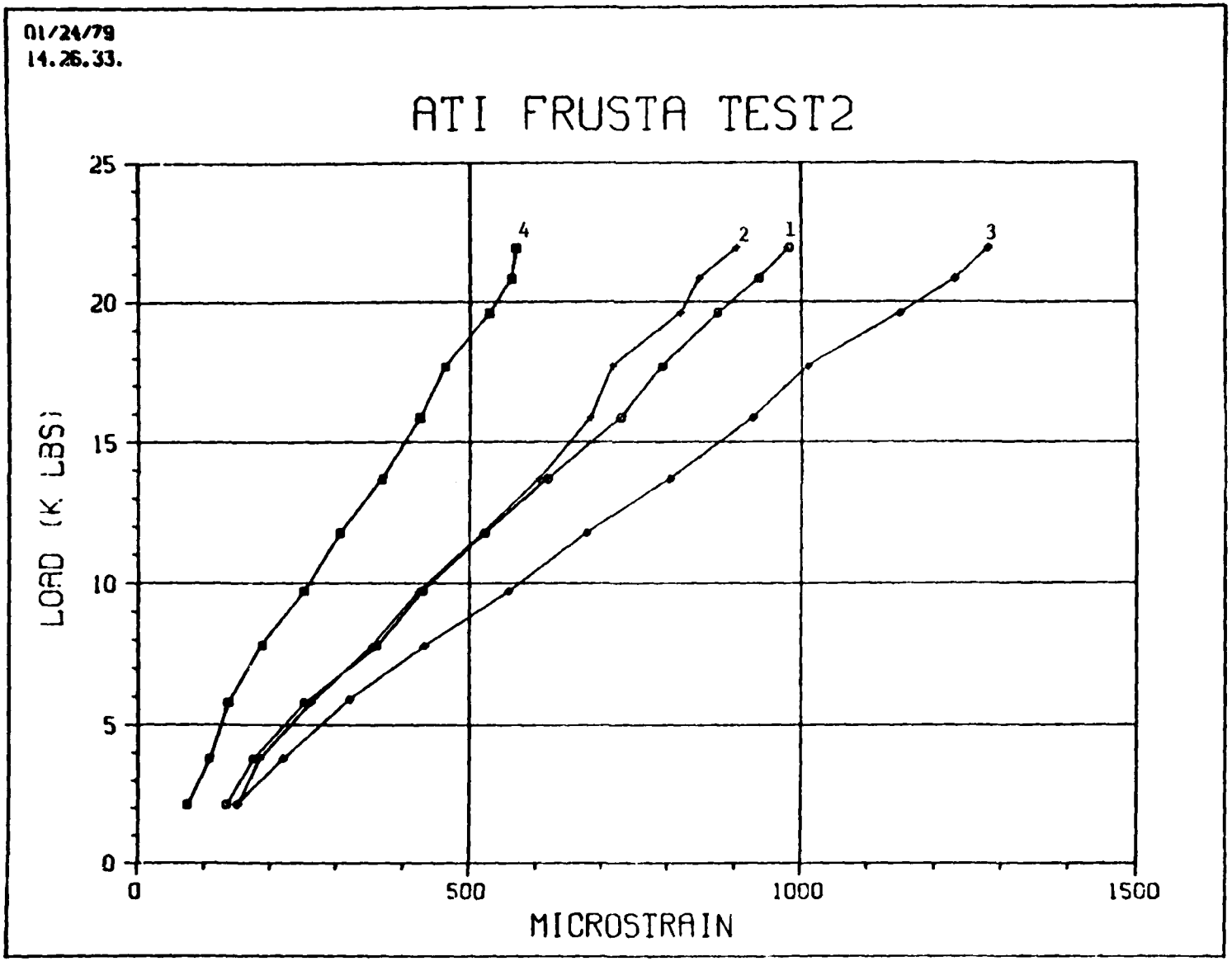

FIGURE B-6. Load vs Strain Data for Gages 1, 2, 3 and 4 on Half Scale Frustum No. 9 Tested in Shear/Bending.

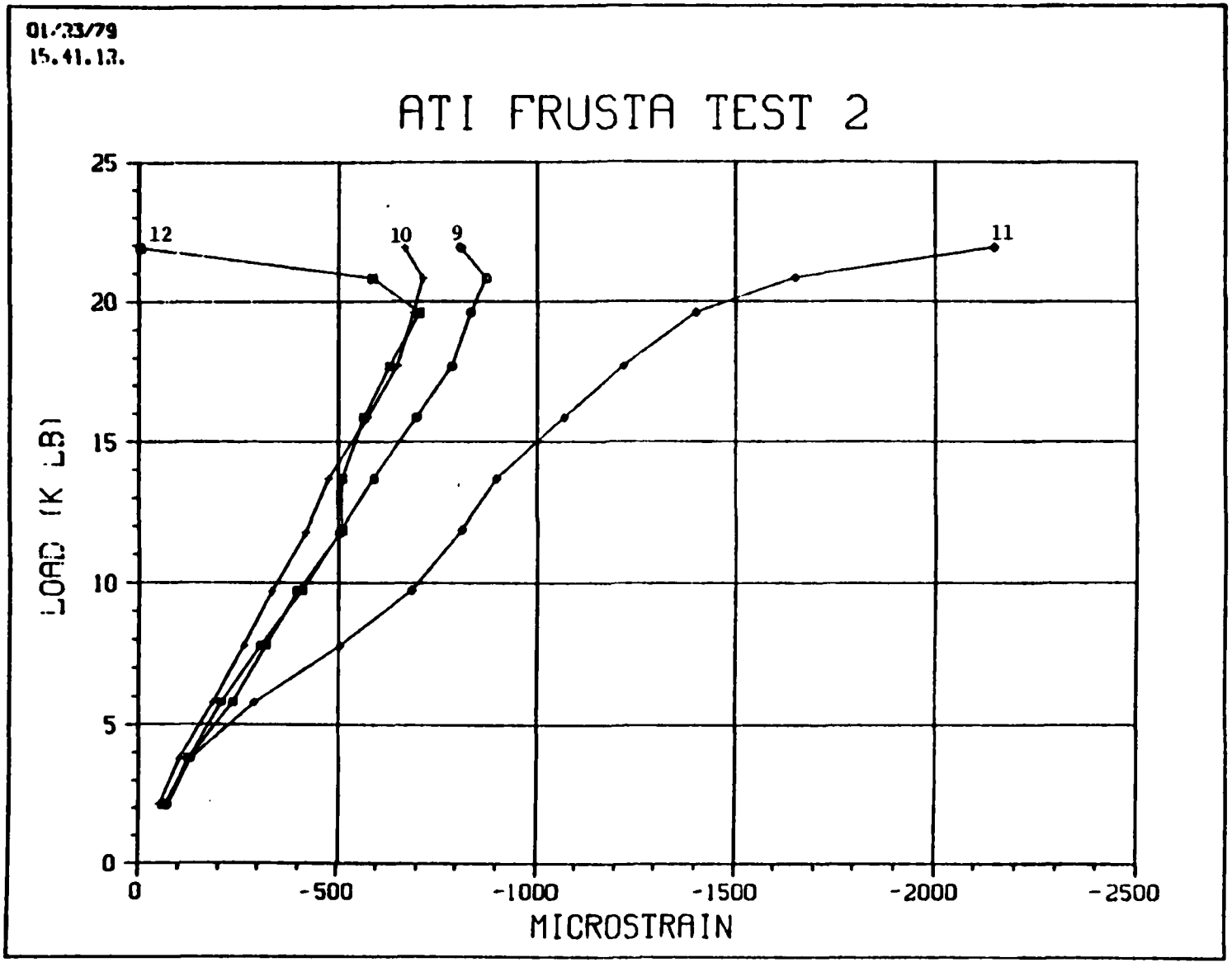

FIGURE B-7. Load vs Strain Data for Gages 9, 10, 11 and 12 on Half Scale Frustum No. 9 Tested in Shear/Bending.

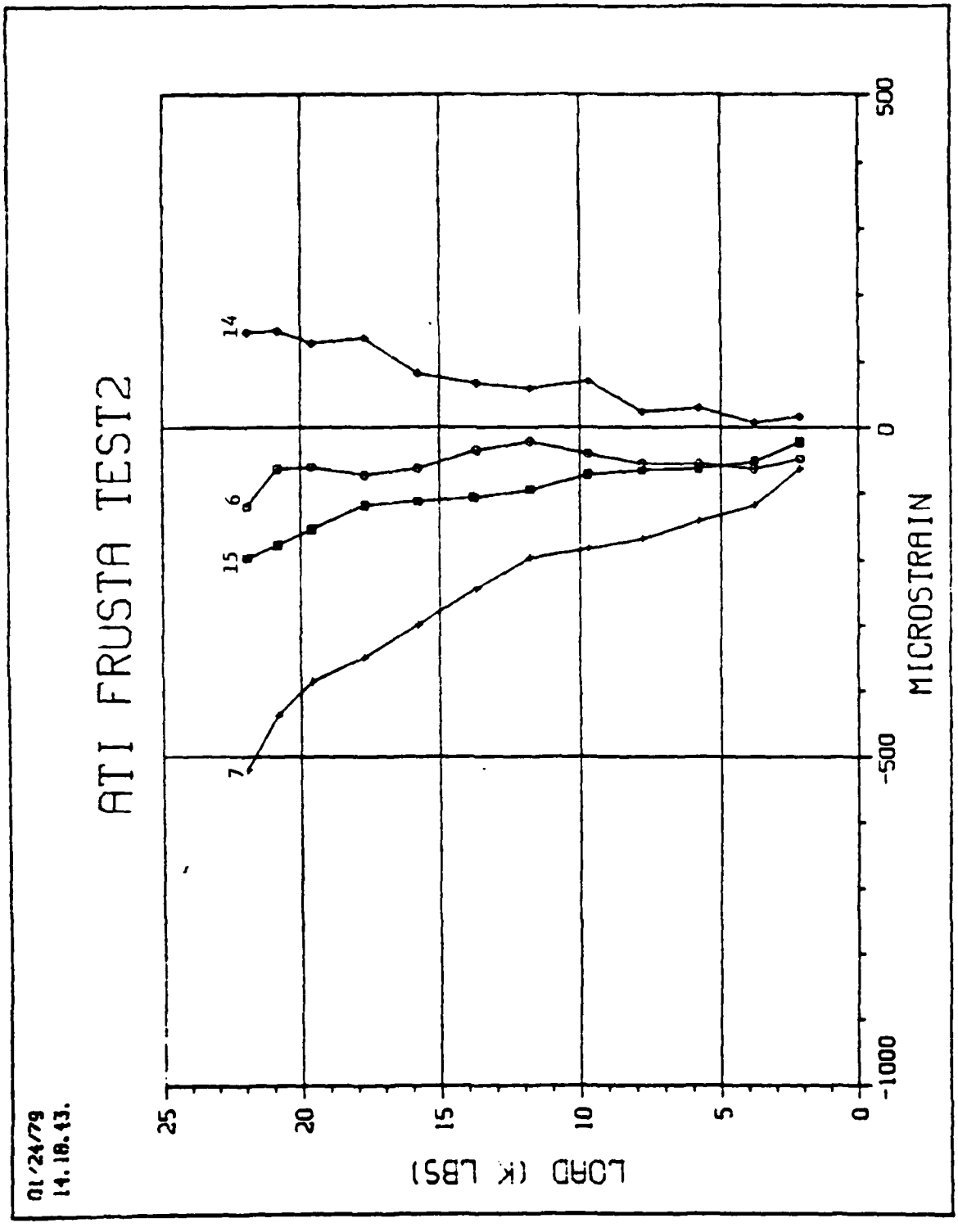

FIGURE B-8. Load vs Strain Data for Gages 6, 7, 14, 15 on Half Scale Frustum No. 9 Tested in Shear/Bending.

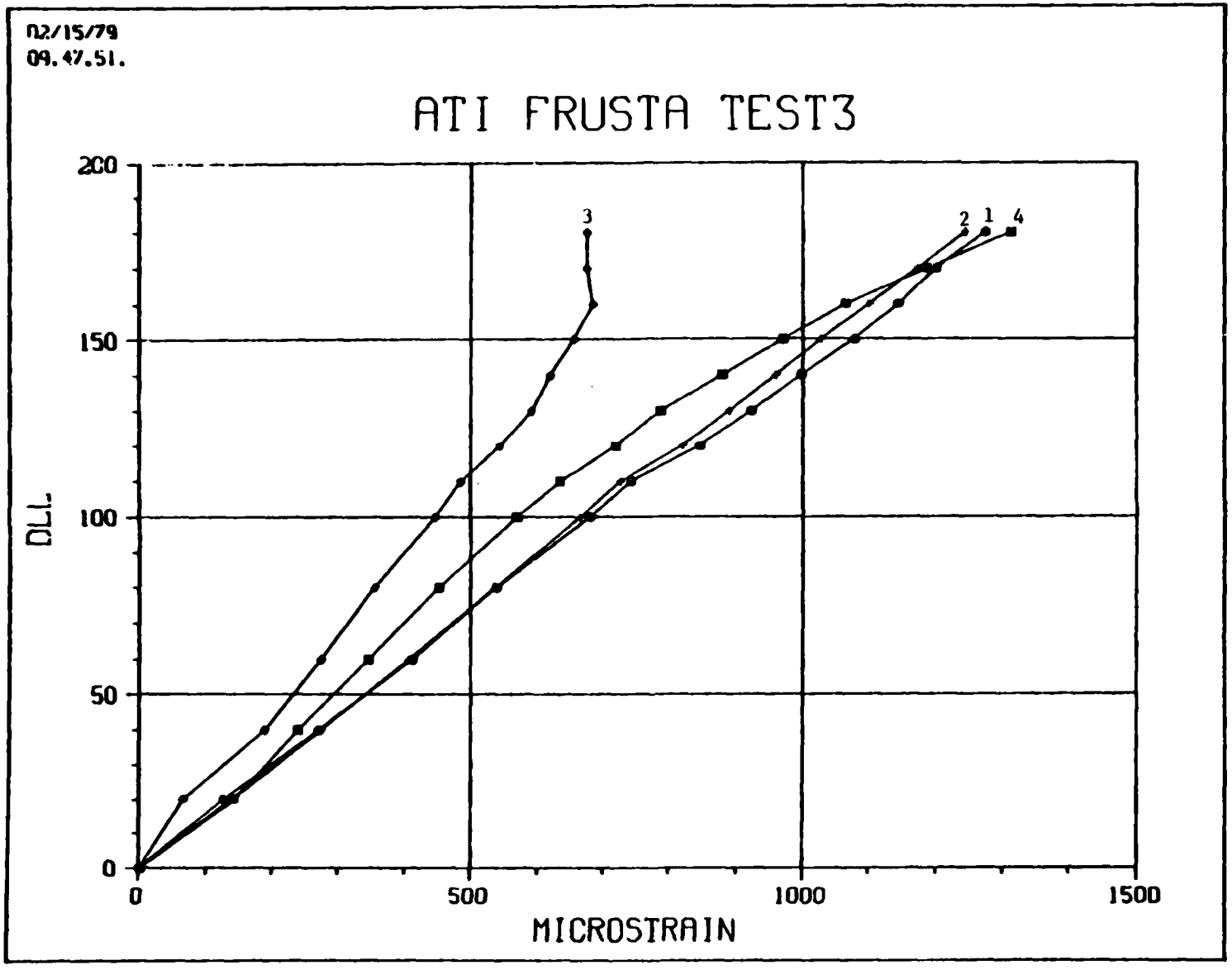

FIGURE B-9. Load vs Strain Data for Gages 1, 2 3 and 4 on Half Scale Frusta No. 12 Tested in Combined Loads.

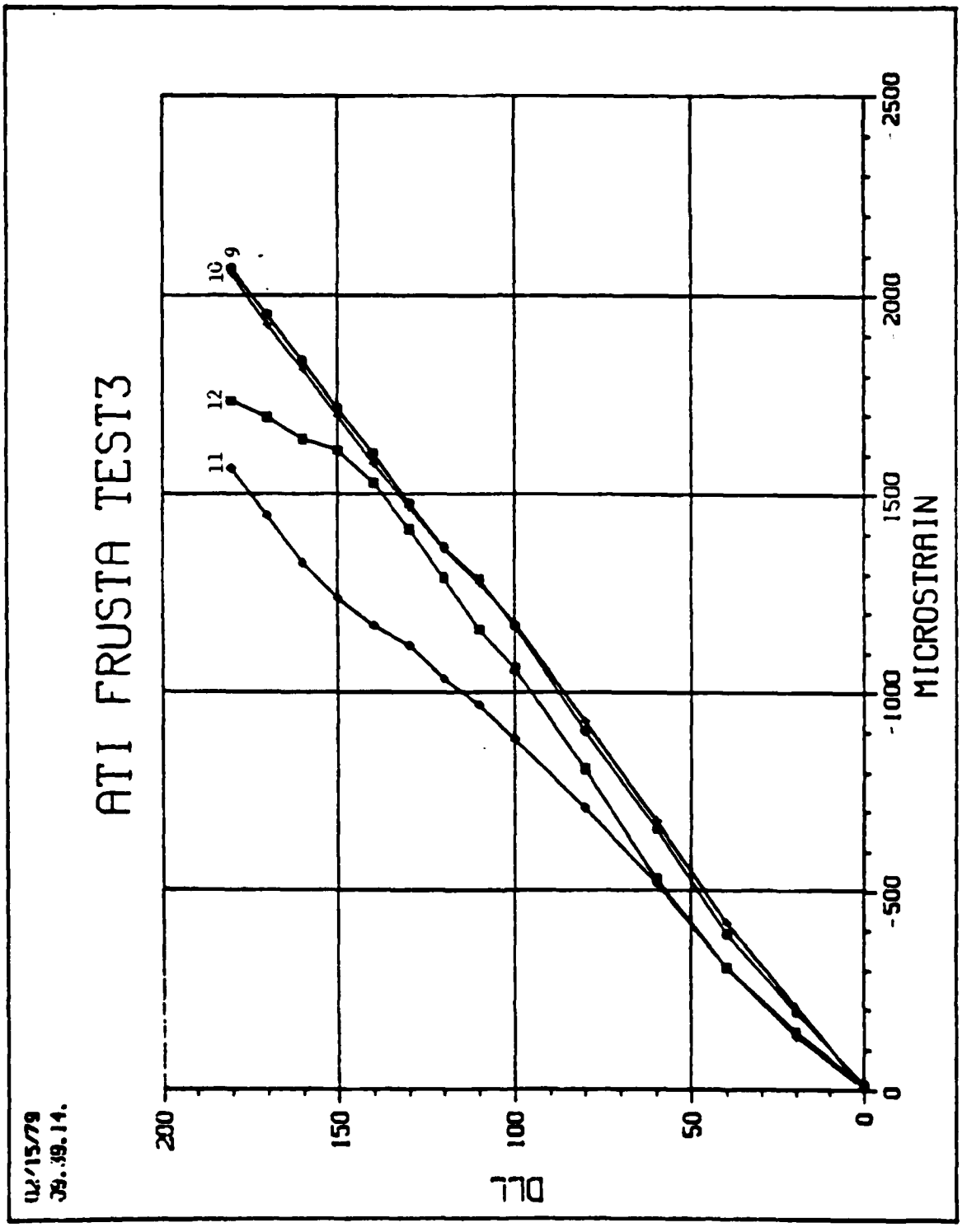

FIGURE B-10. Load vs Strain Data for Gages 9, 10, 11 and 12 on Half Scale Frusta No. 12 Tested in Combined Loads.

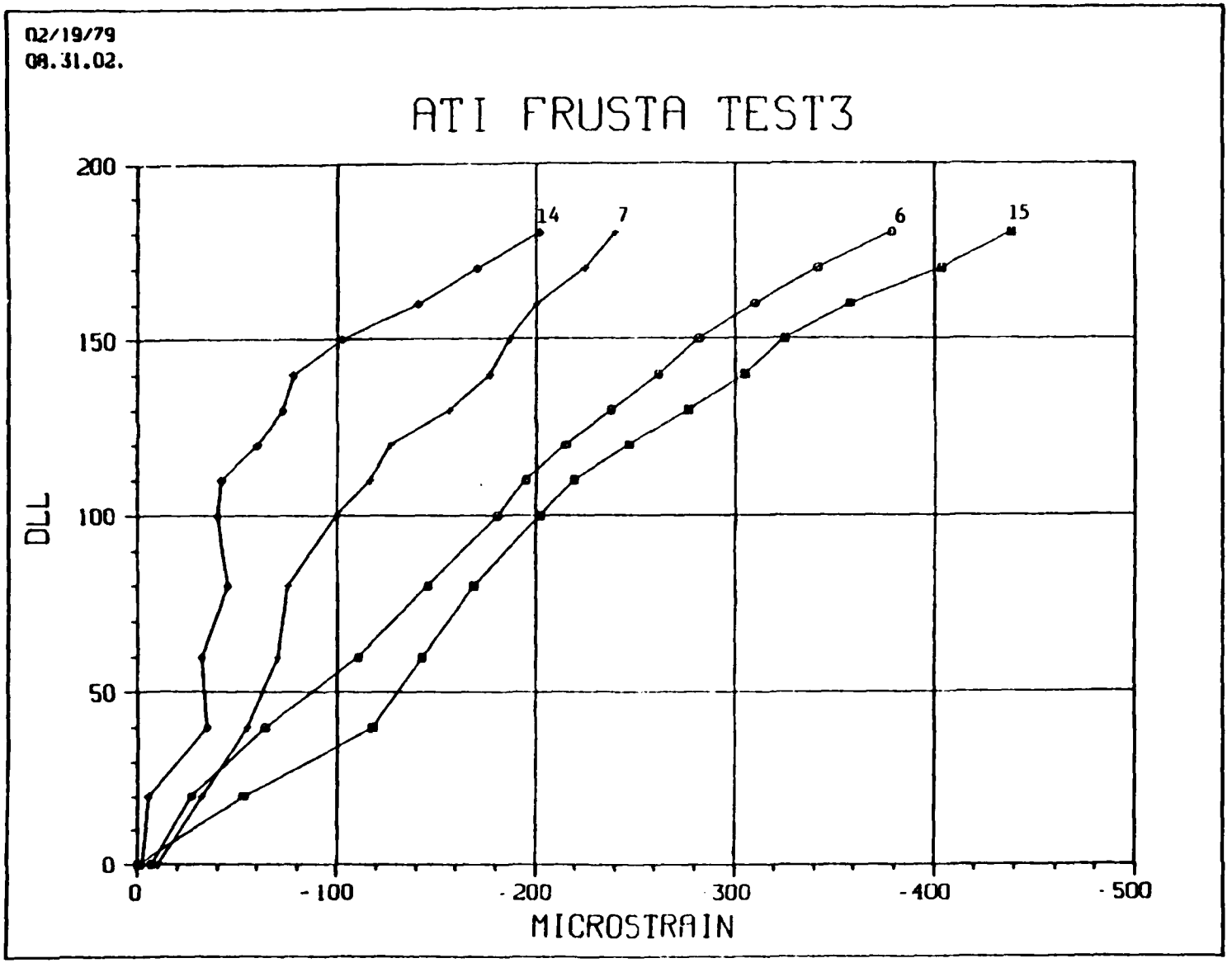

FIGURE B-11. Load vs Strain Data for Gages 6, 7, 14 and 15 on Half Scale Frusta No. 12 Tested in Combined Loads.

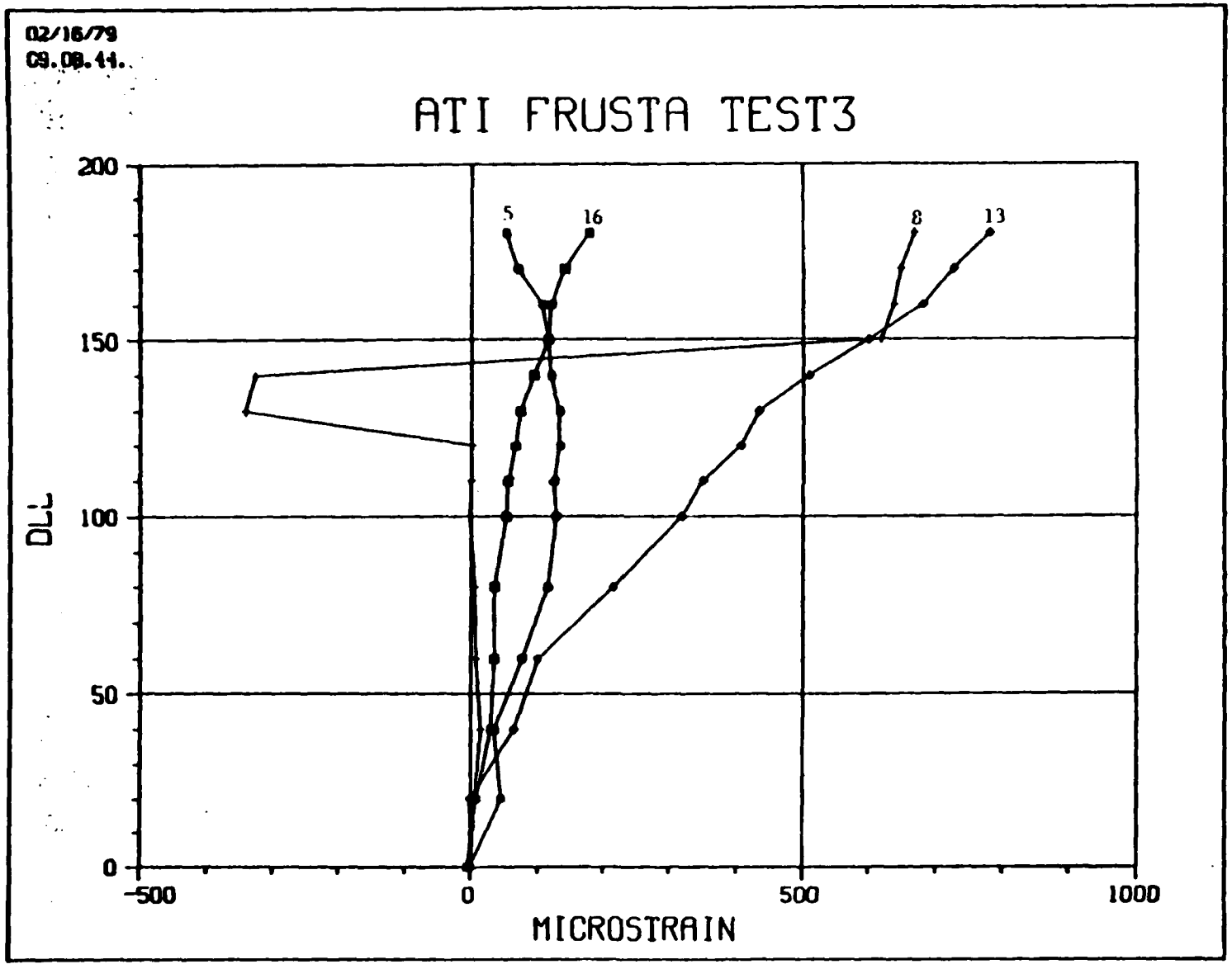

FIGURE B-12. Load vs Strain Data for Gages 5, 8, 13, and 16 on Half Scale Frusta No. 12 Tested in Combined Loads.

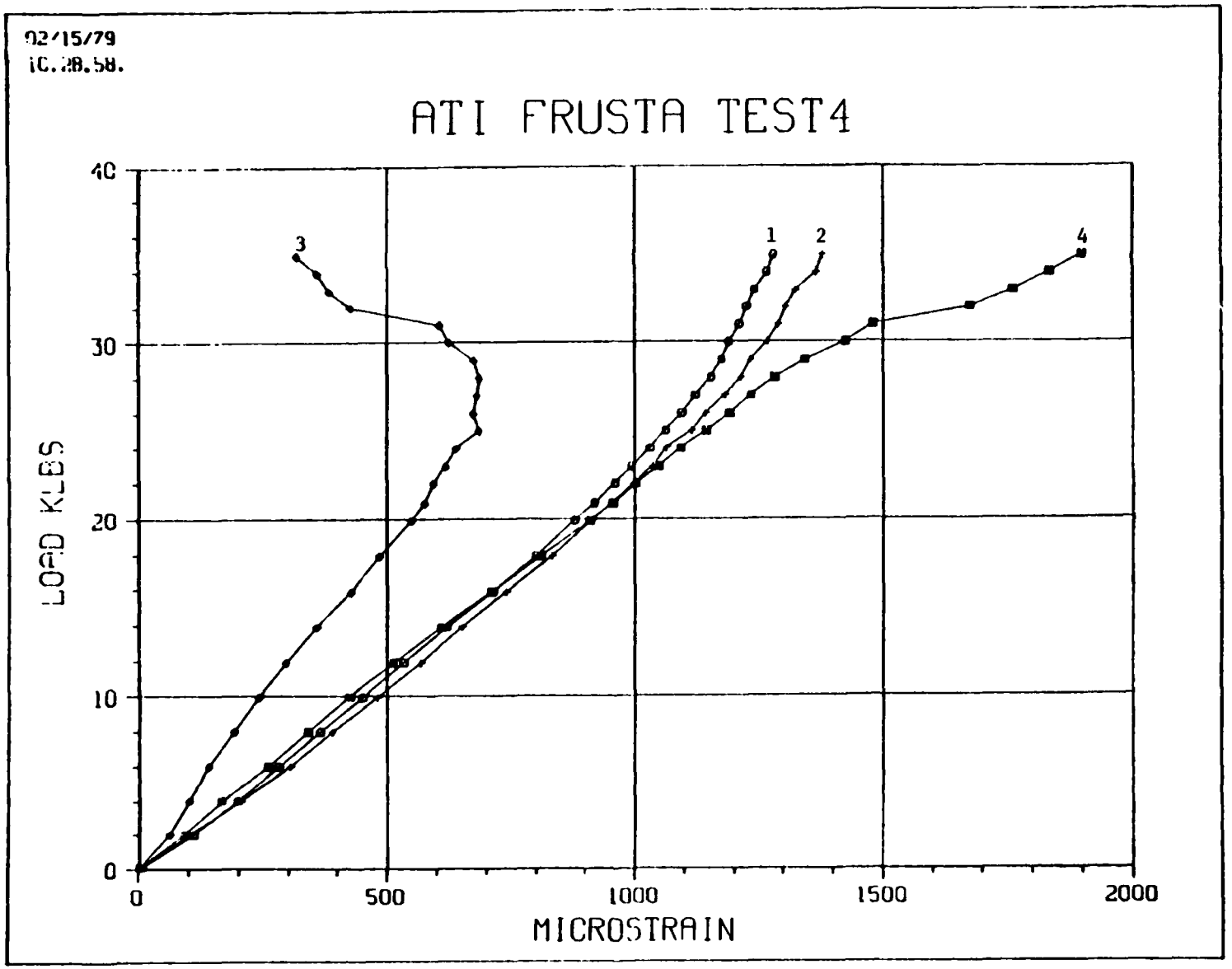

FIGURE B-13. Load vs Strain Data for Gages 1, 2, 3 and 4 on Half Scale Frustum No. IIE Tested in Shear/Bending.

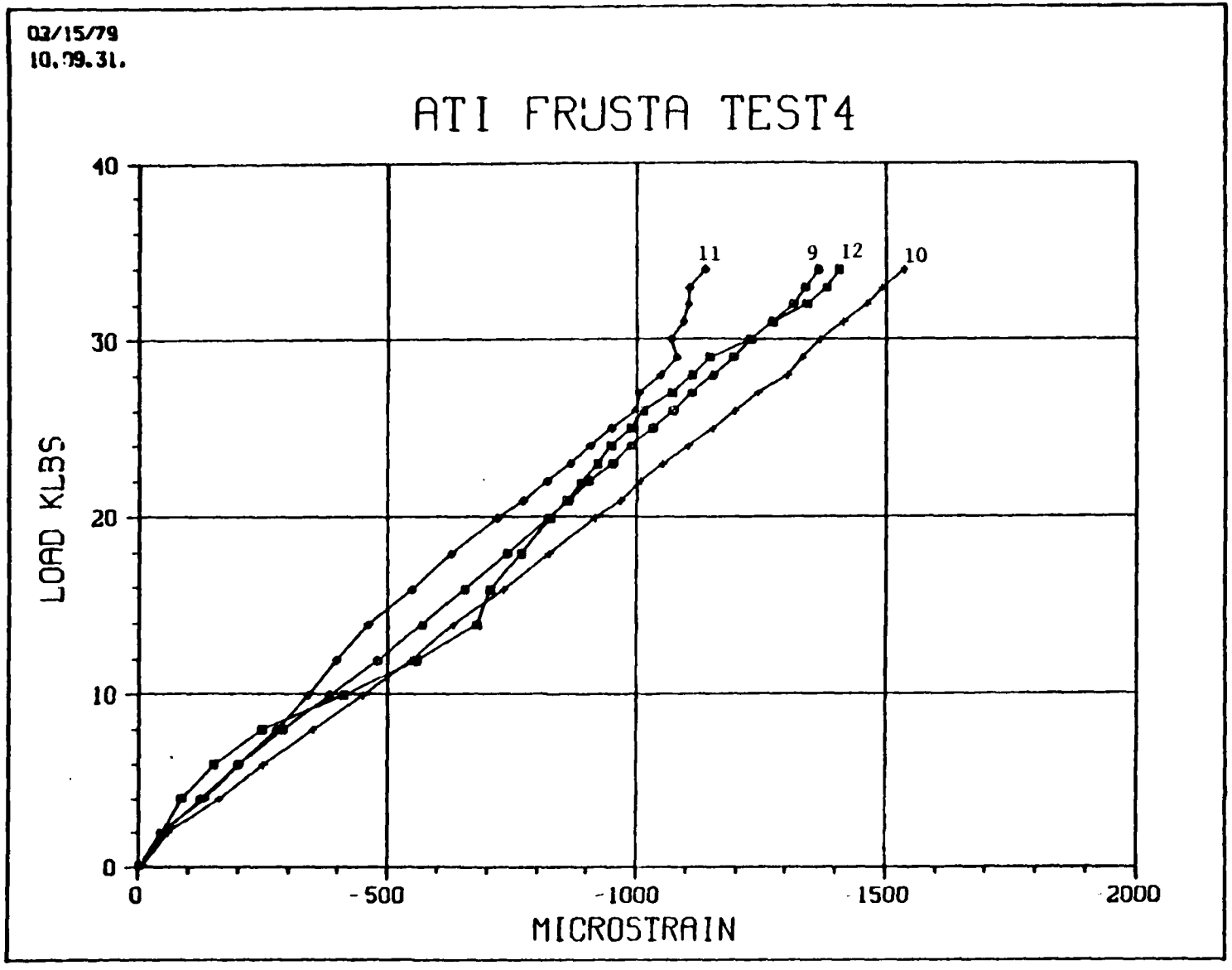

FIGURE B-14. Load vs Strain Data for Gages 9, 10, 11 and 12 on Half Scale Frustum No. 11R Tested in Shear/Bending.

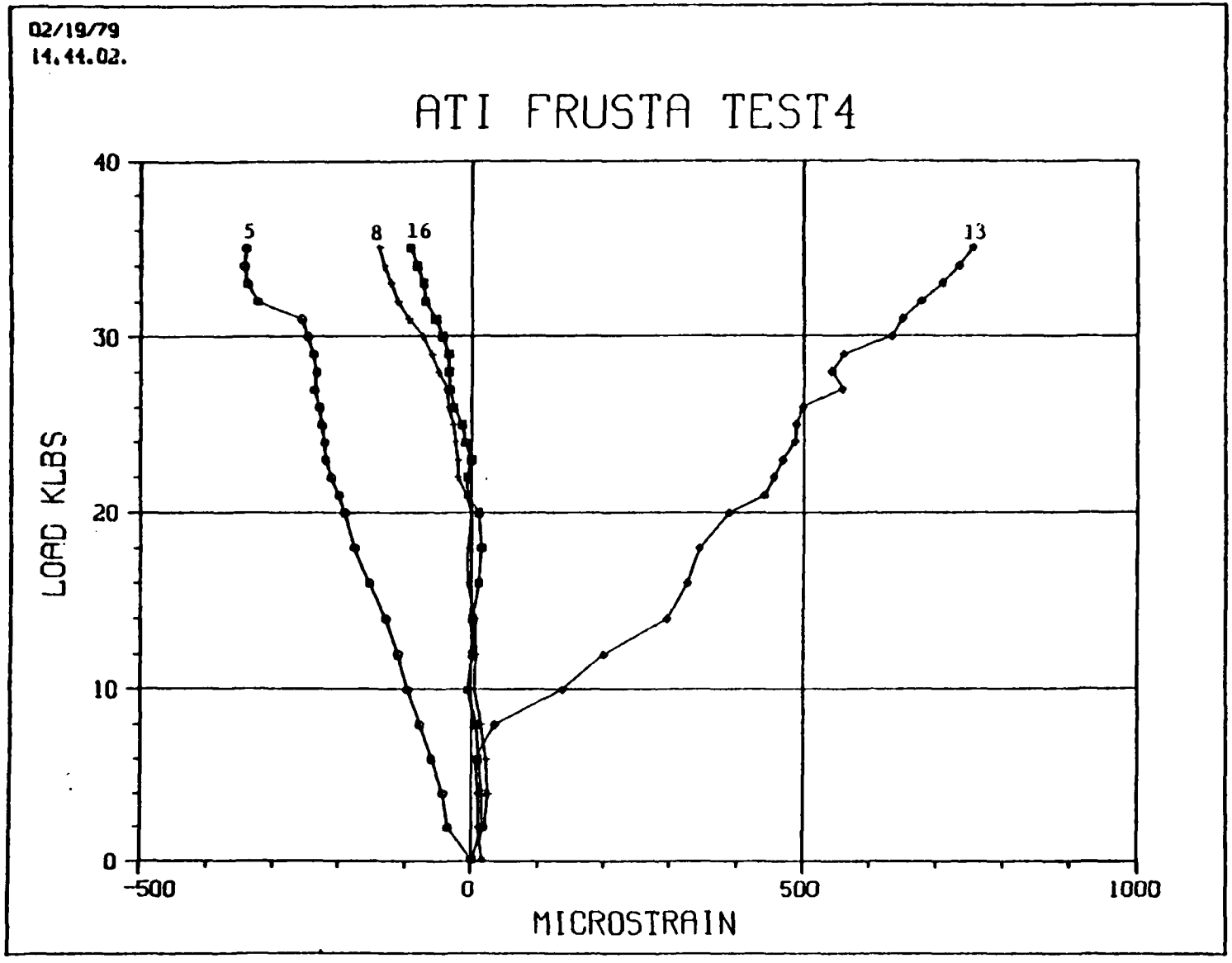

FIGURE B-15. Load vs Strain Data for Gages 5, 8, 13, and 16 on Half Scale Frustum No. 11R Tested in Shear/Bending.

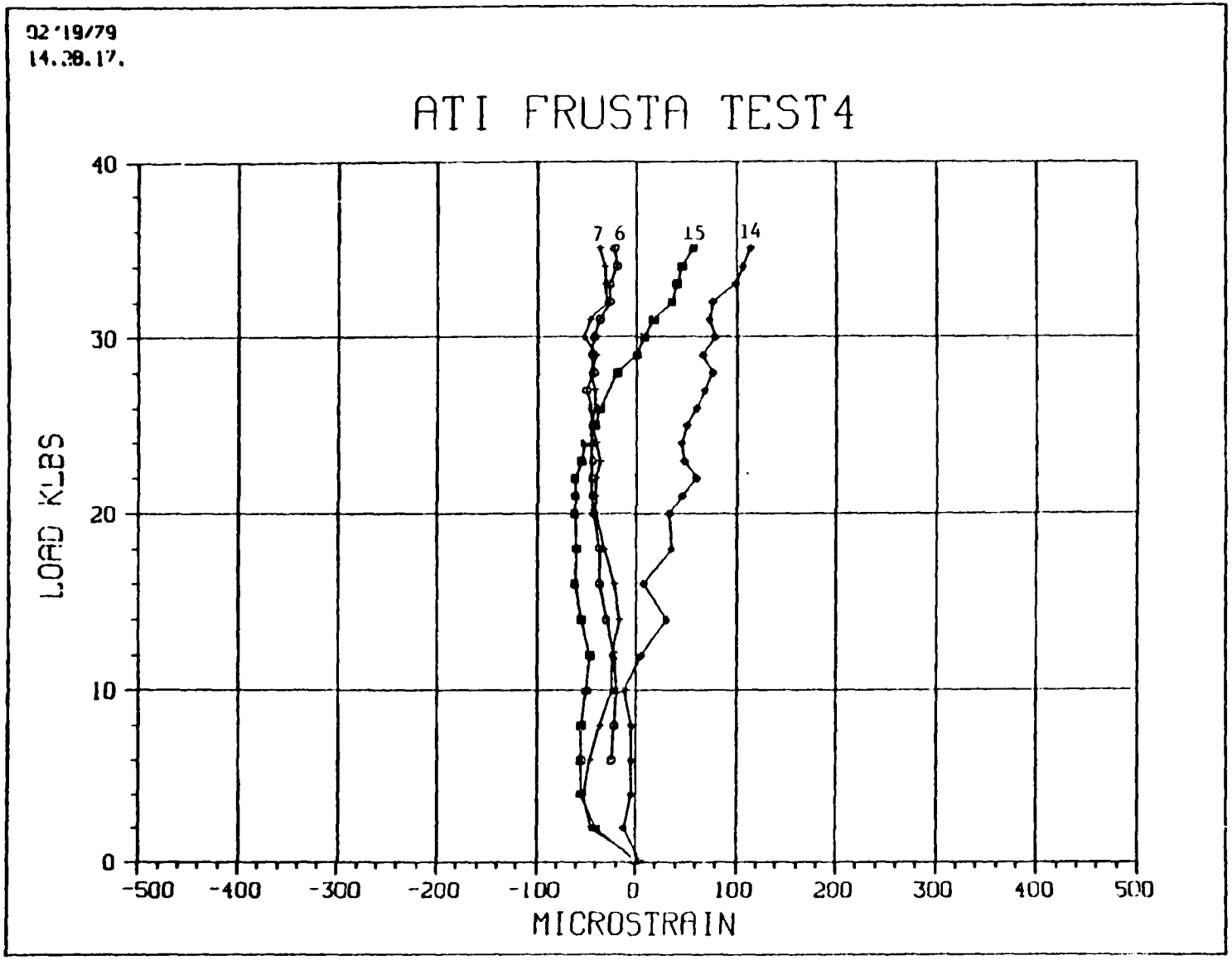

FIGURE B-16. Load vs Strain Data for Gages 6, 7, 14 and 15 on Half Scale Frustum No. 11R Tested in Shear/Bending.

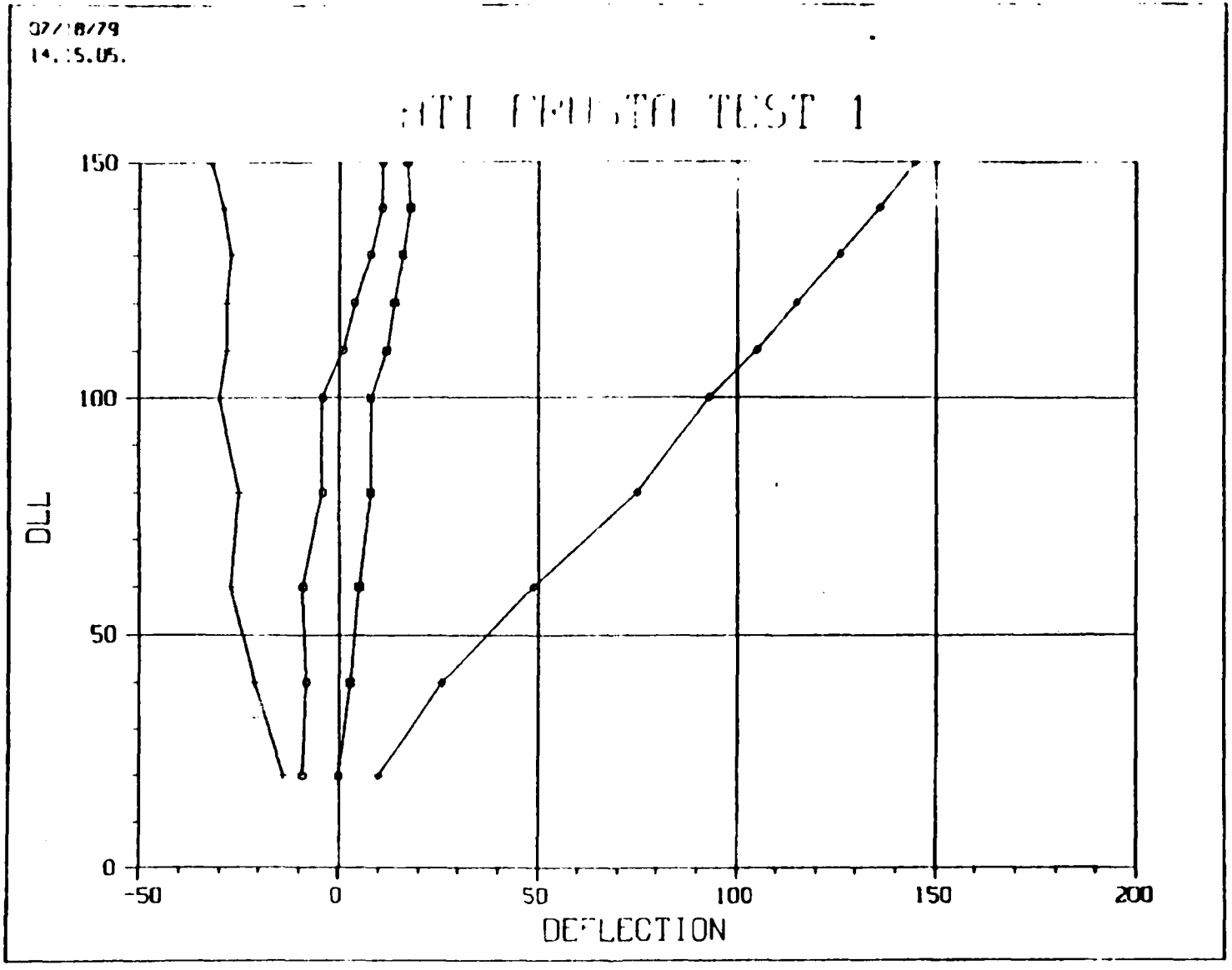

FIGURE B-17. Load vs Deflection for Half Scale Frusta No. 8.

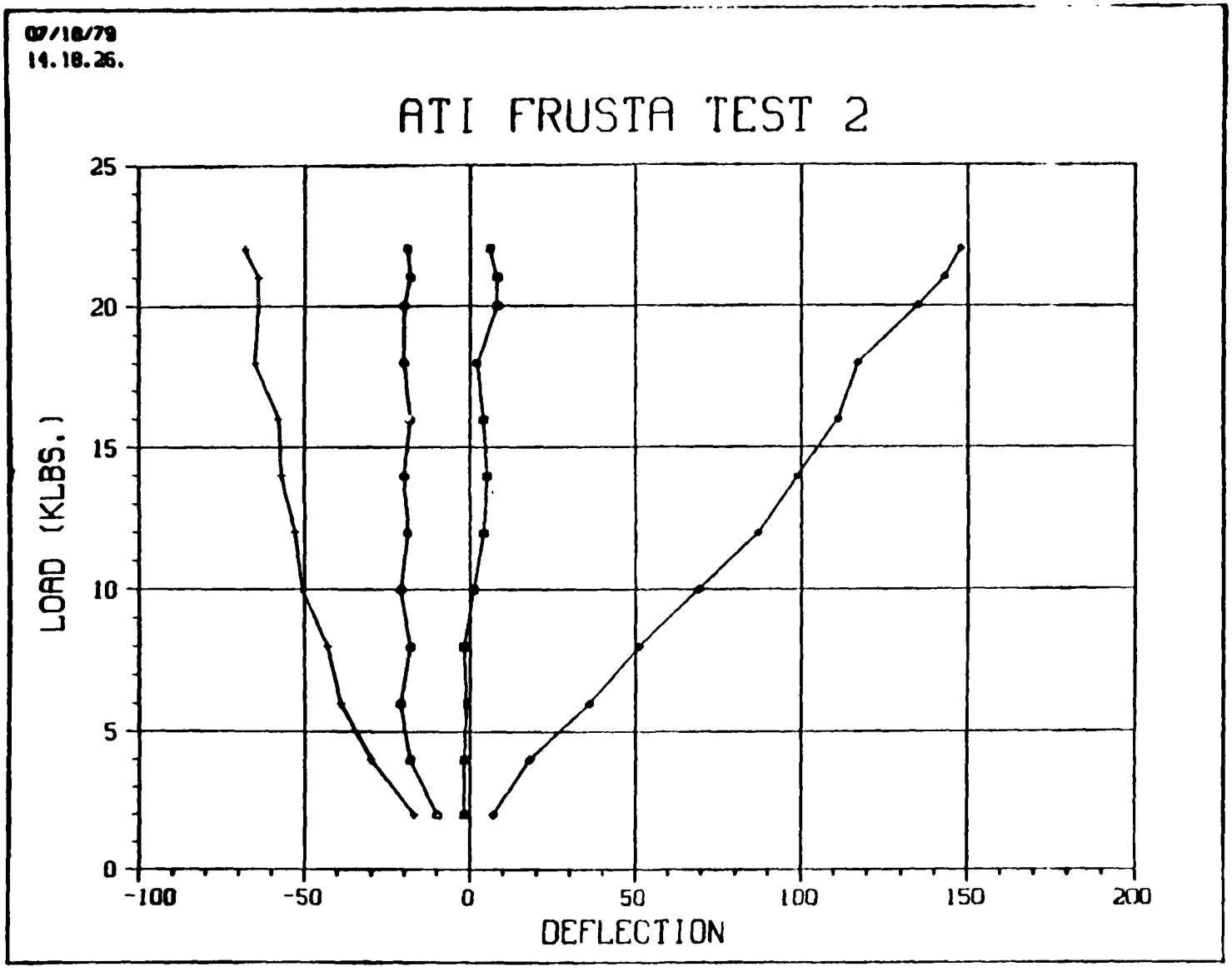

FIGURE B-18. Load vs Deflection for 1.1 Scale Frusta No. 9.

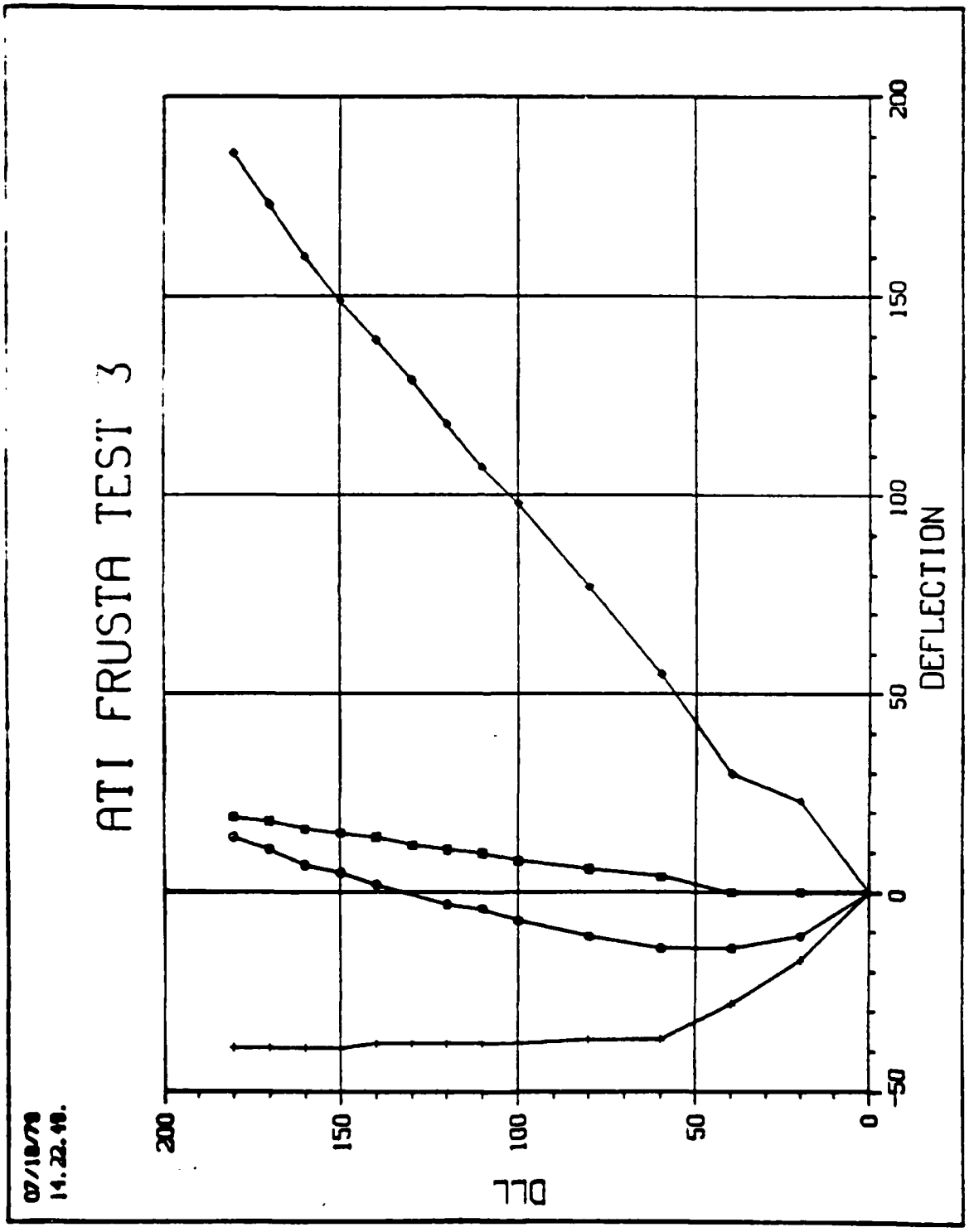

FIGURE B- 19. Load vs Deflection for Half Scale Frusta No. 12.

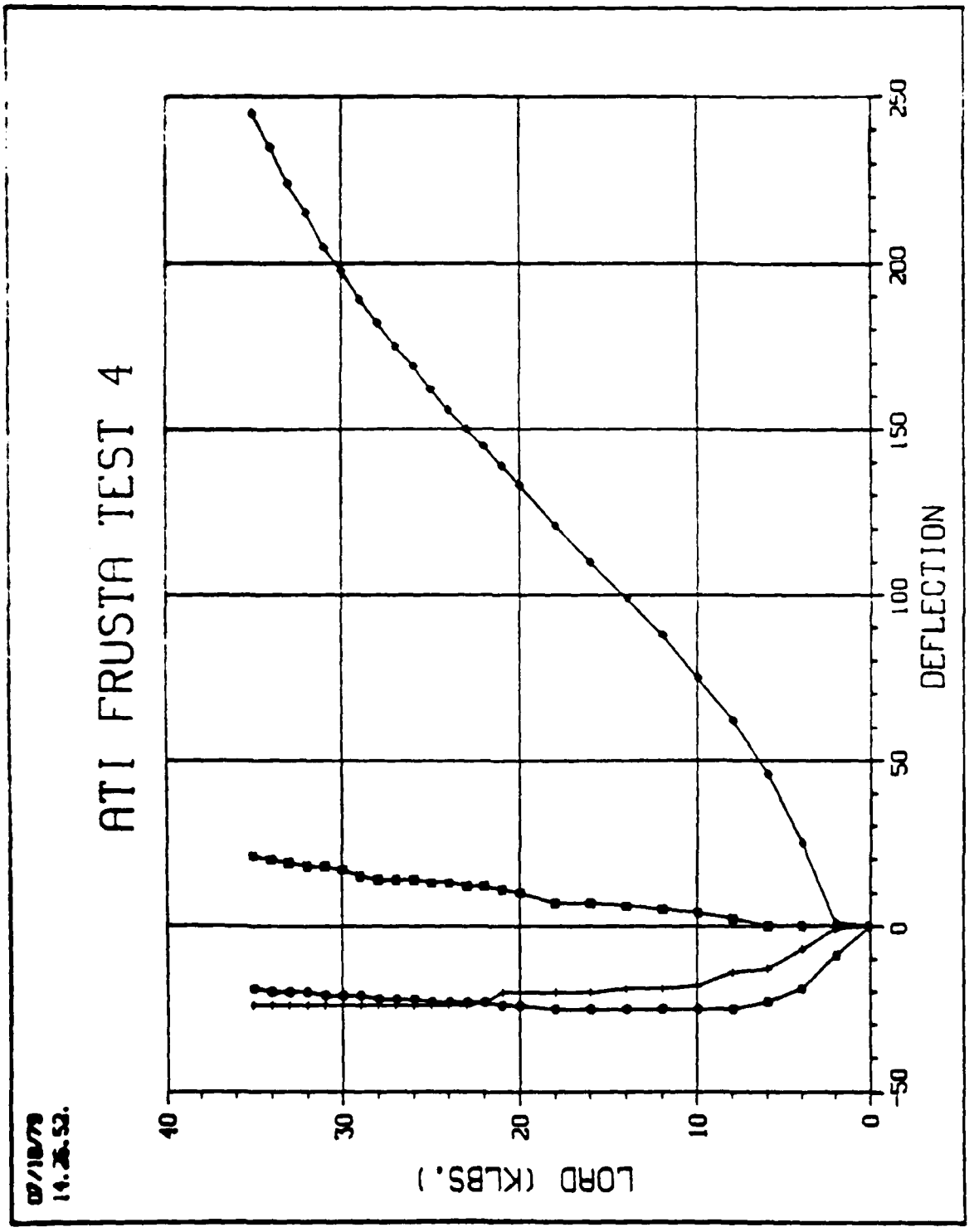

FIGURE B-20. Load vs Deflection for Half Scale Frusta No. 11B.

APPENDIX C

SHOCK SPECTRA

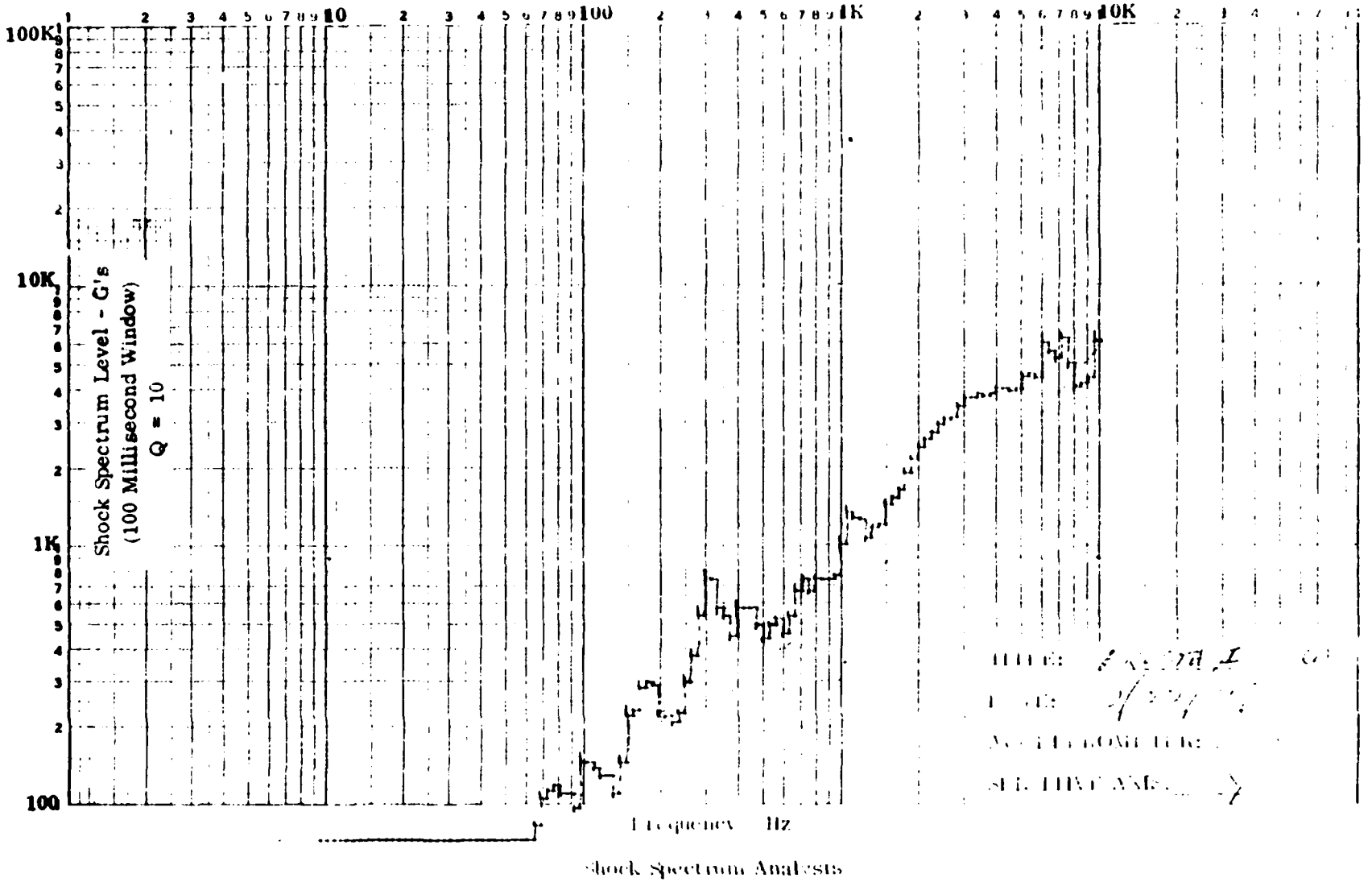

FIGURE C-1. Shock Spectrum at Level 1 on Frustum No. 7

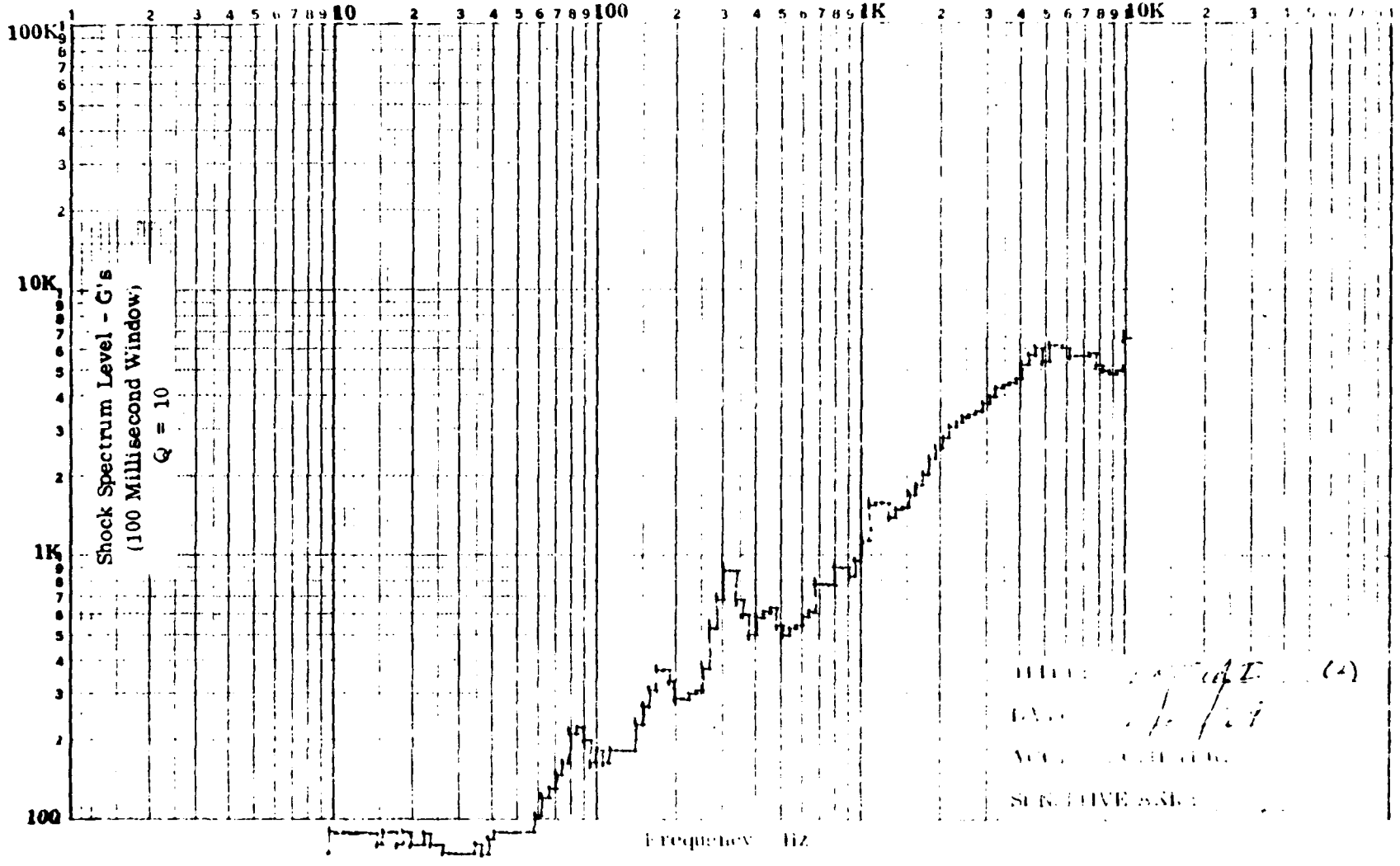

Shock Spectrum Analysis

FIGURE C-2. Shock Spectrum at Level 2 on Frustum No. 7.

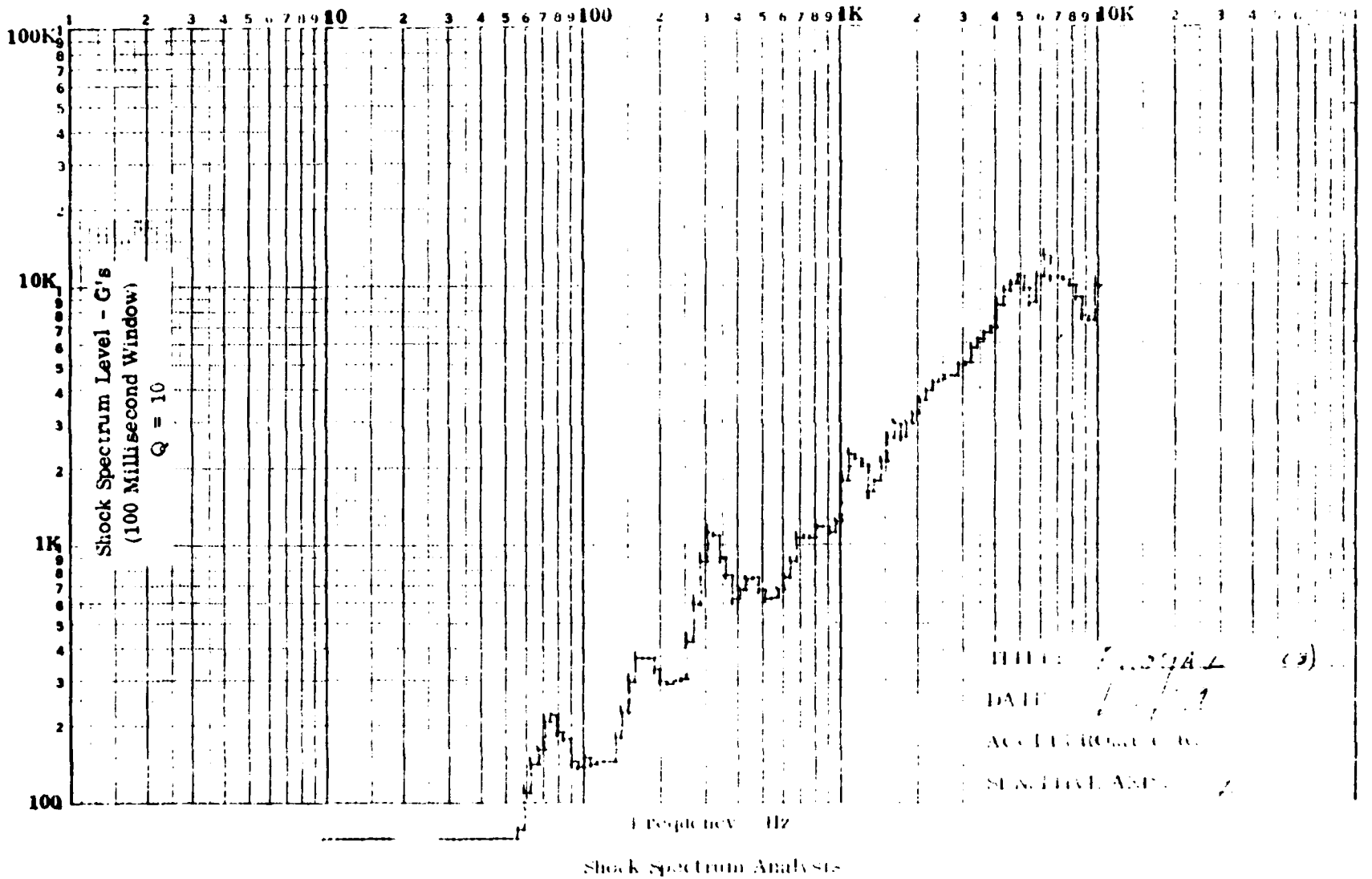

FIGURE C-3. Shock Spectrum at Level 3 on Frustum No. 7.

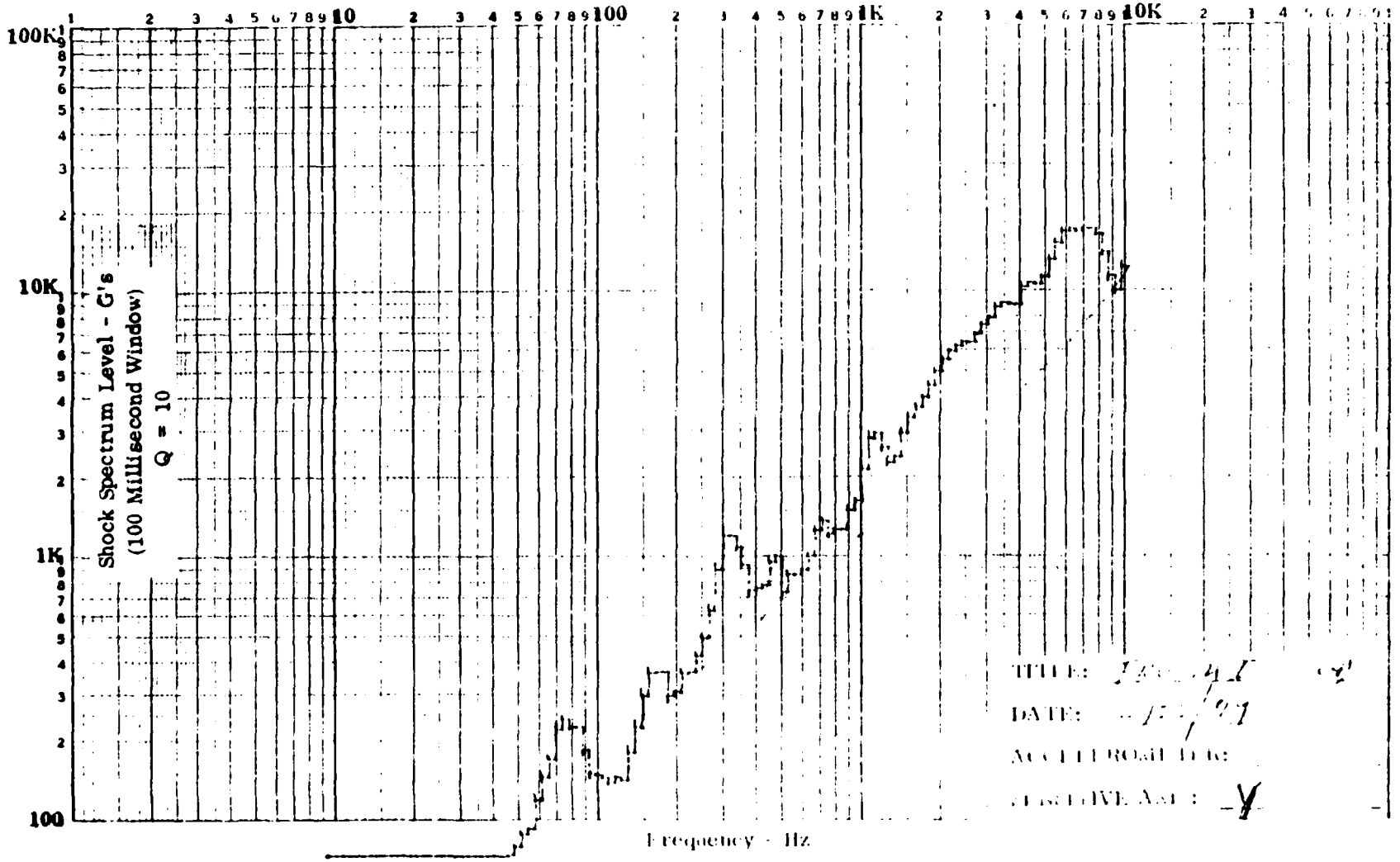

FIGURE C-4. Shock Spectrum at Level 4 on Frustum No. 7.

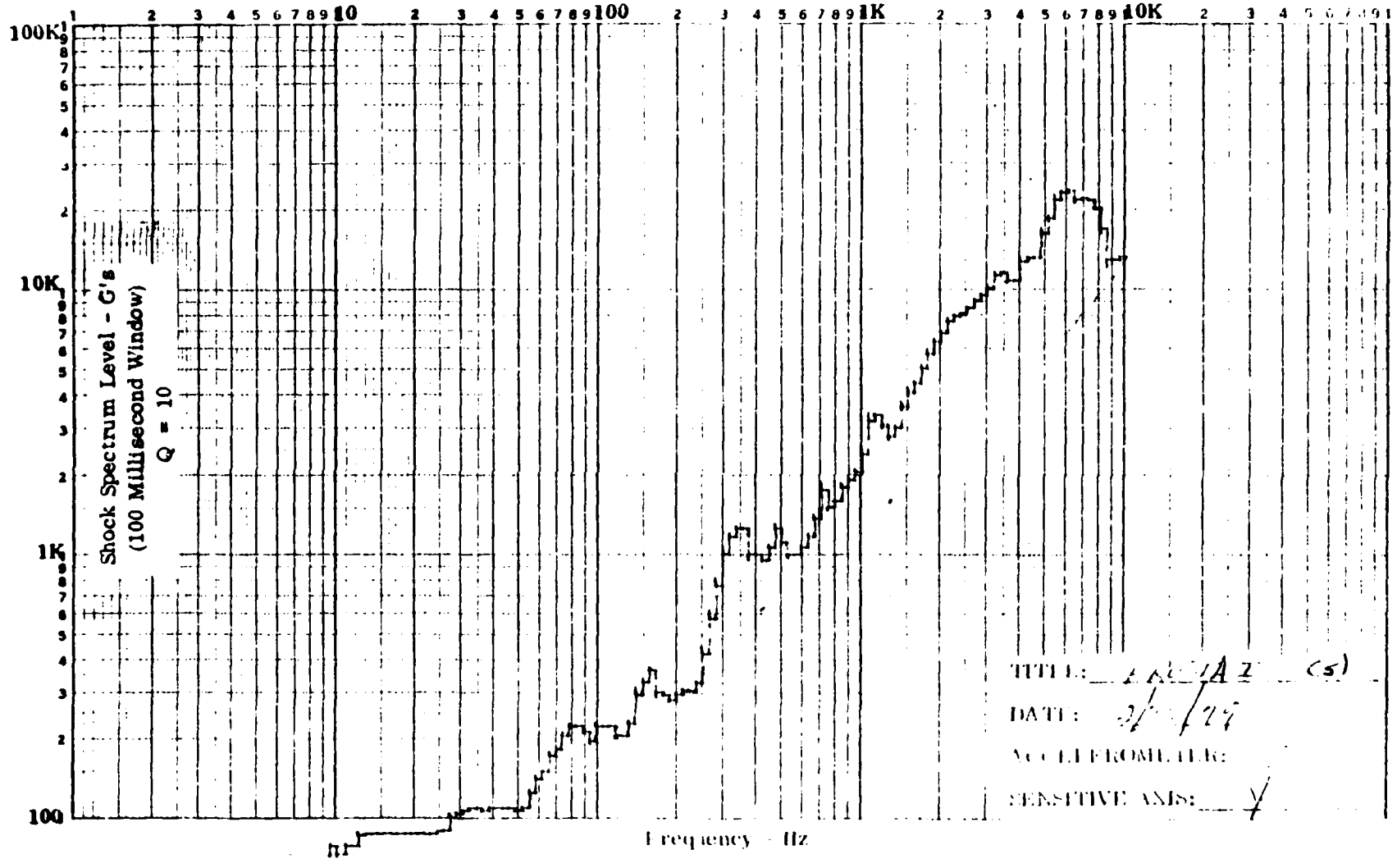

Shock Spectrum Analysis

FIGURE C-5. Shock Spectrum at Level 5 on Frustum No. 7.

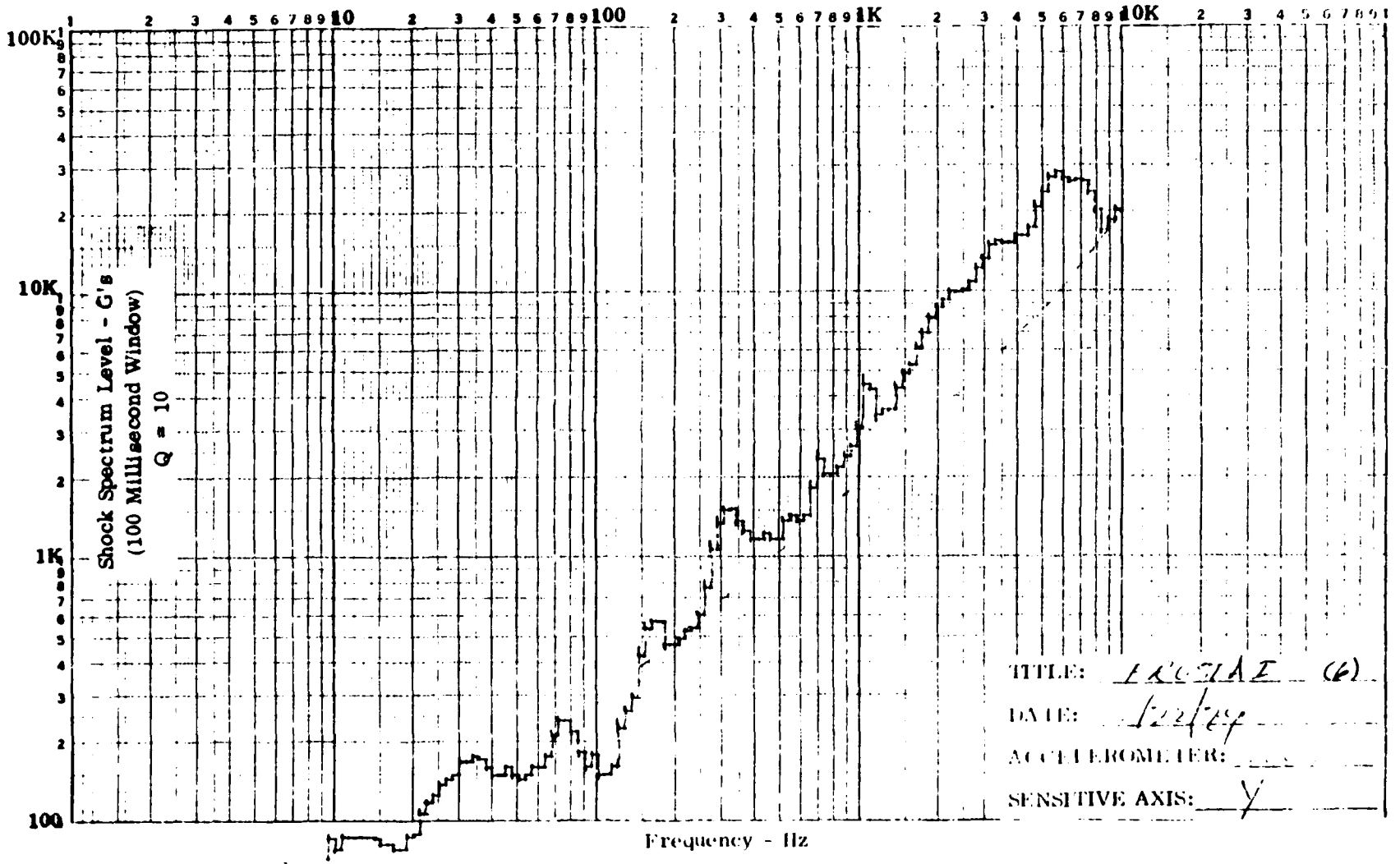

FIGURE C-6. Shock Spectrum at Level 6 on Frustum No. 7.

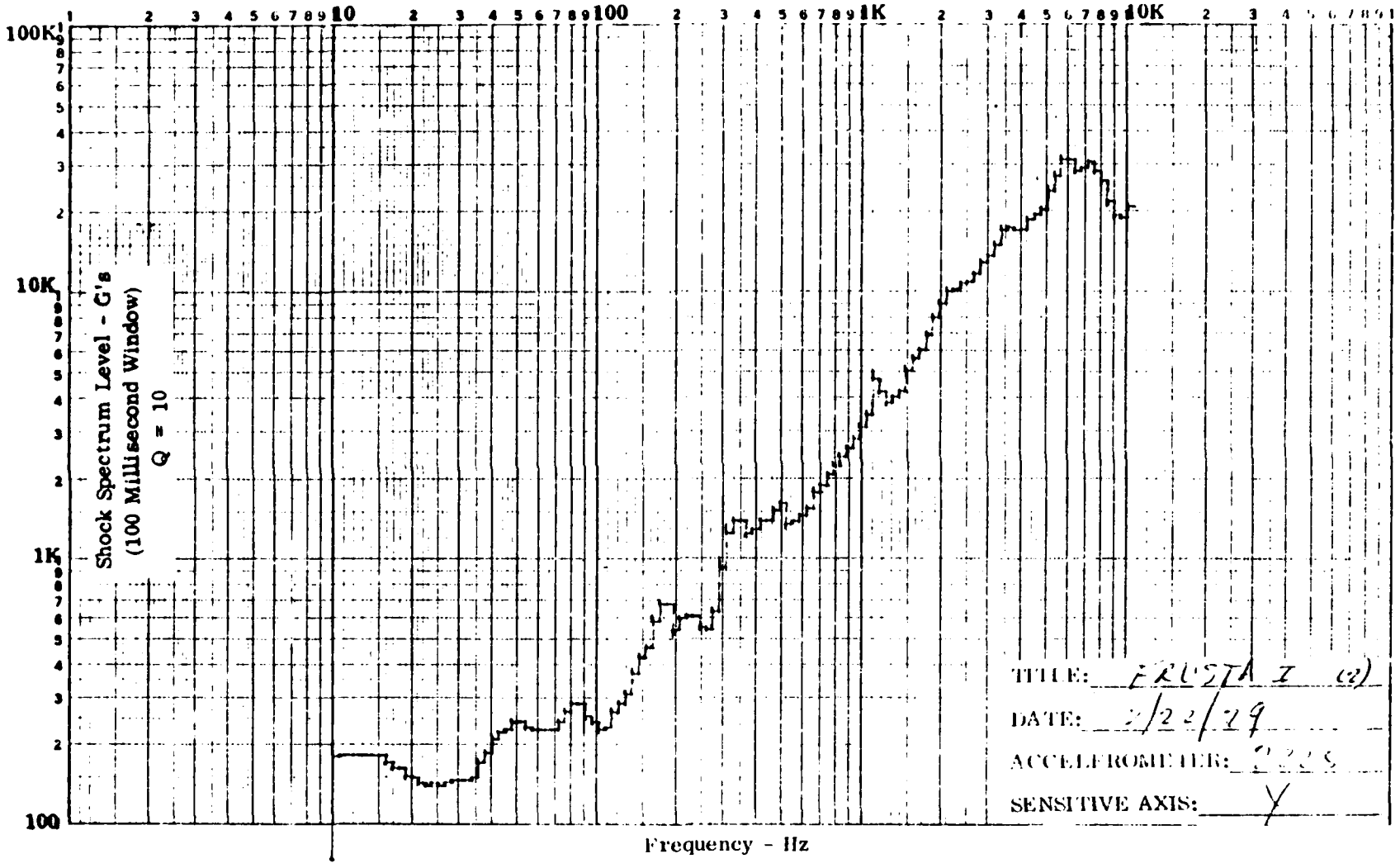

Shock Spectrum Analysis

FIGURE C-7. Shock Spectrum at Level 7 on Frustum No. 7.

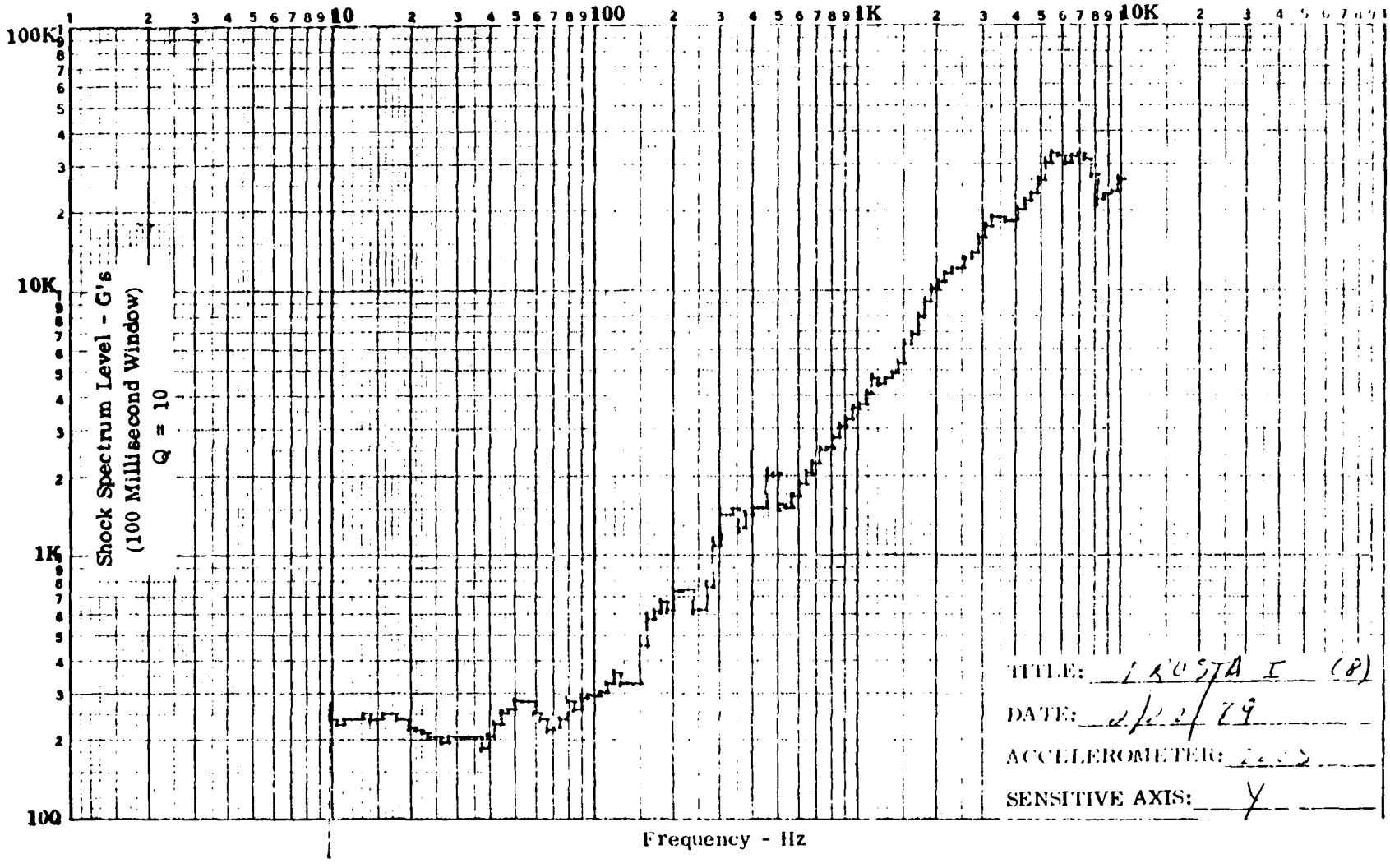

Shock Spectrum Analysis

FIGURE C-8. Shock Spectrum at Level 8 on Frustum No. 7.

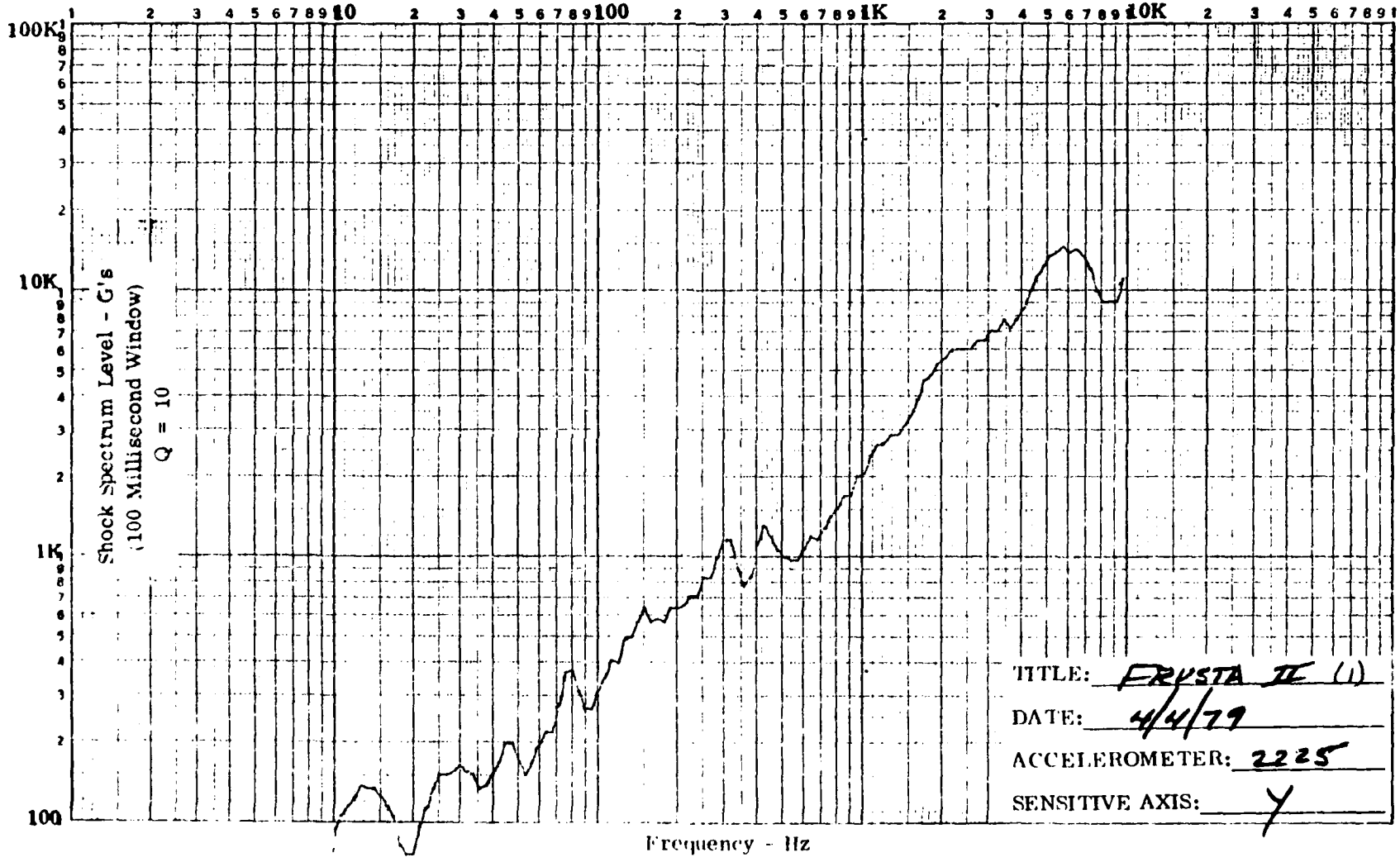

Shock Spectrum Analysis

FIGURE C-9. Shock Spectrum at Level 1 on Frustum No. 10.

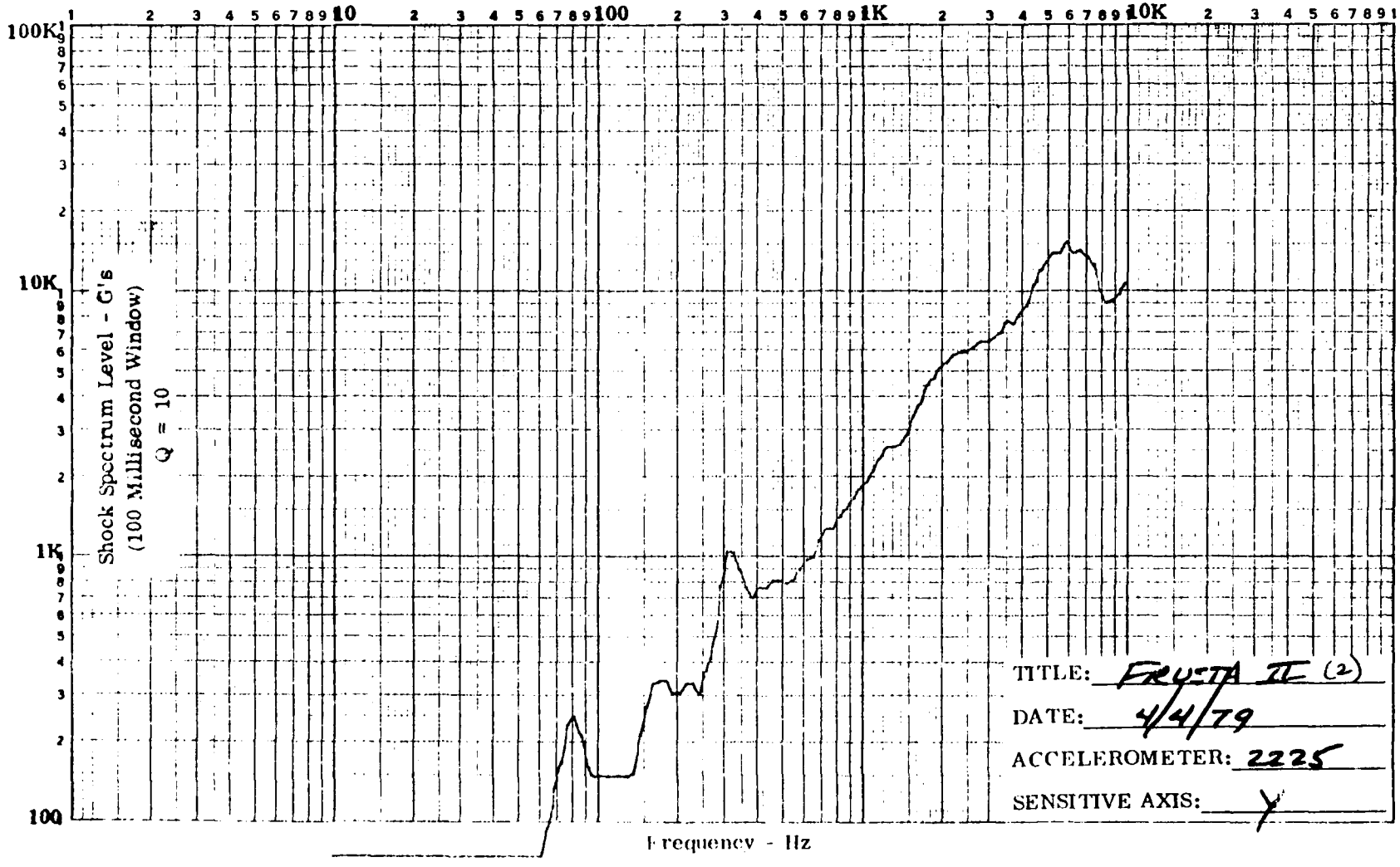

Shock Spectrum Analysis

FIGURE C-10. Shock Spectrum at Level 2 on Frustum No. 10.

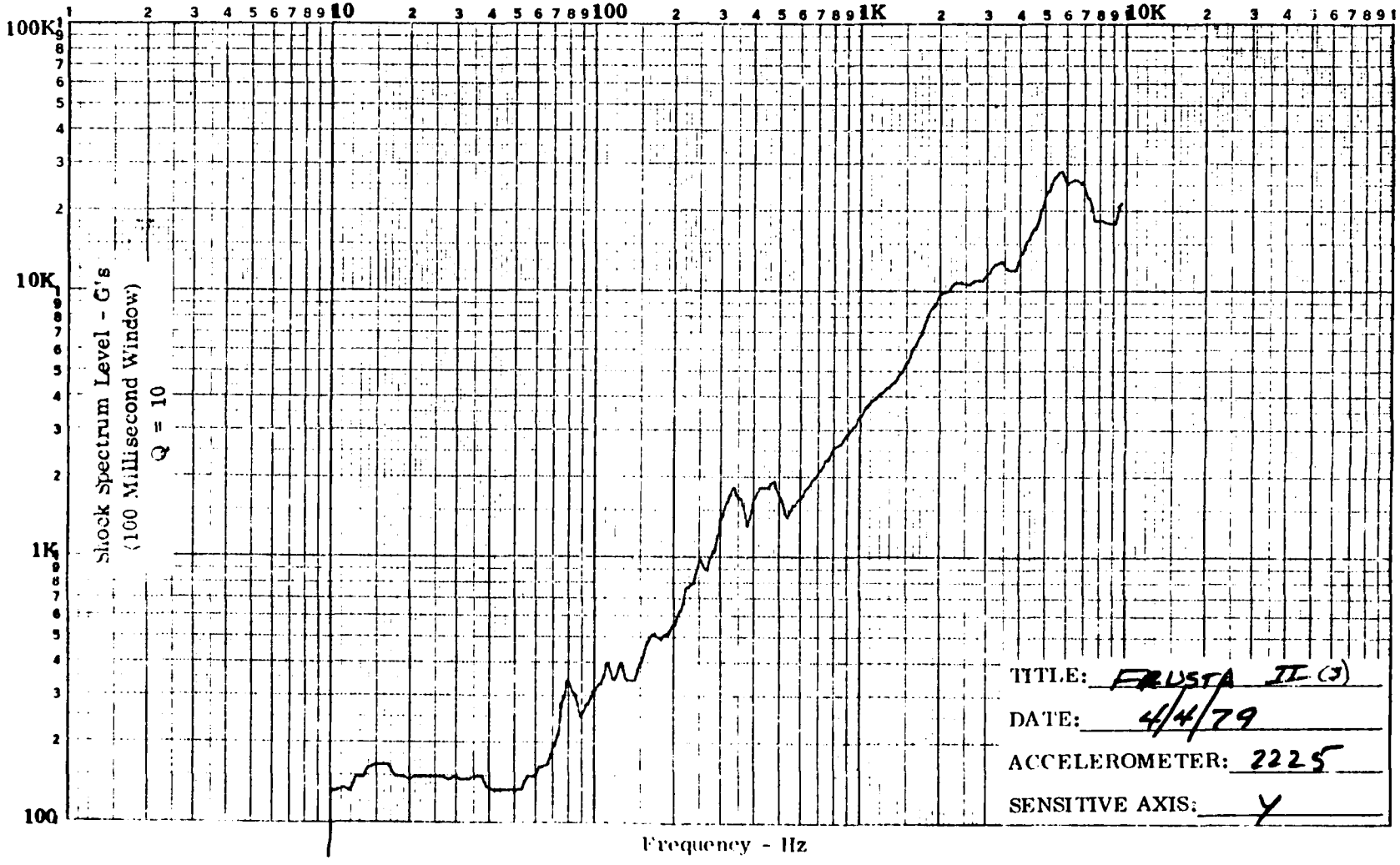

Shock Spectrum Analysis

FIGURE C-11. Shock Spectrum at Level 3 on Frustum No. 10.

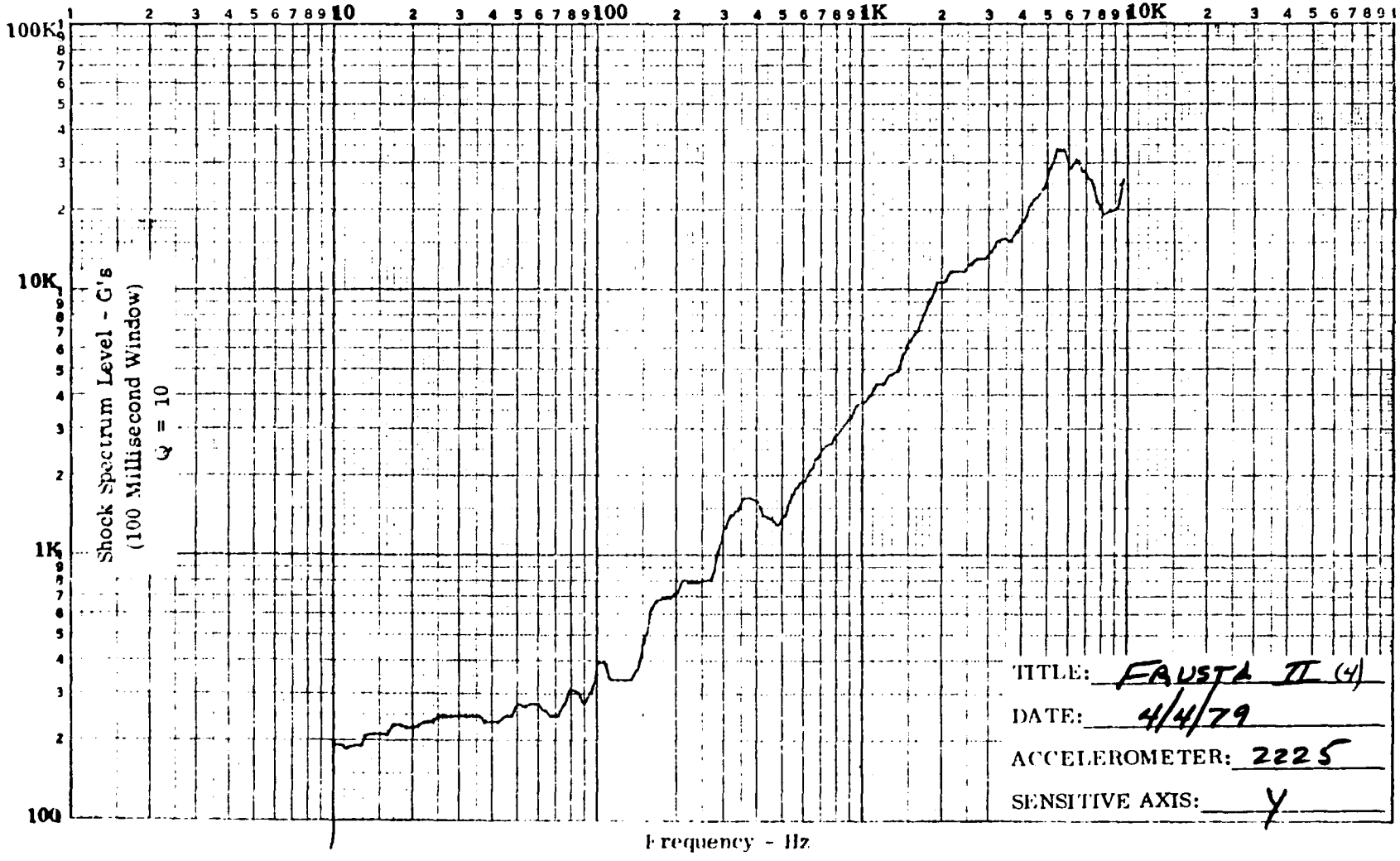

Shock Spectrum Analysis

FIGURE C-12. Shock Spectrum at Level 4 on Frustum No. 10.

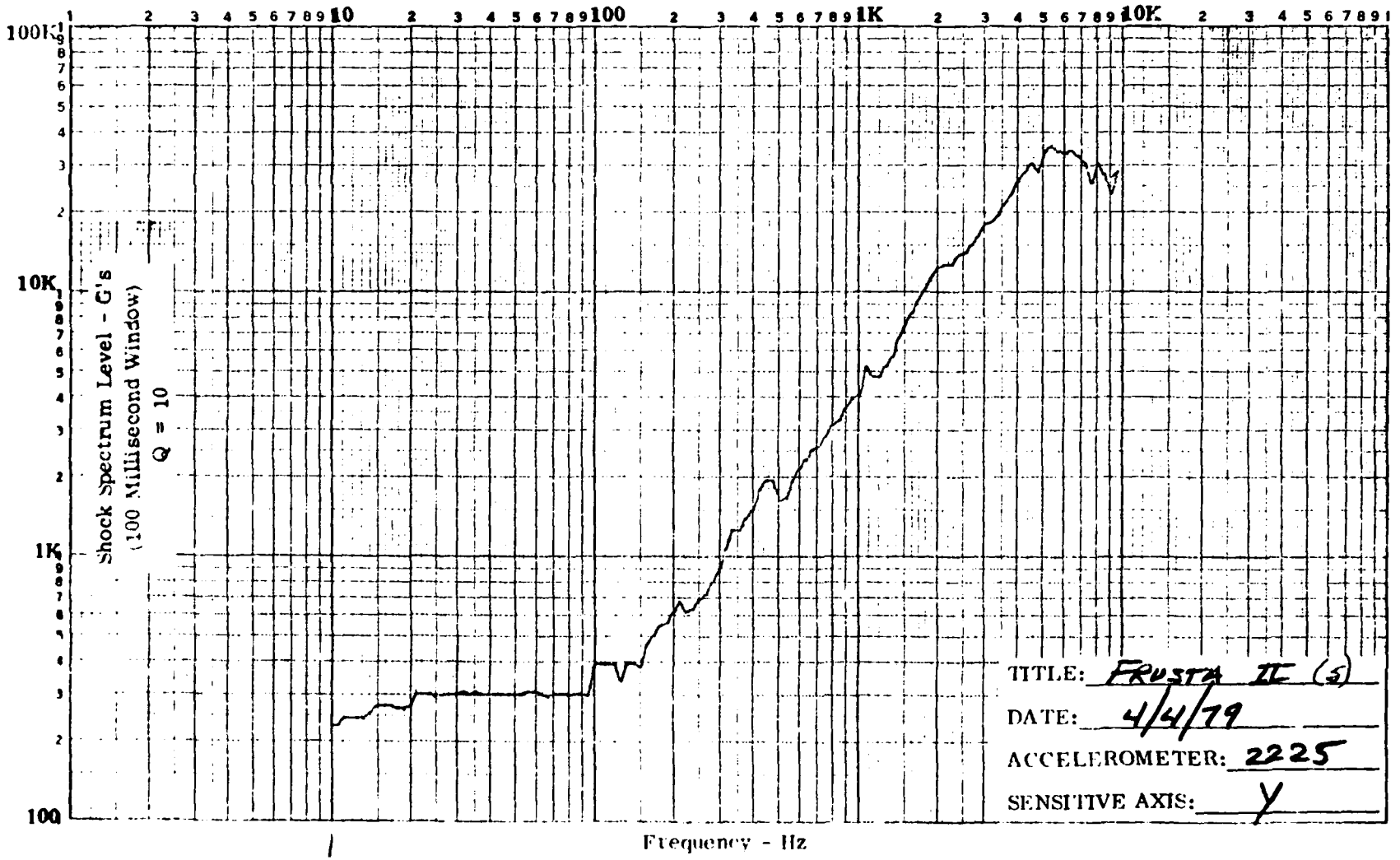

Shock Spectrum Analysis

FIGURE C-13. Shock Spectrum at Level 5 on Frustum No. 10.

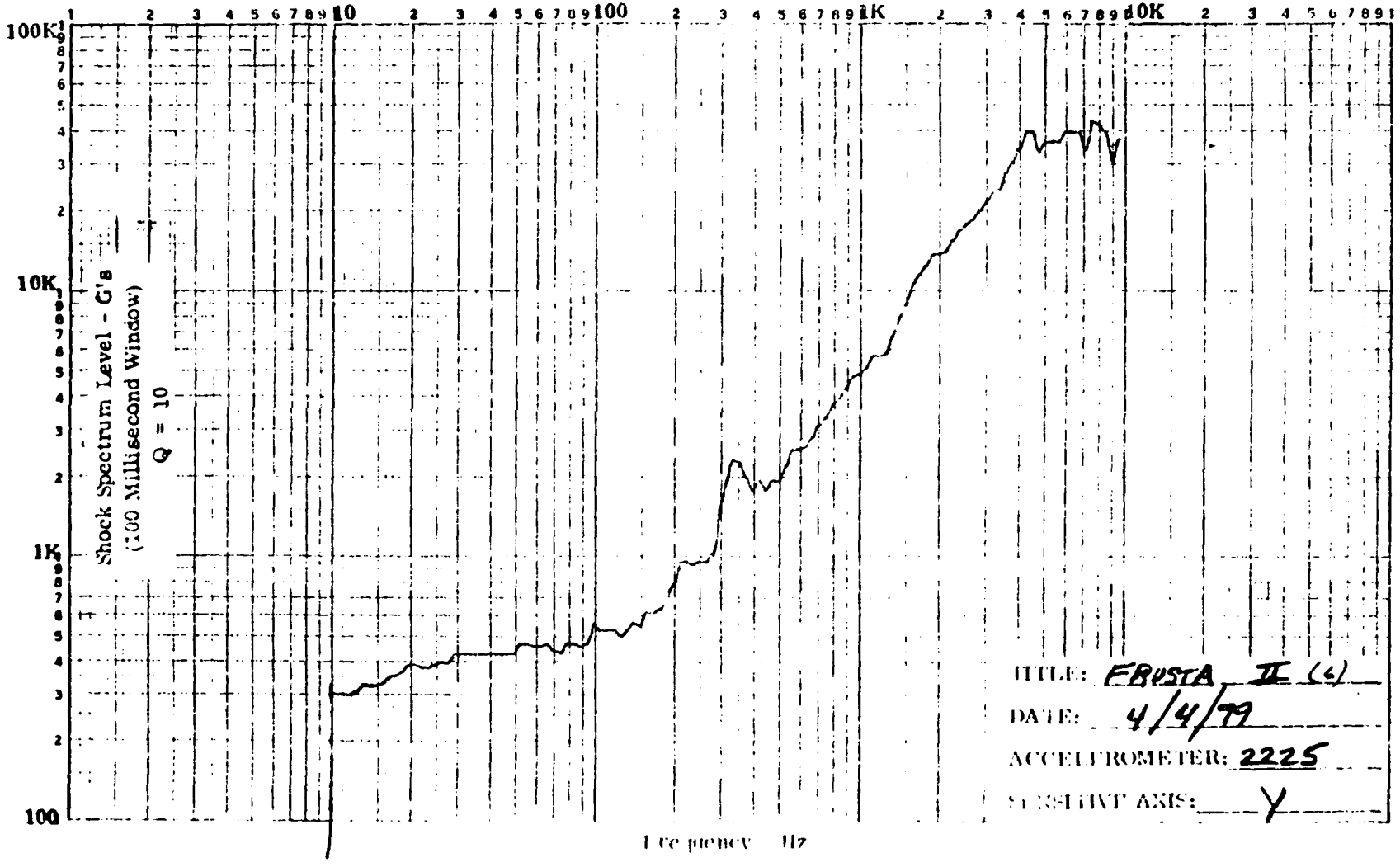

Shock spectrum analysis

FIGURE C-14. Shock Spectrum at Level 6 on Frustum No. 10.

APPENDIX D

GUIDANCE AND CONTROL SECTION
FULL-SCALE STRUCTURE DESIGN

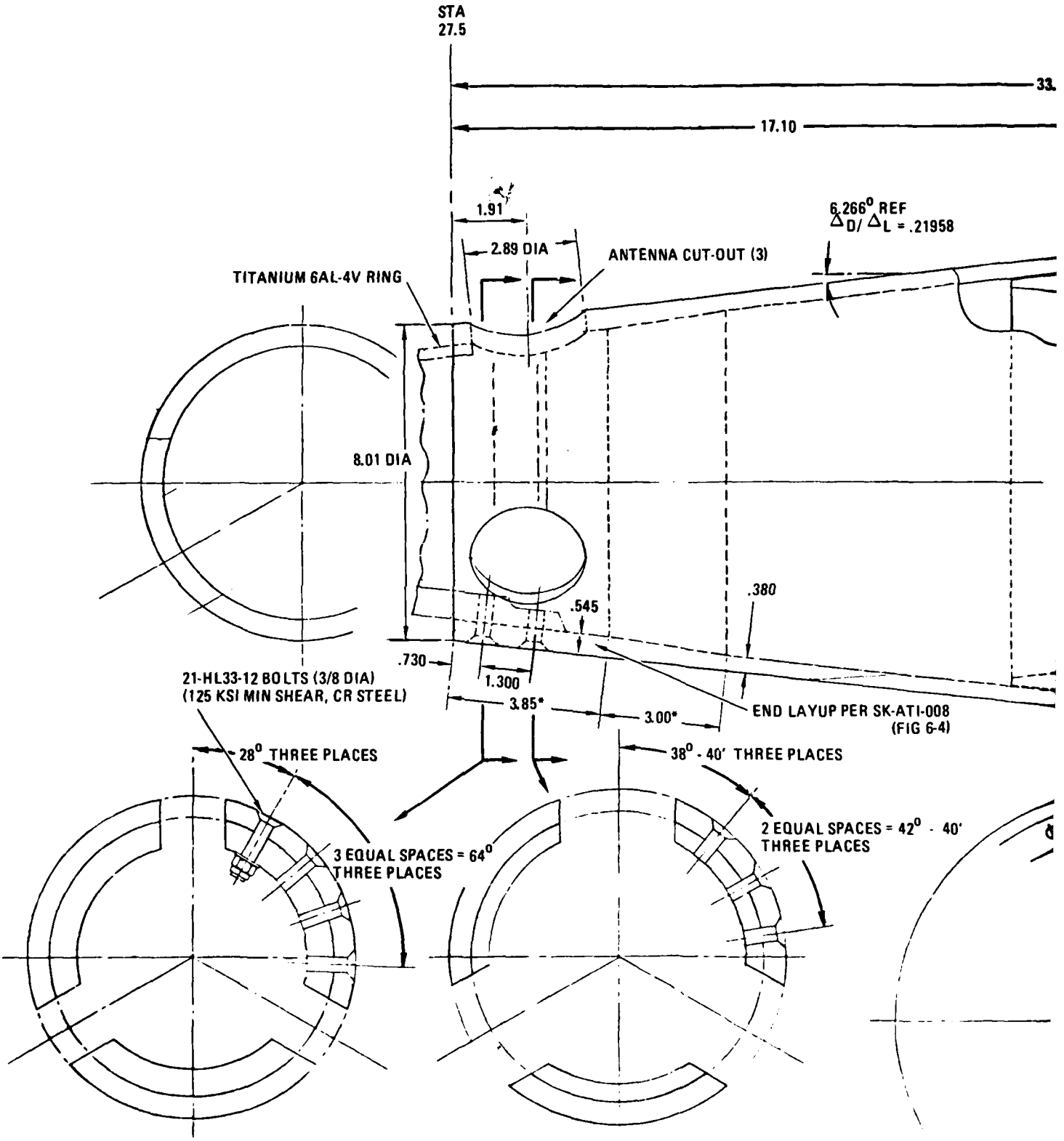
STA
27.5
33.
17.10
1.91
2.89 DIA
6.266° REF
ΔD/ ΔL = .21958
ANTENNA CUT-OUT (3)
TITANIUM 6AL-4V RING
8.01 DIA
.380
.545
.730
1.300
21-HL33-12 BOLTS (3/8 DIA)
(125 KSI MIN SHEAR, CR STEEL)
3.85*
3.00*
END LAYUP PER SK-ATI-008
(FIG 6-4)
28° THREE PLACES
38° - 40' THREE PLACES
3 EQUAL SPACES = 64°
THREE PLACES
2 EQUAL SPACES = 42° - 40'
THREE PLACES

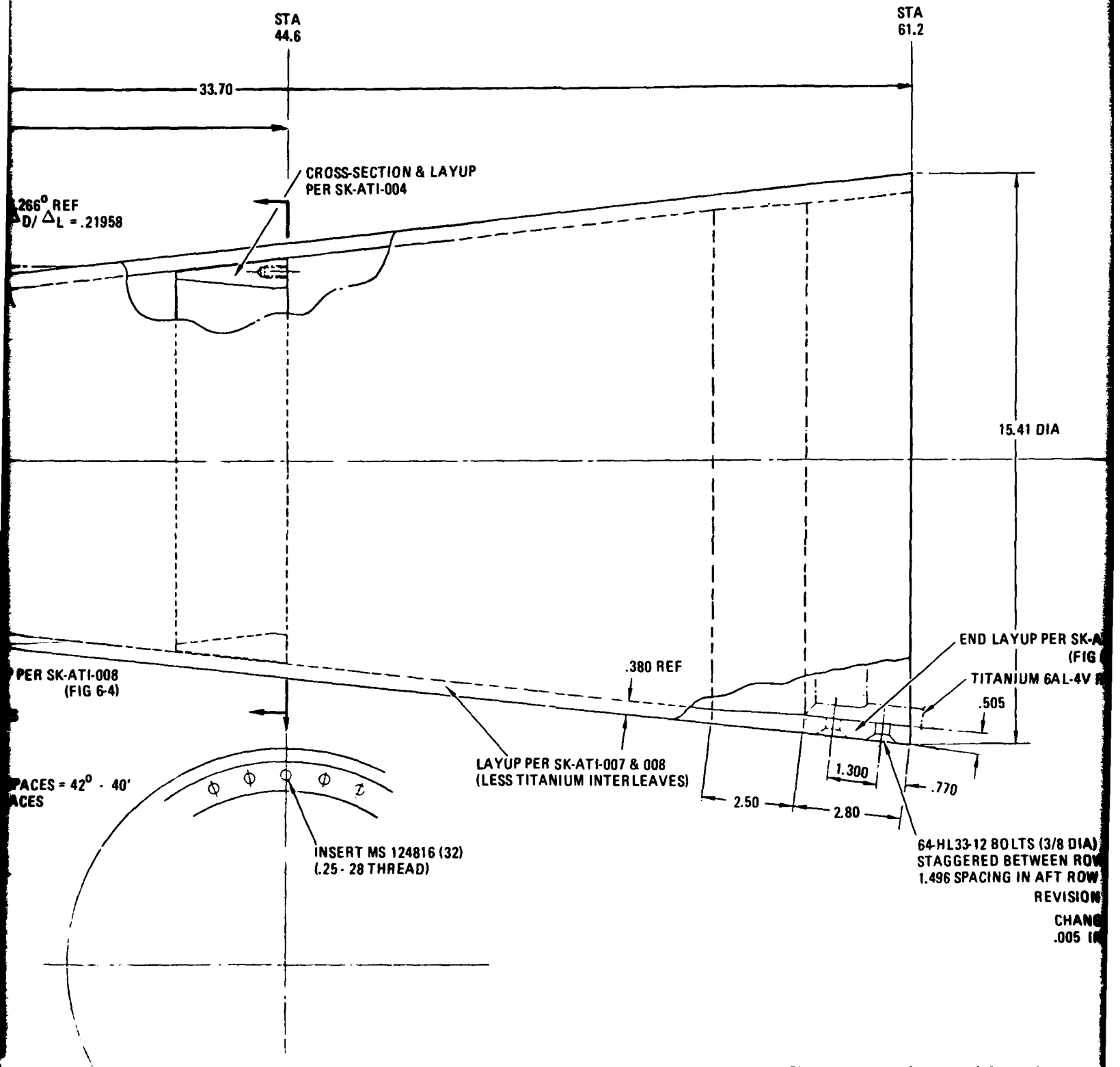

Figure D-1. Guidance and Control Sectio

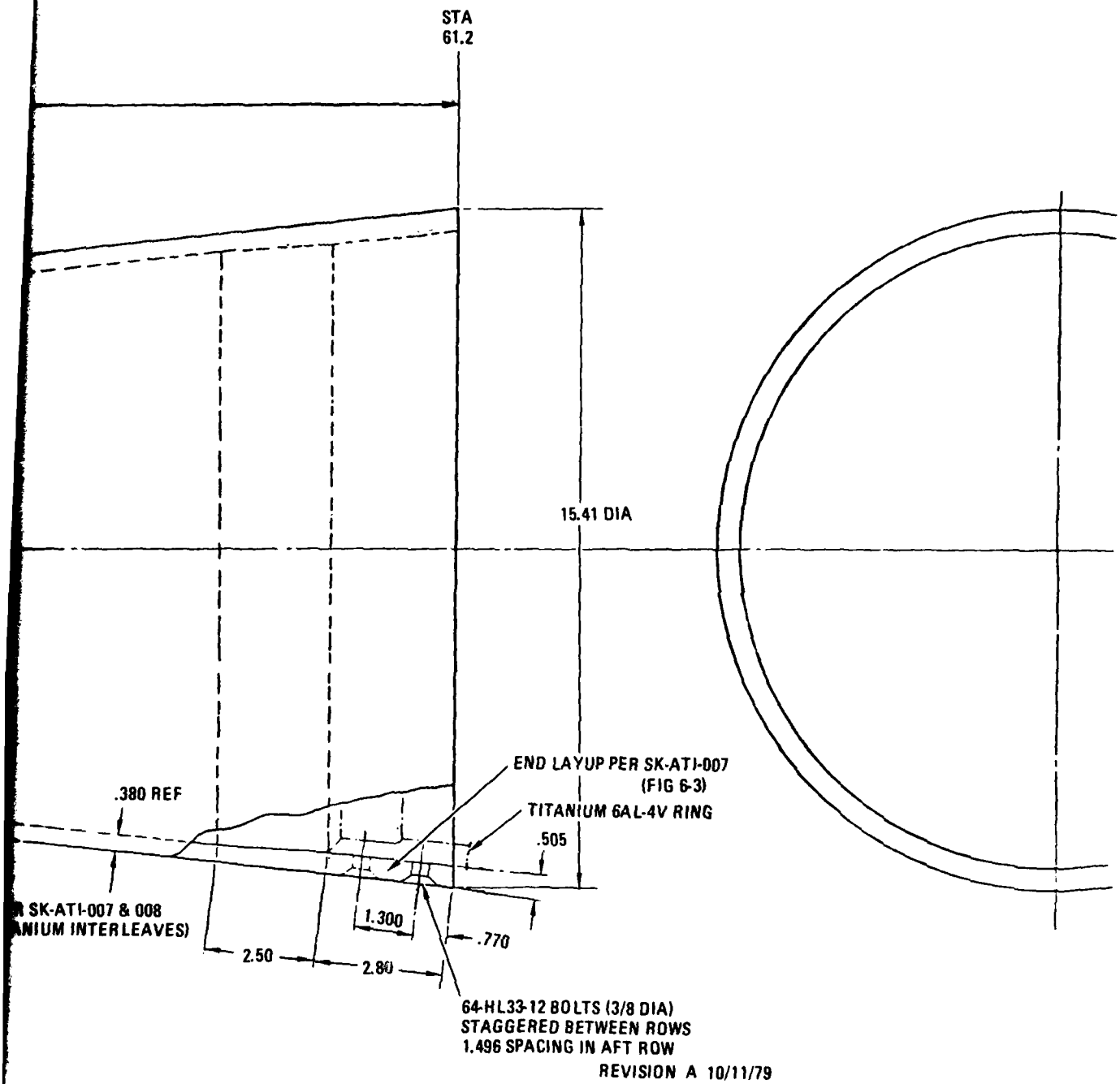

REVISION A 10/11/79

CHANGED END LAYUP CALL-OUT & THICKNESS TO REFLECT
.005 IN LIEU OF .0075 TITANIUM

PRELIMINARY DESIGN DRAWING	
COMPOSITE STRUCTURE ATI	
GENERAL DYNAMICS	14170 SK-ATI-009

653219-50

Figure D-1. Guidance and Control Section Full-Scale Composite Structure

APPENDIX E

FULL SCALE FRUSTUM TEST PLAN

DEVELOPMENT OF ADVANCED INTERCEPTOR SUBSTRUCTURAL MATERIALS

DAAG46-78-C-0056

FULL SCALE FRUSTA TEST PLAN

24 October 1979

by
N. R. Adsit

1.0 INTRODUCTION

Work carried out on previous contracts (DAAG46-76-C-0008, DAAG46-78-C-0056, and DAAG46-79-C-0081) has been concerned with developing the details of an advanced terminal interceptor. These contracts have tested subscale frusta, joint specimens, different types of equipment rings, and a full size forward section. The test data have demonstrated that the technology can be applied to a full size advanced terminal interceptor section.

The objective of this document is to outline the steps in testing a full size ATI section. The purpose of such a series of tests is to demonstrate that a section could withstand all the flight loads and perform its mission.

2.0 FRUSTA SECTION TESTS

The testing plan is divided into five separate tasks. Each task is designed to proof test one part of the structure. The final task would be to carry one of these tests to failure after the first five tests.

Before testing, the equipment ring would be installed and the fastener holes at both ends of the frusta would be drilled. In order to conduct the tests, the loads would be introduced into the ends through rings simulating the actual flight rings. These rings would be fabricated of steel rather than titanium to reduce cost. Also, the lead time in procuring titanium rings for test would be prohibitive. Drawings of the forward and aft rings are shown as Figure 1 which were designed to transfer the end loads to the frustum.

Each frusta will be instrumented to measure the modulus of elasticity of the shell and to measure strain at the suspected critical areas. The outline of the position of the strain gages is shown in Figure 3. This involves the use of 16 axial gages (FAE-25-12SO) and 6 rosette gages (FAER-25R-12SO). Each gage will be installed using Eastman 910 cyanoacrylate adhesive. A three wire system will be installed to prevent lead wire desensitization.

The loads on the frusta at the two most critical conditions are given in Table I. The loads on the equipment ring at these conditions are given in Table II.

2.1 Test I - Axial Load of the Equipment Ring

The first test is to load the equipment ring axial to the axial design limit load at maximum thrust. This test is designed to demonstrate that the equipment ring itself will carry design load and that it is bonded into the frusta correctly.

The test will be carried out in a Universal test machine. A flat, one-inch thick flanged plate of steel will be installed onto the equipment ring. The plate will be loaded from a rod on the test machine. The frusta will rest on the aft end ring (which is flat). The load will be increased in increments of 5,000 lb to 34,000 lb (DLL). Strains and load will be recorded at each increment. The plate on the equipment ring will be left in place for the next two tests.

2.2 Test II Axial Load of Forward End of Frusta

The second test is designed to proof load the forward end of the frusta. This is to substantiate that the forward end with the cut-outs can carry design limit load.

This test will also be carried out in a Universal test machine. The frusta will be put between the heads of the machine and shimmed to ensure uniform loading. A maximum load of 186,400 lb will be used. This load produces a stress equivalent to that caused by axial load and moment at booster burn-out.

The load will be in increments of 20,000 lb to 186,400 lb. Strains and loads will be recorded at each increment. These strains will be used to calculate a modulus of elasticity of the frusta. The best line fit of the data between 0 and DLL will be used to calculate this modulus.

2.3 Test III Axial Load on Frusta & Equipment Ring

This third test is designed to demonstrate that the load will flow around the equipment ring. The maximum loads will be those used in the two previous tests. This loads the shell to DLL at the forward end but only to 50% at the aft end.

The schematic of the test set-up is shown in Figure 3. The tests will be carried out in a Universal test machine. The loads will be applied proportionately in increments. Strain and loads will be recorded at each increment.

2.4 Test IV Combined Loads at Maximum Angle of Attack

The fourth test is a combined loads test. It will use the loads on the structure that occur at the maximum angle of attack (detailed in Tables I and II). The major item of concern is the very high shear discontinuity at station 44.6. The bending moment varies by only a factor of 2 over the total section.

The schematic of the test set-up is shown in Figure 4. The test will require six actuators to produce the desired load pattern. The frusta will be installed into the test fixture using the fasteners called out on the drawing of the graphite/epoxy frusta. The simulated steel end rings will be fastened to the test fixtures so that load will be introduced through them.

After the test cone is installed in the loading fixture, photographs of the test set-up will be made and all instruments will be adjusted to zero for the start of the test. The loads will be increased simultaneously in increments of 10% of Design Limit Load (DLL). Readings of all instrumentation will be made while the load is constant.

2.5 Test V Combined Loads at Booster Cut-Off

The fifth test is the most critical of the tests. The loads are those that occur at booster burn out and are the maximum loads that the structure experiences. They were the loads used to design the structure.

The schematic of the test set-up is the same as shown in Figure 4. Since the loads are substantially different than those in test IV, the actuator may have to be changed.

After the frusta and fixture are ready, the instruments will be adjusted to zero for the start of the test. All six loads will be increased simultaneously in increments of 10% of DLL to 100% DLL. Readings of all loads, strains, and displacements will be made while the loads are constant.

It is anticipated that this test will be carried beyond 100% DLL to failure. In which case the loads would be increased incrementally in 10% increments to failure.

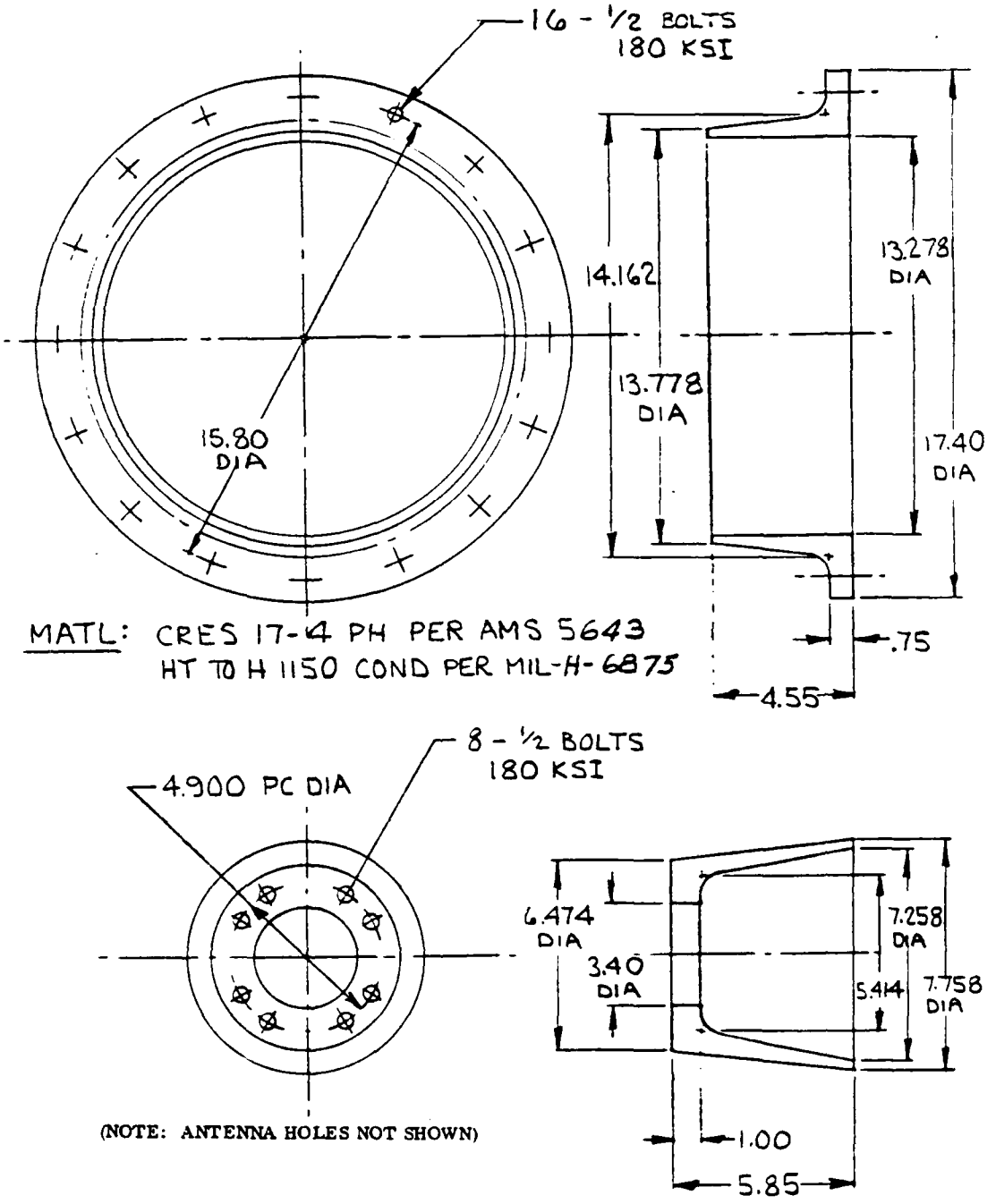

Figure 1. Forward and Aft Rings

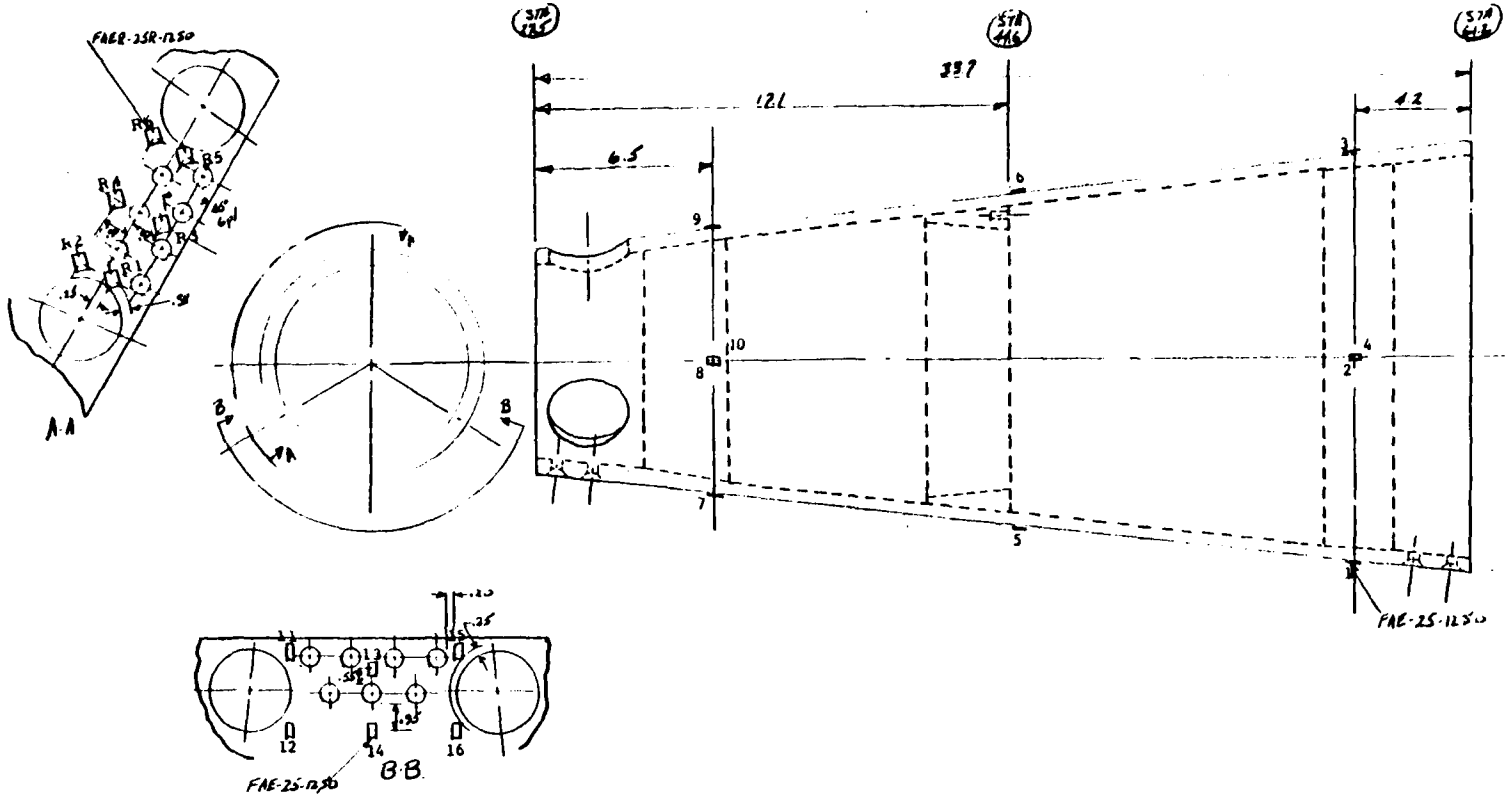

Figure 2. Position of Strain Gages

Table 1. Summary of Maximum Shell Loads For ATI Configuration 4C

Missile Body Forces[1][2] © LIMIT LOADS							
	Station 27.5			Station 61.2			Station 44.6
Load Condition	Axial (Klb)	Shear (Klb)	Moment (in-Klb)	Axial (Klb)	Shear (Klb)	Moment (in-Klb)	Moment (in-Klb)
First-Stage Burnout	−29.7	21.0[3]	282[3]	−77.1	50.7[3]	1306[3]	724
Max. Angle-of-Attack	−0.1	−6.9	205	−4.5	14.2	242	116

Notes:
(1) Trajectory 5-2
(2) Forces positive as shown:
(3) Configuration 4A (Reference 7)

Table 2. Summary of Maximum Equipment Ring Loads

	Equipment Ring Loads Station 44.6	
Load Condition	Axial (Klb)	Shear (Klb)
Maximum Thrust[1]	36.4	12.7
Maximum Angle-of-Attack	−4.5	46.9

[1]Very near first-stage burnout and hence added at that point.

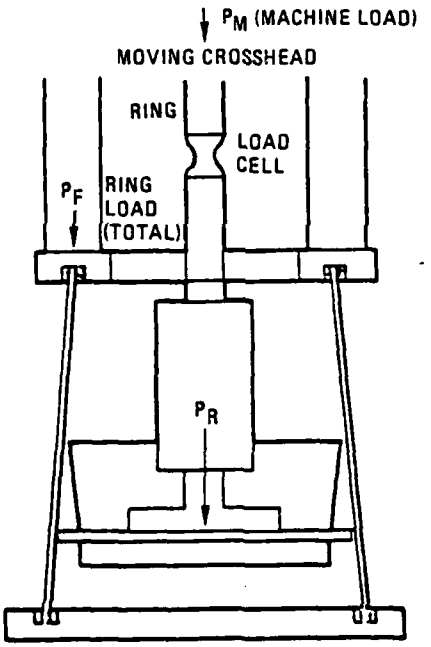

Figure 3. Sketch of Frustum Ring Test

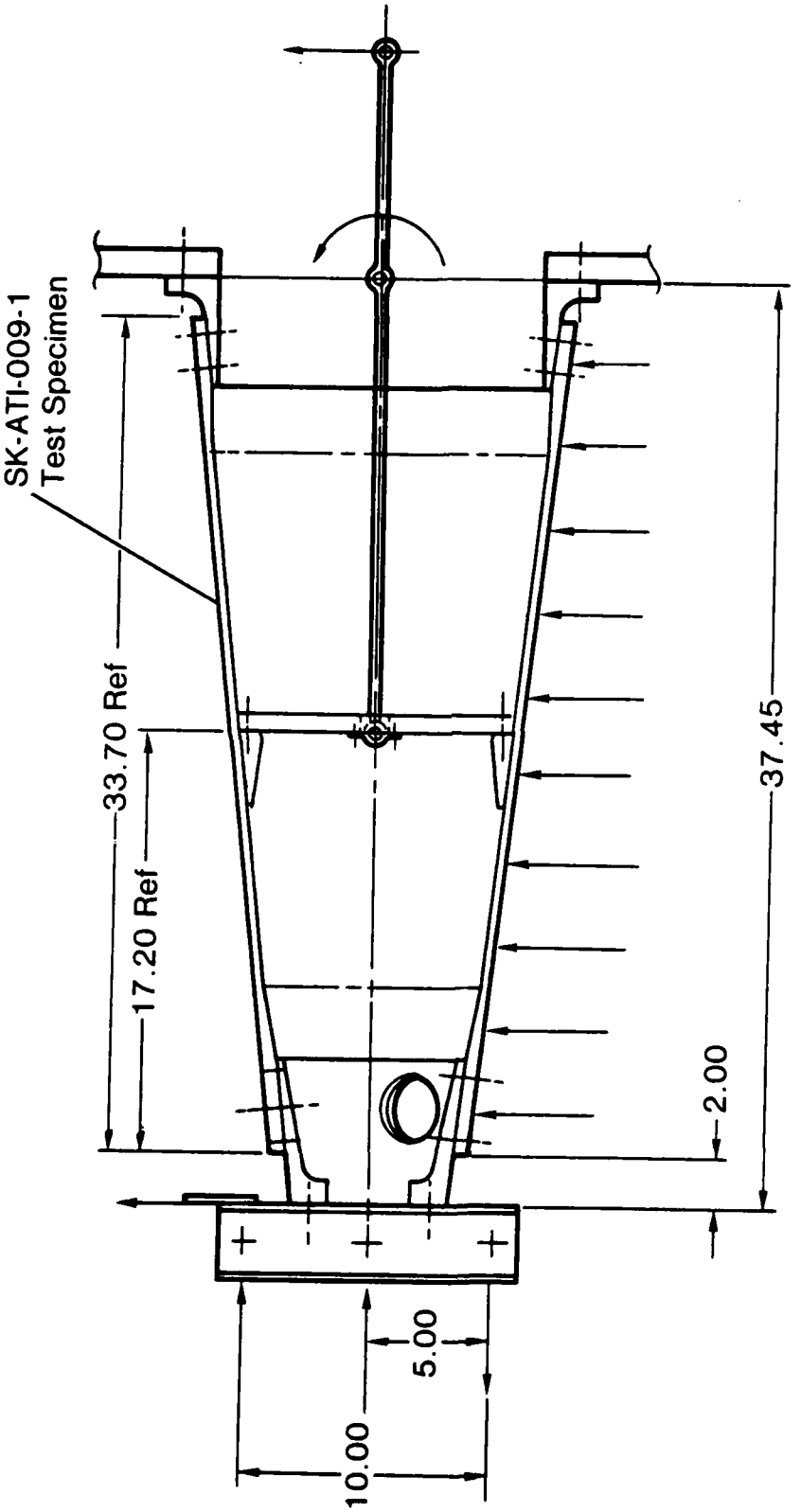

Figure 4. Schematic of Test Setup

DISTRIBUTION LIST
GENERAL DYNAMICS, CONVAIR DIVISION
CONTRACT DAAG46-78-C-0056
Development of Advanced Interceptor Substructural Material

	No. of Copies
Commander US Army Materiel Development and Readiness Command ATTN: DRCLDC, Office of Laboratory Management, R. Gonano 5001 Eisenhower Avenue Alexandria, VA 22333	1
Ballistic Missile Defense Program Office ATTN: DACS-BMT 5001 Eisenhower Avenue Alexandria, VA 22333	1
Director Ballistic Missile Defense Advanced Technology Center ATTN: W. Davis J. Carson Col. J. W. Gillespie W. Davies D. Harmon J. Papadopoulos S. Brockway M. Whitfield P.O. Box 1500 Huntsville, AL 35807	1 1 1 1 1 1 1 1
Ballistic Missile Defense Systems Technology Program ATTN: J. Katechis E. Martz P.O. Box 1500 Huntsville, AL 35807	1 1
Commander US Army Ballistic Missile Defense Systems Command ATTN: N. J. Hurst P.O. Box 1500 Huntsville, AL 35807	1
Commander US Army Missile Research and Development Command ATTN: DRDMI-EAM, W. K. Patterson Redstone Arsenal Huntsville, AL 35809	1

	No. of Copies
Director Defense Nuclear Agency ATTN: SPAS, D. Kohler SPAS, Lt. J. Sommers Washington, DC 20305	 1 1
Office of Deputy Under Secretary of Defense for Research and Engineering (ET) ATTN: J. Persh, Staff Specialist for Materials and Structures The Pentagon, Room 3D1089 Washington, DC 20301	 1
Office of Deputy Chief of Research Development and Acquisition ATTN: DAMA-CSS, J. Bryant The Pentagon, Room 3D424 Washington, DC 20310	 1
Commander Harry Diamond Laboratories ATTN: DRXDO-NP, F. Wimenitz DRXDO-NP, J. Gwaltney 2800 Powder Mill Road Adelphi, MD 20783	 1 1
Commander Air Force Flight Dynamics Laboratory ATTN: AFFDL/FBC, H. A. Wood Wright-Patterson Air Force Base, OH 45433	 1
Commander US Army Combat Development Command Institute of Nuclear Studies ATTN: Technical Library Fort Bliss, TX 79916	 1
Commander AFWAL Materials Laboratory Air Force Systems Command ATTN: W. Kessler H. Materne M. Duhl Wright-Patterson Air Force Base, OH 45433	 1 1 1
Commander Space Division ATTN: SD/YLXT, Lt. Col. Harry L. Staubs Los Angeles Air Force Station Box 92960 Worldway Postal Center Los Angeles, CA 90009	 1

	No. of Copies
Commander BMO/ABRES Office ATTN: BMO/MNRT, Col. R. Smith BMO/MNRTE, Maj. J. Sikra BMO/MNRTE, Maj. K. Yelmgren Norton Air Force Base, CA 92409	 1 1 1
Commander Naval Sea Systems Command ATTN: ORD-03331, M. Kinna Washington, DC 20360	 1
Commander Naval Surface Weapons Center ATTN: W. Carson Lyons J. Foltz R. Feldhuhn Silver Springs, MD 20910	 1 1 1
Sandia Laboratories ATTN: J. K. Cole P.O. Box 5800 Albuquerque, NM 87115	 1
Aerospace Corporation ATTN: W. Riley R. Meyers L. Rubin P.O. Box 92957 Los Angeles, CA 90009	 1 1 1
AVCO Systems Division ATTN: P. G. Rolincik 201 Lowell Street Wilmington, MA 01887	 1
Battelle Columbus Laboratories ATTN: E. Foster 505 King Avenue Columbus, OH 43201	 1
Boeing Aerospace Company ATTN: M. Kushner P.O. Box 3999 Seattle, WA 98124	 2

	No. of Copies
Celanese Corporation ATTN: Howard S. Kliger Morris Court Summit, NJ 07901	1
DWA Composite Specialties, Inc. ATTN: J. F. Dolowy, Jr. 21119 Superior Street Chatsworth, CA 91311	1
Effects Technology, Inc. ATTN: R. Wengler J. Green 5383 Hollister Avenue Santa Barbara, CA 93111	1 1
Fiber Materials, Inc. ATTN: L. Lander G. Williams Biddeford Industrial Park Biddeford, ME 04005	1 1
General Dynamics Corporation Convair Division ATTN: J. Hertz D. Weisinger R. Adsit A. Robertson L. Browning 5001 Kearny Villa Road San Diego, CA 92138	1 1 1 1 1
General Electric Company Advanced Materials Development Laboratory ATTN: P. Gorsuch, Room 4466 J. Brazel, Room 4466 3198 Chestnut Street Philadelphia, PA 19101	1 1
Hughes Aircraft Company ATTN: R. W. Jones Centinela and Teale Streets Culver City, CA 90230	1

	No. of Copies
Lockheed Missiles and Space Company	
Palo Alto Research Laboratory	
ATTN: E. C. Burke	1
D. Aspinwall	1
T. Tietz	1
Dept. 5230, Bldg. 201	
3251 Hanover Street	
Palo Alto, CA 94304	
Lockheed Missiles and Space Company	
ATTN: P. G. Sullivan	1
A. Mietz	1
M. Jacobson	1
H. Armstrong	1
P.O. Box 504	
Sunnyvale, CA 94088	
Martin Marietta Corporation	
ATTN: D. Easter	1
L. Gilbert	1
F. Koo	1
J. Madden	1
G. Wannell	1
V. Hewitt	1
D. Gurley	1
W. Spencer	1
K. Hansen	1
P.O. Box 5837	
Orlando, FL 32805	
Material Concepts, Inc.	
ATTN: S. Paprocki	1
2747 Harrison Road	
Columbus, OH 43204	
McDonnell Douglas Asronautics Company	
ATTN: R. C. Curley	1
H. S. Parachanian	1
L. Cohen	1
P. W. Harruff	1
A. J. Cwiertny	1
R. Zemer	1
5301 Bolsa Avenue	
Huntington Beach, CA 92647	

	No. of Copies
New Technology, Inc. ATTN: B. Neuffer Research Park P.O. Box 5245 Huntsville, AL 38505	1
Prototype Development Associates ATTN: J. Schutzler 1740 Gary Avenue, Suite 201 Santa Ana, CA 92705	1
R&D Associates ATTN: A. Field P.O. Box 9695 Marina del Rey, CA 90291	1
Science Applications, Inc. ATTN: I. Osofsky One Continental Plaza, Suite 310 101 Continental Blvd. El Segundo, CA 90245	1
Southwest Research Institute ATTN: A. Wenzel 8500 Culebra Road San Antonio, TX 78206	1
Terra Tek, Inc. ATTN: A. H. Jones University Research Park 420 Wakara Way Salt Lake City, Utah 84108	1
TRW Defense and Space Systems ATTN: L. Berger P.O. Box 1310 San Bernardino, CA 92402	1
University of California Lawrence Livermore Laboratory ATTN: T. T. Chiao E. M. Wu P.O. Box 808 Livermore, CA 94550	1 1

	No. of Copies
Defense Documentation Center Cameron Station, Bldg. 5 5010 Duke Street Alexandria, VA 22314	2
Director Army Materials & Mechanics Research Center	
ATTN: DRXMR-H, J. F. Dignam	1
DRXMR-H, L. R. Aronin	2
DRXMR-H, S. C. Chou	1
DRXMR-AP	1
DRXMR-PL	1
DRXMR-PR Watertown, MA 02172	2

Army Materials and Mechanics Research Center
Watertown, Massachusetts 02172
DEVELOPMENT OF ADVANCED INTERCEPTOR SUBSTRUCTURAL MATERIAL
J. Hertz and N. R. Adsit
General Dynamics Convair Division

AD

UNCLASSIFIED
UNLIMITED DISTRIBUTION

Key Words

Technical Report AMMRC TR 80-44, August 1980
151 pp – illus – tables, Contract DAAG46-78-C-0065,
DD/A Project 1W16211A661
AMCMS Code 62113.11.07000
Final Report September 1978
to November 1979

Composite Materials
Composite structures
Graphite
Missile Airframes
Interceptors
Epoxy Resins
Fibers

The work reported herein represents a continuation of previous work reported in AMMRC-TR-78-4 and TR 78-38 and is aimed at the development of ultra-high-modulus graphite/epoxy structures for use in future advanced terminal interceptors. The work has produced a preliminary full-scale design and demonstrated, experimentally and analytically, that the design will carry the loads. More study needs to be conducted and some further experimental work is recommended before a full-scale article is tested. Work reported here has concentrated on testing the aft joint and an intermediate ring for holding an equipment package in the frusta.

Army Materials and Mechanics Research Center
Watertown, Massachusetts 02172
DEVELOPMENT OF ADVANCED INTERCEPTOR SUBSTRUCTURAL MATERIAL
J. Hertz and N. R. Adsit
General Dynamics Convair Division

AD

UNCLASSIFIED
UNLIMITED DISTRIBUTION

Key Words

Technical Report AMMRC TR 80-44, August 1980
151 pp – illus – tables, Contract DAAG46-78-C-0056,
DD/A Project 1W16211A661
AMCMS Code 62113.11.07000
Final Report September 1978
to November 1979

Composite Materials
Composite structures
Graphite
Missile Airframes
Interceptors
Epoxy Resins
Fibers

The work reported herein represents a continuation of previous work reported in AMMRC-TR-78-4 and TR-78-38 and is aimed at the development of ultra-high-modulus graphite/epoxy structures for use in future advanced terminal interceptors. The work has produced a preliminary full-scale design and demonstrated, experimentally and analytically, that the design will carry the loads. More study needs to be conducted and some further experimental work is recommended before a full-scale article is tested. Work reported here has concentrated on testing the aft joint and an intermediate ring for holding an equipment package in the frusta.

Army Materials and Mechanics Research Center
Watertown, Massachusetts 02172
DEVELOPMENT OF ADVANCED INTERCEPTOR SUBSTRUCTURAL MATERIAL
J. Hertz and N. R. Adsit
General Dynamics Convair Division

AD

UNCLASSIFIED
UNLIMITED DISTRIBUTION

Key Words

Technical Report AMMRC TR 80-44, August 1980
151 pp – illus – tables, Contract DAAG46-78-C-0056,
DD/A Project 1W16211A661
AMCMS Code 62113.11.07000
Final Report September 1978
to November 1979

Composite Materials
Composite structures
Graphite
Missile Airframes
Interceptors
Epoxy Resins
Fibers

The work reported herein represents a continuation of previous work reported in AMMRC-TR-78-4 and TR 78-38 and is aimed at the development of ultra-high-modulus graphite/epoxy structures for use in future advanced terminal interceptors. The work has produced a preliminary full-scale design and demonstrated, experimentally and analytically, that the design will carry the loads. More study needs to be conducted and some further experimental work is recommended before a full-scale article is tested. Work reported here has concentrated on testing the aft joint and an intermediate ring for holding an equipment package in the frusta.

Army Materials and Mechanics Research Center
Watertown, Massachusetts 02172
DEVELOPMENT OF ADVANCED INTERCEPTOR SUBSTRUCTURAL MATERIAL
J. Hertz and N. R. Adsit
General Dynamics Convair Division

AD

UNCLASSIFIED
UNLIMITED DISTRIBUTION

Key Words

Technical Report AMMRC TR 80-44, August 1980
151 pp – illus – tables, Contract DAAG46-78-C-0056,
DD/A Project 1W16211A661
AMCMS Code 62113.11.07000
Final Report September 1978
to November 1979

Composite Materials
Composite structures
Graphite
Missile Airframes
Interceptors
Epoxy Resins
Fibers

The work reported herein represents a continuation of previous work reported in AMMRC-TR-78-4 and TR-78-38 and is aimed at the development of ultra-high-modulus graphite/epoxy structures for use in future advanced terminal interceptors. The work has produced a preliminary full-scale design and demonstrated, experimentally and analytically, that the design will carry the loads. More study needs to be conducted and some further experimental work is recommended before a full-scale article is tested. Work reported here has concentrated on testing the aft joint and an intermediate ring for holding an equipment package in the frusta.

Army Materials and Mechanics Research Center
Watertown, Massachusetts 02172
DEVELOPMENT OF ADVANCED INTERCEPTOR SUBSTRUCTURAL MATERIAL
J. Hertz and N. R. Adsit
General Dynamics Convair Division

AD ______

UNCLASSIFIED
UNLIMITED DISTRIBUTION

Technical Report AMMRC TR 80-44, August 1980
151 pp – illus – tables, Contract DAAG46-78-C-0056,
D/A Project 1W16211A661
AMCMS Code 62113.11.07000
Final Report September 1978
to November 1979

Key Words

Composite Materials
Composite structures
Graphite
Missile Airframes
Interceptors
Epoxy Resins
Fibers

The work reported herein represents a continuation of previous work reported in AMMRC-TR-78-4 and TR-78-38 and is aimed at the development of ultra-high-modulus graphite/epoxy structures for use in future advanced terminal interceptors. The work has produced a preliminary full-scale design and demonstrated, experimentally and analytically, that the design will carry the loads. More study needs to be conducted and some further experimental work is recommended before a full-scale article is tested. Work reported here has concentrated on testing the aft joint and an intermediate ring for holding an equipment package in the frusta.

Army Materials and Mechanics Research Center
Watertown, Massachusetts 02172
DEVELOPMENT OF ADVANCED INTERCEPTOR SUBSTRUCTURAL MATERIAL
J. Hertz and N. R. Adsit
General Dynamics Convair Division

AD ______

UNCLASSIFIED
UNLIMITED DISTRIBUTION

Technical Report AMMRC TR 80-44, August 1980
151 pp – illus – tables, Contract DAAG46-78-C-0056,
D/A Project 1W16211A661
AMCMS Code 62113.11.07000
Final Report September 1978
to November 1979

Key Words

Composite Materials
Composite structures
Graphite
Missile Airframes
Interceptors
Epoxy Resins
Fibers

The work reported herein represents a continuation of previous work reported in AMMRC-TR-78-4 and TR-78-38 and is aimed at the development of ultra-high-modulus graphite/epoxy structures for use in future advanced terminal interceptors. The work has produced a preliminary full-scale design and demonstrated, experimentally and analytically, that the design will carry the loads. More study needs to be conducted and some further experimental work is recommended before a full-scale article is tested. Work reported here has concentrated on testing the aft joint and an intermediate ring for holding an equipment package in the frusta.

Army Materials and Mechanics Research Center
Watertown, Massachusetts 02172
DEVELOPMENT OF ADVANCED INTERCEPTOR SUBSTRUCTURAL MATERIAL
J. Hertz and N. R. Adsit
General Dynamics Convair Division

AD ______

UNCLASSIFIED
UNLIMITED DISTRIBUTION

Technical Report AMMRC TR 80-44, August 1980
151 pp – illus – tables, Contract DAAG46-78-C-0056,
D/A Project 1W16211A661
AMCMS Code 62113.11.07000
Final Report September 1978
to November 1979

Key Words

Composite Materials
Composite structures
Graphite
Missile Airframes
Interceptors
Epoxy Resins
Fibers

The work reported herein represents a continuation of previous work reported in AMMRC-TR-78-4 and TR-78-38 and is aimed at the development of ultra-high-modulus graphite/epoxy structures for use in future advanced terminal interceptors. The work has produced a preliminary full-scale design and demonstrated, experimentally and analytically, that the design will carry the loads. More study needs to be conducted and some further experimental work is recommended before a full-scale article is tested. Work reported here has concentrated on testing the aft joint and an intermediate ring for holding an equipment package in the frusta.

Army Materials and Mechanics Research Center
Watertown, Massachusetts 02172
DEVELOPMENT OF ADVANCED INTERCEPTOR SUBSTRUCTURAL MATERIAL
J. Hertz and N. R. Adsit
General Dynamics Convair Division

AD ______

UNCLASSIFIED
UNLIMITED DISTRIBUTION

Technical Report AMMRC TR 80-44, August 1980
151 pp – illus – tables, Contract DAAG46-78-C-0056,
D/A Project 1W16211A661
AMCMS Code 62113.11.07000
Final Report September 1978
to November 1979

Key Words

Composite Materials
Composite structures
Graphite
Missile Airframes
Interceptors
Epoxy Resins
Fibers

The work reported herein represents a continuation of previous work reported in AMMRC-TR-78-4 and TR-78-38 and is aimed at the development of ultra-high-modulus graphite/epoxy structures for use in future advanced terminal interceptors. The work has produced a preliminary full-scale design and demonstrated, experimentally and analytically, that the design will carry the loads. More study needs to be conducted and some further experimental work is recommended before a full-scale article is tested. Work reported here has concentrated on testing the aft joint and an intermediate ring for holding an equipment package in the frusta.